Study of Friction and Wear Behavior Based on Different Lubricants and Materials

by

Sanjeev K C

A dissertation submitted to the Graduate Faculty of
Auburn University
in partial fulfillment of the
requirements for the Degree of
Doctor of Philosophy

Auburn, Alabama
December 11, 2021

Keywords: Friction, Wear, Bio-oil, Additive Manufacturing, Tribology, Soybean

Approved by

Robert L. Jackson, Chair, Professor, Department of Mechanical Engineering
Sushil Adhikari, Co-Chair, Professor, Department of Biosystems Engineering
Jay M. Khodadadi, Professor, Department of Mechanical Engineering
Jeffrey C. Suhling, Professor, Department of Mechanical Engineering

Abstract

Tribology is the study of friction, wear, and lubrication between the contacting bodies and requires a deeper understanding of multiple disciplines. This study was mainly focused on two main areas: the tribological study of additively manufactured parts and bio-based lubricants (first, second and third generation of biomass) as alternatives to conventional base oils.

First, additively manufacturing parts of 17-4 precipitation hardening (PH) stainless steel (SS) were made using laser-based powder beam fusion (LB-PBF), and wrought conventional parts were also made. Both samples were tested using a tribometer under dry and lubricated conditions at 10N and 30N applied loads. The wear rate for both dry and lubricated conditions were found to be proportional to the load under the same loading condition. LB-PBF 17-4 PH SS has a slightly higher hardness value (417 ± 21 HV) than the CM 17-4 PH SS (392 ± 24 HV) due to the finer microstructure produced as a result of a higher cooling rate. This variation in hardness number results in less wear in the LB-PBF sample than the conventional wrought sample. Wear results tested in the dry condition had more adhesive wear while the mechanism changed to abrasion during the lubricated condition. The surface roughness of the LB-PBF specimens was measured to be 1.93 μm, while it was 0.88 μm for the CM ones. Asperities were more likely to be in contact for the LB-PBF samples during the lubricated condition. This could be the reason for variation in the wear rate for the lubricated condition where conventional wrought had lower wear than the LB-PBF samples. There was a difference in the friction between each test condition, but not between the conventional wrought and LB-PBF samples. The average dry coefficient of friction (COF) at 30 N is 0.9 while the dry COF at 10 N is 1.15. SEM and optical images confirmed that

the dominating mechanism for wear during the dry condition was due to adhesion whereas abrasion was the dominant mechanism during the lubricated condition.

Secondly, the importance of sustainable lubricants is very important and several vegetable-based oils with different oleic content were compared with a standard mineral base oil for friction, wear, and chemical properties. A ball-on-disk tribometer test was performed to analyze the tribological properties of the oil under 50 N of applied load and at varying speeds. The viscosity of the conventional soybean oil increased as the temperature increased past approximately 100^{o}C and could be the result of the heavier molecular fraction of the oil. Plenish and Vistive had lower viscosities than the mineral base, even at 100^{o}C. The Plenish oil samples' wear areas were comparable to the mineral oil samples with 0.25% of a conventional additive package. This demonstrates the potential of the renewable source as a base lubricant that may not require as many additives as mineral oils. The presence of higher oleic content oils had C=O as a functional group identified from a Fourier Transformation Infrared (FTIR) test. This C=O bond helped to attract oil toward the metal surface to form a film layer. Vegetable oils have a lower COF as compared to mineral oil in the boundary lubrication regimes. The presence of oxygenates in the vegetable oil reacts with the surface and improves the lubricity of the oil. Similar to the previous study, abrasion was found to be the dominant wear mechanism and was identified due to directional grooves on the metal surfaces.

Similarly, second and third generation biomasses were used to make bio-oils from fast pyrolysis (using poultry and pine), gasification ("gasitar" using pine), and hydrothermal liquefaction processes (using *Scenedesmus* and *Nannocholoropsis*). The friction and wear tests were conducted using a ball on the disk tribometer test. The results showed that the COFs were around 0.02 for both gasitar and *Scenedesmus* bio-oil; whereas, catalytic and non-catalytic

pyrolysis oils had COFs around 0.1. Wear results indicated that catalytic pyrolysis bio-oil had a lower wear cross-sectional area compared to all other tests. The chemical analysis of bio-oil samples indicated that gasitar had lower oxygen and higher hydrocarbon composition, pyrolysis bio-oil had higher oxygenates, and algal bio-oils had a higher nitrogenates composition. The study showed that catalytic pyrolysis bio-oil and gasitar have good prospects to be used as lubricants, however, catalytic pyrolysis bio-oil chemical analysis indicated the presence of oxygenating groups which could have a cascading effect at an elevated temperature. Optical images indicated that for algal and poultry bio-oil scuffing was the dominant wear mechanism where abrasive wear was more dominant for the other bio-oils.

Acknowledgements

I would like to express my deepest appreciation to my major advisor, Dr. Robert L. Jackson for his continuous support and mentorship during my entire time at Auburn University. His support, motivation, and guidance helped me to complete this dissertation. I am equally thankful to my co-advisor Dr. Sushil Adhikari, for his constant motivation, support, and guidance. I would also like to thank Dr. George Flowers for constantly supporting me with the graduate assistantship support. Thank you again from the bottom of my heart Dr. Jackson, Dr. Adhikari, and Dr. Flowers. I would also like to thank my committee members Dr. Jay M. Khodadadi and Dr. Jeffrey C. Suhling for their valuable suggestions along the way.

I would also like to thank Dr. Brian Via for serving as a university reader on such a short notice. I would also like to thank Dr. Oladiran Fasina, Dr. Nima Shamsaei for allowing me to use their lab space. I would also like to thank Dr. Marian Kennedy from Clemson University who helped me drive our additive manufacturing study. I would also like to thank Mr. David Patrick from Physics Department who provided me the opportunity to work as a teaching assistant during my stay at Auburn University.

I am thankful for all my past and present members of Dr. Jackson and Dr. Adhikari's research group, and it was a pleasure to get to know and learn from them. I would like to thank Dr. Rajdeep Shakya for his constant support, Dr. Zhouhong Wang, Dr. Hyungseok Nam, Dr. Swarna Shah, Nikhil Jain, Dr. Rakish Shrestha, and Dr. Vivek Patil for their constant help and support during my research work. I would like to thank Ujjain Pradhan, Thomas Loxley, Sanjita Wasti, Dr.

Ravishankar Mahadevan, Anshu Shrestha, Alex Locker, Bijen Shrestha, and Dr. Philip Cross for their help.

I would also like to thank the Mechanical Engineering Department, Biosystems Engineering Department, Graduate School, and Physics Department for giving me this wonderful opportunity to pursue my graduate study. I would also like to thank all my friends in Auburn who helped me get settled in with ease and for all the good time shared (too many names to be listed here). I am also grateful to my colleagues from Amazon especially Dan Comperchio, Dr. Hao Jan Liu (Max), Christian Brewer, Jan Wuttig, Joshua Otemba, and Mohit Srivastava for their help in managing my workload.

I would like to acknowledge Zeeland Farm Services, Inc, (Zeeland, MI), DowDuoPont (Wilmington, DE), The Lubrizol Corporation (Wickliffe, OH), and Petro-Canada Lubricants Inc. (Calgary, Canada) for their support. I would also like to thank United Soybean Board for financially supporting our vegetable-based oil study.

Finally, and most importantly, I am grateful to my wife Binita, my parents (Krishna and Sujata KC), and my siblings (Sudeep, Bimal, and Upama) for their constant support throughout my Ph.D. I am especially thankful to them for reminding and pushing me each day to work harder to finish this dissertation. This dissertation is dedicated to you all!

Table of Contents

List of Tables

List of Figures

List of Abbreviations

AISI	American Iron and Steel Institute
AM	Additive Manufactured
ASTM	American Society for Testing and Materials
CAD	Computer Aided Design
CM	Conventional Manufactured
COF	Coefficient of Friction
EIA	Energy Information Administration
ESO	Epoxidized Soybean Oil
ESP	Electrostatic Precipitator
FTIR	Fourier Transformation Infrared
HHV	Higher Heating Value
HTF	High Temperature Filter
HTL	Hydrothermal Liquefaction
ISO	Internation Organization for Standardization
LB-AM	Laser Based Additive Manufactured
LB-PBF	Laser Based Powder Beam Fusion
MoDTP	Molybdenum Dithiophosphate
NTP	Normal Temperature and Pressure

PCM	Pulse Code Modulation
PH	Precipitation Hardening
PSD	Particle Size Distribution
PUFA	Polyunsaturated Fatty Acids
SEM	Scanning Electron Microscope
SS	Stainless Steel
TAN	Total Acid Number
TGA	Thermogravimetric Analysis
ZDDP	Zinc dialkyldithiophosphates

Chapter 1: Introduction

1.1 Background

Tribology is the branch of science that deals with friction, wear, and lubrication of two contacting surfaces. Tribology is derived from the Greek word *Tribos* which means rubbing [1]. It is mainly focused on reducing friction between the interacting surfaces in relative motion [2]. Tribology requires interdisciplinary knowledge of physics, mathematics, chemistry, material science, and engineering, making it complex as well as interesting at the same time. Numerous textbooks, journals, and proceedings are present in tribology, however the term tribology is still new to the general public [3,4]. The world is full of machines and any moving parts contacting each other is related to tribology since it deals with the study of understanding the science behind the interfaces. This knowledge helps in reducing the need for maintenance, improves life span, reduces energy consumption, and improves the reliability of interacting machine components [5]. Therefore, it has become an integral part of the design phase that has substantial benefits during the operation period of the machine.

According to Dowson [6], the history of tribology can be found as far as 3500 before Christ (B.C.), when fire was generated by rubbing pieces of wood. During the 3500-900 BC pieces of evidence were found indicating the use of animal fat or bitumen as lubricants in cylindrical pieces. There was an era of Leonardo da Vinci which included many aspects of machine elements as shown in many drawings called codices [7]. He is considered to be the first well-known tribologist. The developments were followed by other remarkable works on gears and pieces of machinery and research from Hooke's (relationships of rolling friction), Newton (viscosity), Euler (definition of friction), and Amontons (law of friction) [2].

The first industrial revolution occurred between the period of 1750-1850 when friction was postulated by Coulomb that adhered the laws of Leonardo da Vinci and Amontons [8]. Posiseuille flow and Navier Stokes equations were derived during this era. From 1850 to 1940, hydrodynamic studies were carried out and Reynolds developed his equation for hydrodynamic pressure that is the basis for the calculation of full-film bearings desgin [9]. During 1940-1960, the effect of elastic deformation of contacting bodies and its dependency on the viscosity of lubricant pressure were evaluated to determine the minimum film thickness by numerical solutions [10]. Other notable achievements during this period were the Bowden and Tabor relationship for friction coefficient and hardness of the asperity; Archard's equation for the volume of worn material; Sommerfeld's analytical solution for Reynolds's equation; and the Stribeck curve showing the relationship between friction, load, speed, and viscosity.

The word tribology came into existence from 1960 to 1990 and is characterized as the birth of the defined field of tribology which was dated in a report by Jost in 1966 [11]. With the help of computing advancement, elastohydrodynamic numerical calculations were extended to point contact [12]. Various types of computational and experimental studies were conducted on low friction bearings such as air lubricated [13], magnetic bearings [14], and hydrostatic lubrication [15].

1.1.1 Friction

Friction is an integral part of life and one of the primary examples of friction is our control during walking. Friction is defined as tangential resistance to motion. Friction is undesired in most machine operations as it reduces performance, material, and component failure due to resistance.

Therefore, reducing friction by using lubricants, low friction materials, and improvement in designs are employed to reduce friction. The coefficient of friction (COF) is the ratio of frictional force resisting the motion between two surfaces to the normal force pressing the two surfaces. Many researchers have called COF a product of the evolved works of many philosophers, scientists, and engineers [16].

$$COF\ (\mu) = \frac{F}{N}$$

where, F = frictional force

N = normal force

There are mainly two types of friction, static and dynamic, as depicted in Figure 1. Static friction is the friction between two or more objects that are not in motion with respect to each other. Kinetic friction is the friction between two or more objects that are in motion with respect to each other. Static friction in Figure 1 is when the load doesn't move relative to the flat surface when applying the force. Kinetic friction Is when the load starts to move relative to the flat surface due to the applied load.

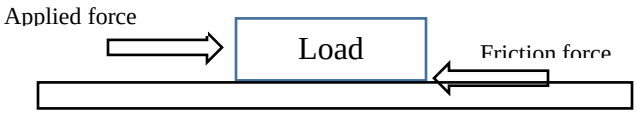

Figure 1.1: Demonstration of static and dynamic forces

Based on the experiment from many researchers there are five observation of dry friction:

1) Friction is independent of area of contact
2) Friction is proportional to normal load i.e. Fα N
3) Kinetic friction is independent of magnitude of sliding velocity

4) Coefficient of static friction is slightly greater than the coefficient of kinetic friction

5) To initiate relative motion, applied force must be equal or greater than the static friction

However, these observations do not hold universally.

1.1.2 Wear

Similar to friction, material removal can be both desirable and undesirable. Materials are removed for polishing, machining, and shearing to obtain a desired product in manufacturing, whereas undesired removal is referred as wear. Wear is defined as an undesirable removal of material from one of the two surfaces that are in relative motion. The materials are removed starting from the asperity contacts and are dependent on operating conditions and material properties. Wear reduction is directly related to operational and maintenance savings in industrial applications. Wear can be classified as zero wear and measurable wear [17]. Zero wear is referred as polishing since the materials are removed in a way that asperities are gradually worn to obtain a smooth surface. Measurable wear is due to undesired removal of materials caused by friction and an increase in surface roughness. One of the prominent forms of measurable wear is pitting. Contact stresses are developed due to repeated loading and when the contact stress exceeds the surface fatigue (one type of wear) strength then material starts to wear off.

Wear can be classified into six major classes depending on the type of wear mechanism:

- Abrasive wear: Abrasive wear occurs due to the sliding of hard materials against soft surfaces. Scratching, micro-cutting, micro-fracture, micro fatigue, and removal of materials grains are based on abrasive wear.
- Adhesive wear: This wear depends on the affinity between the two contacting surfaces. If a steel pin surface is pushed on a indium surface and retracted, then a layer of the indium

gets transferred to the steel pin due to the affinity between steel and indium. Sometimes materials get welded together due to scuffing and tear out the particles, which is referred to as scoring.

- Corrosive wear: Corrosive wear is caused due to chemical reaction between the material and corroding medium followed by mechanical action to trigger the wear. Corrosive wear is a combination of chemical reaction and mechanical action.
- Erosive wear: It is caused by the impacting particles on the solid surfaces and depends on particle velocity, impact angle, and size of the abrasive particles. A typical example of this wear is dust particles impacting turbine blades.
- Fatigue wear: Fatigue wear is mainly caused by the cyclic loading. When multiple cyclic loading is applied to the surface then the contact stress exceeds material strength and crack is initiated [17]. The cracks propagate and materials are removed from the surface eventually, sometimes by the abrasive or adhesive mechanism.
- Fretting wear: This occurs due to high-frequency movement of the surfaces in which relative sliding are on a micron level. Generally, the wear debris remains in the contacting surface and accelerates the wear process.

1.1.3 Lubrication

Lubrication is a process of reducing undesirable wear and friction by the introduction of lubricants to reduce solid contact between two surfaces. A lubricant is a substance that is introduced to reduce friction and wear. Apart from reducing friction and wear, lubricants can help for cooling, cleaning, protection, suspending, and the transfer of power. When the two contacting surfaces are separated by the lubricant then it is referred to as thick or full-film lubrication. When the lubricant is unable

to separate the contacting surfaces and asperities begin contacting then it is referred as thin or mixed and boundary lubrication. Based on the mechanism, lubrication can be classified as boundary, mixed, elastohydrodynamic, and hydrodynamic. These lubricant regimes are classified by a dimensionless film parameter known as specific film thickness (Λ) [17].

$$\Lambda = \frac{h_{min}}{\sqrt{R_{rms,a}^2 + R_{rms,b}^2}}$$

where, h_{min} = minimum film thickness

$R^2_{rms,a}$ = root mean square (rms) surface roughness of surface a

$R^2_{rms,b}$ = root mean square (rms) surface roughness of surface b

Based on Hirani [17], the lubrication mechanism based on specific film thickness are classified as:

- Boundary lubrication (approx. $\Lambda < 1$): Associated with metal to metal contact under heavily loaded condition with a thin film layer in between the contacting surfaces. Usually occurs during the start and shutdown of machines.
- Mixed lubrication ($1 < \Lambda < 3$): As the sliding speed increases, a wedge of lubricant film is created between the surfaces in motion which reduced the coefficient of friction and wear, and is referred as mixed lubrication regime.
- Elasto-hydrodynamic ($3 < \Lambda < 5$): This lubrication regime occurs when a rolling motion exists between the moving elements and the contact zone. This regime has a small contact area creating high contact pressures. This regime is sometimes
- Hydrodynamic lubrication ($\Lambda > 5$): As the speed increases the oil film separates the two contacting surfaces and there is little risk of asperity contact. This lubrication regime is referred as hydrodynamic regime and this is a desirable condition for the operation to reduce wear and friction. Viscosity of oil plays a very important role in this lubrication

regime since the separation between two surfaces should be maintained under every operating condition. If the lubricant is too viscous then lubricant resistance will reduce the efficiency.

1.1.4 Additives

Lubrication is an important aspect in reducing friction and wear, and the hydrodynamic lubrication regime is most preferable [18]. Additives are not needed as extensively in these cases. However, with the constant interaction of high speed, high temperature, and high load, additives are required in lubricants to enhance properties. Additives are selected based on the type of application and its role in that application. Additives need to be readily soluble and should be uniformly dispersed in the base oil to enhance the properties. Based on Hirani [17], depending on the application additives are classified as:

- Detergent and dispersant additive: These additives are used to remove and neutralize harmful products. Detergents help to prevent sludge and varnish while reducing the amount of acidic materials. Dispersants are used to suspend/disperse harmful products.
- Anti-wear additive: These additives are used to prevent metal to metal contact under light loads, for heavy loads extreme pressure additives (helps to reduce wear under extreme pre) are required. Chemical decomposition and absorption mechanism are used to form a protective layer on the metal surface.
- Anti-foaming agents: Foams are produced during lubrication that hinders flow rate and increases oxidation. Detergent and dispersant additives tend to promote foam so anti-foaming additives are added to reduce foam formation.

- Anti-oxidant additive: Oxidation accelerates during high temperature and pressure operations and results in corrosion of the materials including lubricants. Corrosion results in viscous drag in the pumping lubricant and eventually power loss. Therefore, anti-oxidant additives helps to prevent corrosive agents.
- Pour point depressants: This additive is used to reduce the pour point (lowest temperature at which the lubricant will flow) so that the lubricant can operate at a lower temperature. These additive helps to encapsulate waxy crystals to stop their growth at lower temperature.

1.2 Recent Technological Advancement Effecting Tribology

1.2.1 Additive Manufacturing (AM)

Additive manufacturing (AM) is a technology to create complex parts and prototypes by forming layer by layer three-dimensional objects using computer-aided design (CAD). AM was initially used to produce prototypes, however with the advancement in technology such as laser-based additive manufacturing (LB-AM), AM is leaping into the manufacturing world. The advantage of this technology, in particular, is to produce complex parts as one integrated components compared to the traditional assembled way, which helps to reduce cost and labor. There have been many instances of its applications such as in unmanned aerial vehicles, fuel nozzles, houses, biomedical implants, and more [19][20][21]. Several studies are being conducted to improve the properties of AM parts such as fatigue, surface roughness, porosity, and grain size [22][18]. There is a huge prospect in this technology and improvements in properties would help this technology to be utilized in a widespread manner.

1.2.2 Bio-derived oils

There is a shift towards the circular economy and creating a sustainable world resulting in more focus on biomass sources energy. Thermochemical processes is one of the methods to convert biomass into useful products, the other being biochemical processes. Thermochemical processes convert lignocellulose raw material to useful products with pathways such as gasification and pyrolysis [23]. Pyrolysis is a process of converting biomass to liquid fuel by rapidly heating biomass at a temperature of about 500^{o}C at a short residence time and in the absence of oxygen. Biomass contains a mixture of hemicellulose, cellulose, lignin along with other organics that have different degradation rates [24]. This process requires rapid heating of biomass to convert into coke, condensable and non-condensable vapors, followed by immediate cooling of vapors to obtain dark bio-crude. This liquid yield contains polar organics and water which constrains its application directly and requires further processing to achieve end products such as lubricants [25].

On the other hand, gasification is a process to convert biomass into gas/vapor phase (syngas) and solid phase (char). Gasification, just like pyrolysis, requires the biomass to be decomposed at a higher temperature of around 900^{o}C under limited supply of oxygen to yield syngas (CO, H_2, CO_2, CH_4, H_2O, and N_2). Tar and char are other byproducts of the gasification process [26]. The syngas can be used to produce liquid transportation fuels, chemicals, and jet fuel range. Gasifying agents such as air is more suitable for heat and power applications, whereas steam and oxygen would help to produce H_2 for use in fuel cells via the Fischer-Tropsch synthesis method [27]. One of the issues with the gasification process is tar formation which is mainly composed of compounds with molecular weights higher than benzene [28].

1.3 Problem Statement

As discussed earlier, tribology requires knowledge of interdisciplinary subjects ranging from material science to fluid mechanics. With the advancement of technology, tribological knowledge is becoming more important and requires a deeper understanding of material and processes. AM is evolving as a new wave in the manufacturing world and a tribological study of AM-produced parts is very important. Studies on AM were more focused on the grain size, manufacturing process, operating condition, fatigue, fracture, and cracks. However, the tribological behavior of AM parts under dry and lubrication conditions as compared with the conventional wrought sample would provide vital information for further advancement and application of this technology.

In the past, studies for lubrication were mostly based on the conventional base oils and improving their properties by application of additives. With the concern about climate change and greenhouse gases, there is a need to research alternatives to conventional base oils. Vegetable-based oil is favorable for lubrication because of inherent fatty acids that have been historically used for lubrication purposes. Previous studies were more focused on converting vegetable-based oil to biofuel and less on the lubrication aspects. A comparative study of vegetable oil as a lubricant and conventional oil with additives under variable speeds will help to provide more insight into the tribological properties of vegetable-based oil.

Although vegetable oil is a good alternative to conventional lubricants, the debate of food vs energy would hinder at some point with the increase in demand. So, using alternative raw material to produce bio-based lubricant is imminent. Second and third generations of biomass such as agricultural wastes, poultry litter, and algae are some of the raw materials that could be converted to bio-based liquid via thermochemical conversion. These bio-based lubricants could

potentially be a good alternative to conventional lubricants and a tribological study would help to shed more light on this aspect of bio-based lubricants.

1.4 Research Objectives

Tribology is an important aspect of everyday life and plays a very important role in many applications. Tribology is required for the longevity of the system, reduce maintenance and save cost. With the advancement of technology, tribological studies for additive manufacturing and renewable lubricants have become more exciting and challenging. The overall goal of this study is focused on two aspects of tribology: 1) material of the moving parts, and 2) sustainable lubricants from the first, second, and third generation of biomass.

Objective 1: Study of tribological behavior of 17–4 PH stainless steel fabricated by traditional manufacturing and laser-based additive manufacturing methods

In this part, the tribological properties of additively manufactured parts using laser beam powder bed fusion method and conventional wrought samples were tested using a pin on disk tribometer test under dry and lubricated conditions. Details of this part are given in Chapter 2.

Objective 2: Study of the friction and wear properties of high oleic vegetable-based and mineral oils

In this part, friction, wear, and chemical properties of several vegetable-based oils with different oleic content were compared with a standard mineral base oil with inherent chemistries. A pin on disk tribometer test was conducted at varying speeds to understand the influence of oleic acid content on friction and wear properties. Details of this part are given in Chapter 3.

Objective 3: Study of friction and wear properties of biomass-derived oils via thermochemical conversion processes

In this part, the tribological properties of second and third-generation bio-mass derived oils were produced using thermochemical processes. Bio-derived oils were tested for chemical, friction, and wear properties and compared against the standard mineral base oils under a constant load and constant speed. Details of this part are given in Chapter 4.

The overall conclusions of the parts and recommendations for future work are summarized in Chapter 5.

1.5 References:

[1] B. N. T. Persson, “History of Tribology,” in *Encyclopedia of Lubricants and Lubrication*, T. Mang, Ed. Berlin, Heidelberg: Springer Berlin Heidelberg, 2014, pp. 791–797.

[2] E. Ciulli, “Tribology and Industry: From the Origins to 4.0,” *Front. Mech. Eng.*, vol. 5, 2019.

[3] R. P. Glovnea, A. V. Olver, and H. A. Spikes, “Effectiveness of boundary lubricant additives on some coated surfaces,” *Tribol. Interface Eng. Ser.*, vol. 48, pp. 135–143, Jan. 2005.

[4] A. N. Farhanah and S. Syahrullail, “Tribological behavior of the refined, bleached, and deodorized palm kernel as an alternative lubricant,” *Sci. Iran.*, vol. 25, no. 3B, pp. 1169–1178, 2018.

[5] S. J. Shaffer, “Tribology 101 – Introduction to the Basics of Tribology,” *Bruker*, 2013.

[6] D. Dowson, “History of Tribology in America,” *J. Lubr. Technol.*, vol. 103, no. 3, 1981.

[7] I. M. Hutchings, “Leonardo da Vinci’s studies of friction,” *Wear*, vol. 360–361, 2016.

[8] C. A. Coulomb, *Théorie des machines simples en ayant égard au frottement de leurs parties et a la roideur des cordages*. New York: Readex Microprint, 1968.

[9] O. Reynolds, “The Royal Society is collaborating with JSTOR to digitize, preserve, and extend access to Proceedings of the Royal Society of London. ® www.jstor.org,” *Society*.

[10] D. Dowson and G. R. Higginson, “Chapter 6 - Elasto-Hydrodynamic Theory,” in *International Series on Materials Science and Technology*, D. Dowson and G. R. B. T.-E.-H. L. Higginson, Eds. Pergamon, 1977, pp. 65–77.

[11] H. P. Jost, “Lubrication (Tribology) Education and Research, A Report on the Present Position and Industry’s Needs. London,” 1966.

[12] B. J. Hamrock and D. Dowson, *Ball bearing lubrication : the elastohydrodynamics of elliptical contacts*. New York: Wiley, 1981.

[13] W. A. Gross, *Gas film lubrication*. New York, NY: Wiley, 1962.

[14] F. C. Moon, *Superconducting Levitation: Applications to Bearing and Magnetic Transportation*. 2007.

[15] R. Bassani and B. B. T.-T. S. Piccigallo, Eds., "Hydrostatic Lubrication," in *Elsevier*, vol. 22, Elsevier, 1992, pp. 54–86.

[16] P. J. Blau, "The significance and use of the friction coefficient," *Tribol. Int.*, vol. 34, no. 9, pp. 585–591, 2001.

[17] H. Hirani, *Fundamentals of Engineering Tribology with Applications*. 2016.

[18] S. KC, P. D. Nezhadfar, C. Phillips, M. S. Kennedy, N. Shamsaei, and R. L. Jackson, "Tribological behavior of 17–4 PH stainless steel fabricated by traditional manufacturing and laser-based additive manufacturing methods," *Wear*, vol. 440–441, p. 203100, 2019.

[19] L. Robinson and J. Scott, "Layers of Complexity: Making the Promises Possible for Additive Manufacturing" *JOM*, vol. 66, no. 11, pp. 2194–2207, Nov. 2014.

[20] M. Foust, D. Thomsen, R. Stickles, C. Cooper, and W. Dodds, "Development of the GE Aviation Low Emissions TAPS Combustor for Next Generation Aircraft Engines," in *50th AIAA Aerospace Sciences Meeting including the New Horizons Forum and Aerospace Exposition*, American Institute of Aeronautics and Astronautics, 2012.

[21] Y. Tadjdeh, "Navy Beefs Up 3D Printing Efforts With New 'Print the Fleet' Program," *Natl. Def.*, vol. 99, no. 731, pp. 24–27, Sep. 2014.

[22] R. Shrestha, J. Simsiriwong, and N. Shamsaei, "Fatigue behavior of additive manufactured 316L stainless steel parts: Effects of layer orientation and surface

roughness," *Addit. Manuf.*, vol. 28, pp. 23–38, Aug. 2019.

[23] N. Canabarro, J. F. Soares, C. G. Anchieta, C. S. Kelling, and M. A. Mazutti, "Thermochemical processes for biofuels production from biomass," *Sustain. Chem. Process.*, vol. 1, no. 1, p. 22, 2013.

[24] A.V. Bridgwater, D. Meier, and D. Radlein, "An overview of fast pyrolysis of biomass," *Org. Geochem.*, vol. 30, no. 12, pp. 1479–1493, 1999.

[25] R. Mahadevan, R. Shakya, S. Neupane, and S. Adhikari, "Physical and chemical properties and accelerated aging test of bio-oil produced from in situ catalytic pyrolysis in a bench-scale fluidized-bed reactor," *Energy and Fuels*, vol. 29, no. 2, pp. 841–848, 2015.

[26] N. S. Barman, S. Ghosh, and S. De, "Gasification of biomass in a fixed bed downdraft gasifier – A realistic model including tar," *Bioresour. Technol.*, vol. 107, pp. 505–511, 2012.

[27] M. Panahi, E. Yasari, and A. Rafiee, "Multi-objective optimization of a gas-to-liquids (GTL) process with staged Fischer-Tropsch reactor," *Energy Convers. Manag.*, vol. 163, pp. 239–249, 2018.

[28] H. Nam, D. A. Rodriguez-Alejandro, S. Adhikari, C. Brodbeck, S. Taylor, and J. Johnson, "Experimental investigation of hardwood air gasification in a pilot scale bubbling fluidized bed reactor and CFD simulation of jet/grid and pressure conditions," *Energy Convers. Manag.*, vol. 168, pp. 599–610, 2018.

Chapter 2: Tribological behavior of 17-4 PH stainless steel fabricated by traditional manufacturing and laser-based additive manufacturing methods

Abstract

This chapter discusses the investigation of the wear and mechanical properties of additively manufactured (AM) 17-4 precipitation hardening (PH) stainless steel (SS) and compares to those of conventionally manufactured (CM) wrought specimens. Disk shape specimens were fabricated by either a laser beam powder bed fusion (LB-PBF) process or a conventional manufacturing method. Wear resistance of LB-PBF 17-4 PH SS specimens were compared to that of CM ones, for both dry and lubricated conditions under 10 N and 30 N applied loads. The wear rate for both LB-PBF and CM 17-4 PH SS was found to have a proportional relation with the applied load. The CM 17-4 PH SS specimens tended to have a higher wear rate than LB-PBF ones when tested dry, while the trend reversed for the lubricated condition. This is because the lubrication changed the dominant wear mechanism from adhesion to surface fatigue and abrasion. This trend was found to be similar for both AM and CM specimens. This was attributed to the low wear rate in lubricated condition, and high wear rate in dry condition, regardless of the type of specimens (i.e. LB-PBF or CM 17-4 PH SS). The results showed that AM parts have good potential to be an alternative to wrought counterparts in terms of friction and wear behavior.

**This work has been published in Wear, vol, 440, pp. 203100, 2019*

2.1 Introduction

Additive manufacturing is being explored as a process of producing customized components for aerospace, biomedical, automotive and food industries [1]. Additive manufacturing involves joining materials layer upon layer to manufacture parts from three-dimensional (3D) CAD data, providing opportunities to fabricate parts with complex geometries. Among various additive manufacturing methods, laser beam powder bed fusion (LB-PBF) is one of the most common processes for fabricating metallic components [2]. In this process, parts are fabricated by repetitive melting and fusing a thin layer of powder to the previously fused layers, using a high-powered laser source to successively build components from bottom to top, to form the final geometry.

Despite many advantages provided by additive manufacturing, the presence of defects inherent to the process is known as its drawback, delaying the adoption of this technology for many industrial applications [3]. Such defects may include entrapped gas pores, lack of fusions, and surface roughness, which can be detrimental to the structural integrity of additively manufactured (AM) parts [4, 5]. While there have been several studies evaluating tensile and fatigue behaviors of AM materials as compared to their wrought counterparts [6-10], not much attention has yet been given to wear behavior of AM materials.

Among various additive manufactured materials, the low carbon martensitic/austenitic 17-4 precipitation hardening (PH) stainless steel (SS) has drawn much attention because of its excellent mechanical properties such as high tensile/impact strength, fracture toughness, and corrosion resistance [11]. Nezhadfar et al. [6] recently studied the microstructure and mechanical properties of LB-PBF 17-4 PH SS under various heat treatments. They reported that the tensile properties of LB-PBF 17-4 PH SS could be comparable and even better than that of wrought counterparts for the same heat treatment condition. This has been attributed to the finer

microstructure obtained in LB-PBF 17-4 PH SS due to rapid solidification during manufacturing. However, they observed lower fatigue resistance for LB-PBF 17-4 PH SS as compared to that of wrought counterparts, which was due to the presence of either surface roughness in the as-built specimens, or internal porosities for the machined specimens, similar to the observations reported in the literature for other materials [12, 13].

Wear is another potential mode of failure in structural components that are caused by gradual deformation and removal of surface material. Wear rate is one of the critical factors governing the application of manufactured parts into a moving system. Hence, it is critical to understand the friction and wear properties of AM parts in comparison to that of their wrought counterparts. There are different classifications used to describe different mechanisms occurring in wear. Some of the most common wear mechanisms that are relevant to this work are: (a) abrasive wear, which is defined by plowing of asperities resulting in material removal, (b) adhesive wear, which is defined by material removal due to welding or sticking between surfaces, and (c) surface fatigue, which is due to crack propagation due to repeated surface loading and unloading [14]. Wear is often measured via mass or volume removed. If this volume is divided by the sliding distance, the resulting value is known as wear rate. If the wear rate is also divided by the applied load, it is known as the specific wear rate.

There have been prior studies on the wear properties of wrought 17-4 PH SS, which explored the influence of heat treatment and surface modification on the wear resistance. Bressan et al. [15] studied the influence of hardness on the wear resistance of wrought 17-4 PH SS (i.e. AISI Type 630) under different heat treatment conditions (CA-H900, CA-H1025, and CA-H1150) and observed that a decrease in pin hardness (i.e. CA-H1150) resulted in lower pin wear resistance which agrees with the postulate from Archard [16]. Wear increased with larger differences in

hardness values between the ball and disk specimens used in their study. Similarly, Mahesha et al. [17] investigated the tribological wear behavior of wrought AISI 630 SS (i.e. 17-4 PH SS) considering three factors; normal load, sliding distances, and sliding velocity. They found that load is a more dominant factor relative to the sliding distance and sliding velocity in affecting the wear volume loss and specific wear rate. They observed that sliding distance itself, and interaction between load and sliding distance also play a vital role on wear volume loss.

Poor tribological properties have been reported for wrought 17-4 PH SS due to its lower surface hardness relative to common steel bearing materials, such as 52100 high carbon chrome steel. In the past, research has also shown that the addition of nitrogen via thermal implantation can improve wear performance, which may be due to topographical alternation during implantation [18]. Research has also shown that the treatment of plasma diffusion at low temperature enhances wrought 17-4 PH SS wear resistance properties [19]. The improved resistance was mainly due to thermionically providing nitriding and carburizing treatments on precipitation of stainless steel. Similar research was also conducted by Liu et al. [20] to improve wear resistance by plasma nitro-carburizing. The longer treated specimen (8h) had comparatively the lowest friction coefficient and the best corrosion resistance. It is noted in Ref. [15] that 17-4 possesses outstanding oxidation resistant properties. However, others note that during wear oxidation plays a role [21], but these are at temperatures elevated well above room temperature. Nonetheless, oxidation could play a role in the wear measured in the current study.

In the area of friction and wear testing of additively manufactured surfaces, Buciumeanu et al. [22] investigated the tribocorrosion behavior of Ti-6Al-4V manufactured by laser engineered net shaping, hot pressing, and cast processes. In their work, they found that when submerged in

saline the specific wear rate of the laser engineered net shaping material was lower than the material of the other two processes.

This paper mainly focuses on the comparative study of friction and wear properties of LB-PBF 17-4 PH SS with that of the CM wrought counterparts. The tribological behavior of the material is investigated for dry and lubricated conditions under several loads. The results will help determine if LB-PBF 17-4 PH SS could be an alternative to CM wrought in terms of tribological performance (i.e. wear and friction).

2.2 Experimental Methods

2.2.1 Material and specimen fabrication

Disks of 17-4 PH SS specimens were cut from a wrought cylindrical specimen manufactured through conventional methods and were referred to as the CM specimens in this study. The resulting disks were 7 mm thick and 70 mm in diameter. In addition, AM specimens were fabricated via EOS M290, a laser beam powder bed fusion (LB-PBF) method, under the argon environment. A picture of the resulting 17-4 PH CM specimen is shown in Figure 2.1.

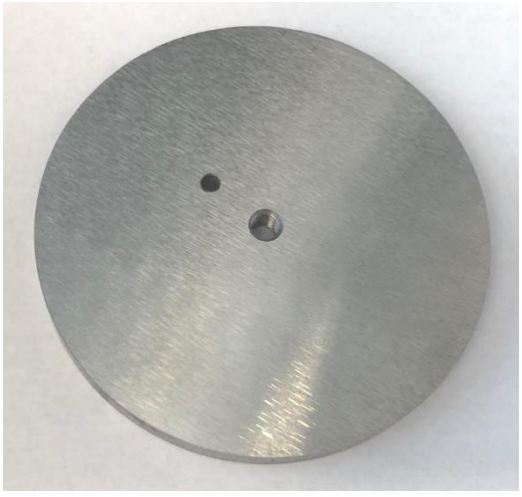

Figure 2.1: Picture of a CM 17-4 PH SS disk specimen. (diameter 6.98 cm)

The process parameters for 17-4 PH SS recommended by EOS are listed in Table 2.1**.** Argon atomized 17-4 PH SS powder with the particle size distribution (PSD) of 15-45 µm, provided by LPW Technology Inc., and was used for this study. The chemical composition of the virgin powder is listed in Table 2.

Table 2.1: Process parameters for LB-PBF 17-4 PH SS provided by EOS Company

Laser power (W)	**Scanning speed (mm/s)**	**Hatching distance (µm)**	**Layer thickness (µm)**
220	755.5	100	40

Table 2.2: Chemical composition of 17-4 PH stainless steel powder provided by LPW Inc.

	C	**Cr**	**Ni**	**Cu**	**Mn**	**Si**	**Nb**	**Mo**	**N**	**O**	**P**	**S**	**Fe**
(wt. %)	0.01	15.6	4.03	3.89	0.24	0.29	0.33	<0.01	0.01	0.05	0.004	0.003	Bal

All specimens were then subjected to CA-H900 heat treatment conditions. This heat treatment procedure includes a solution heat treatment (i.e. condition A (CA)) step; heat treating at 1050 °C for 30 min, followed by air cooling to room temperature. The second step is holding the specimens at 482°C for 1 hour, and then air cooling them to room temperature (H900). The microstructure of LB-PBF 17-4 PH SS that has undergone the CA-H900 condition has been compared to that of the wrought counterpart elsewhere [10]. It has been shown that LB-PBF 17-4 PH SS possesses

similar microstructure as the wrought counterpart, however, due to the high cooling rate during the additive manufacturing process, it is comprised of finer grains.

The surface of specimens was further grinded to remove contaminants and roughness from the heat treatment procedure and manufacturing process. Representative tensile stress strain curves of the materials are provided in Figure 2.2. It can be seen that the LB-PBF 17-4 PH SS possesses higher yield strength than the wrought material, which is due to the finer microstructure of LB-PBF 17-4 PH SS based on the Hall-Petch relationship [23].

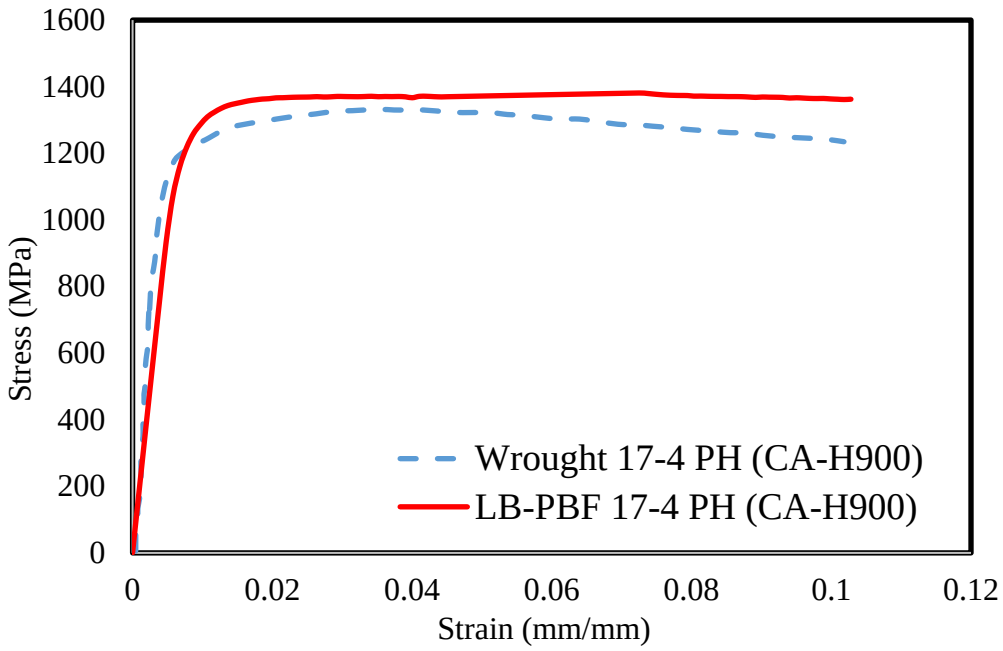

Figure 2.2. Tensile stress strain curves for the considered materials.

2.2.2 Micro-hardness testing

Selected specimens were cross sectioned and progressively polished to reach a mirror-like surface finish prior to the micro-hardness testing. Micro-hardness test was performed on both CM and LB-PBF 17-4 PH SS specimens using a LECO DM400 hardness tester based on the ASTM

E384 standard method. The load used for the hardness test was 1kgf with a dwell time of 10 s. For certainty, 3-5 indentations were conducted, and the average hardness is reported.

2.2.3 Friction and wear testing

The coefficient of friction (COF) and wear rate was characterized with a ball-on-disk method using a Bruker UMT-3 as shown schematically in Figure 2.3 (a) 52100 high carbon chrome steel balls with a diameter of 10 mm were used to load against the disk specimens. The steel balls have a Rockwell C hardness between 60 and 67. Prior testing, the specimens, and balls were cleaned using a sequence of acetone and then methanol, followed by cleaning with lent free wipes to avoid any residual dust or contaminant. Each ball and disk were then weighed in an analytical balance with a resolution of 0.0001 g to determine their initial mass. Figure 3 (b) shows the actual setup for the ball on disk tribometer test equipment.

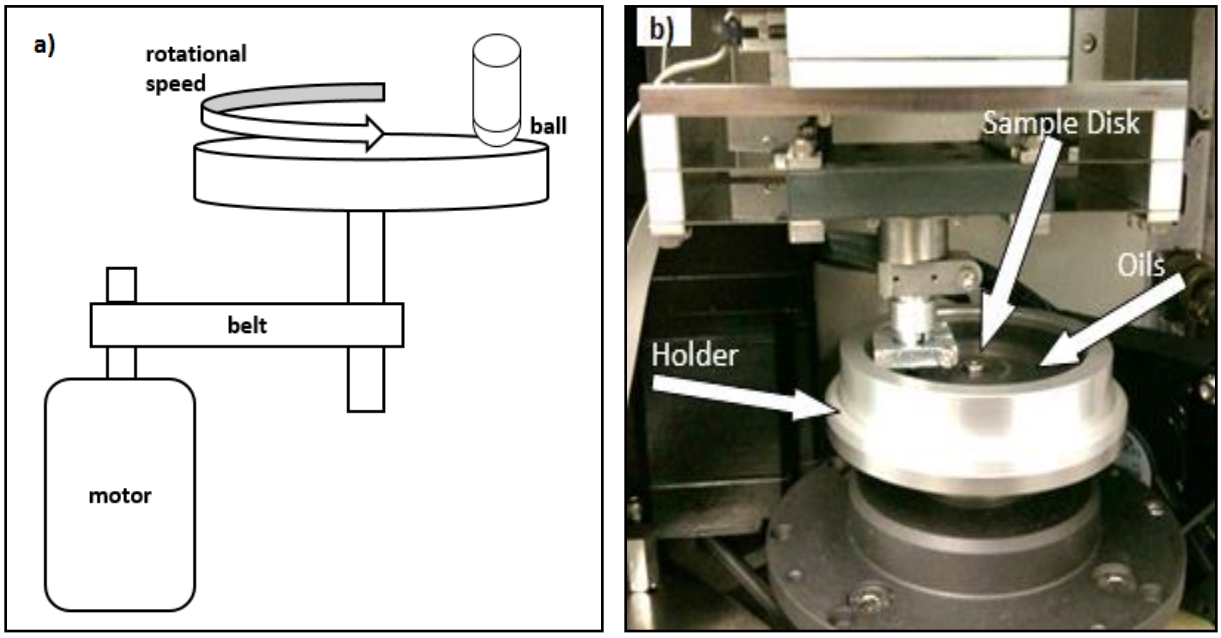

Figure 2.3. (a) Schematic of a ball on disk test, and (b) test setup for a test.

The specimens were tested for dry conditions with two different loads of 10 N and 30 N, and with a single load of 30 N for the lubricated condition. The wear of the specimens was then analyzed using a stylus profilometer. The linear sliding velocity was held at 0.6 m/s for the tests in a dry condition for 4000s. For the lubricated conditions, the specimens were submerged in the oil and tests were run using a linear sliding velocity of 0.1 m/s for 4000s. Therefore the sliding distance of the dry tests was longer than the lubricated tests, but this was accounted for when calculating the wear rate. The lower speed was used for the lubricated condition to insure solid contact and boundary lubrication. Three tests were performed for each condition with random order of runs to reduce the possibility of bias in the results due to external, unknown influences. After each test, ball and disk were both cleaned with acetone followed by methanol prior to weighing for mass. Table 2.3 shows the test conditions with the experiment run number for each case.

Table 2.3: Experimental matrix

Load (N)	10			30			30		
Lubricant	NA			NA			Synthetic		
Linear Velocity (m/s)	0.6			0.6			0.1		
Rotating Speed rpm	260			327			43		
Replicates	1	2	3	1	2	3	1	2	3
	Order of Runs (1-18)								
Wrought	2	9	14	1	8	17	4	10	13
LB-PBF	3	7	16	6	11	18	5	12	15

The wear rate was calculated from the measured profile of the worn grooves using a Vecco Dekatak 150 stylus surface profilometer with a stylus radius of 2.5 µm. The stylus was used to measure the profile of the worn surface of the test specimen over a length of 3 mm with a lateral resolution of 1 µm and a vertical resolution of 1 nm. The data were then plotted to extract the wear groove profile, while the rest of the unworn surface data were fitted linearly (see Figure 2.4). The groove and linear lines were plotted separately to calculate the wear cross sectional area. Three scans on each specimen were run in order to check variation in the results. The results for the cross-sectional area of each scan were averaged and the wear volume was evaluated by multiplying the average cross-sectional area by the track radius. Generally, the volumetric wear rate is then given by

$$Q = V/S \qquad (1)$$

where, Q (mm^3/m) is referred to as the wear rate, and V is the cumulative lost volume per sliding distance, S. Figure 2.4 represents the typical wear profile from the profilometer with the fitted line on the wear groove.

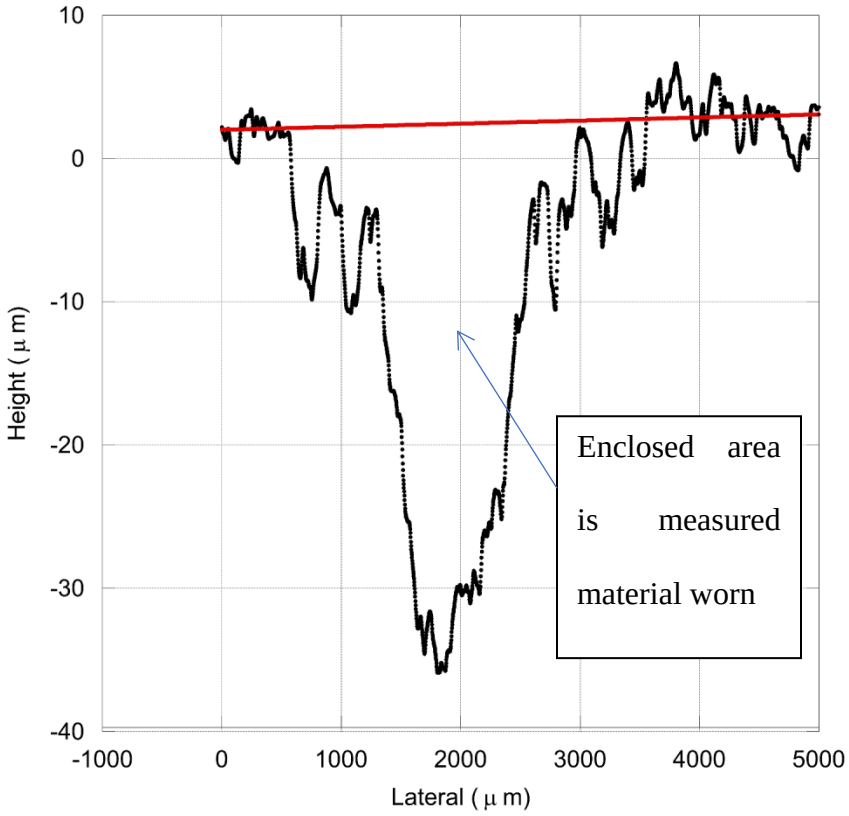

Figure 2.4. Typical wear groove profile (LB-PBF 17-4 PH SS Dry 10 N-specimen 18)

2.3 Experimental Results and Discussion

2.3.1 Hardness

The results of the micro hardness tests show that the LB-PBF 17-4PH SS has a slightly higher hardness value (417 ± 21 HV) than the CM 17-4 PH SS (392 ± 24 HV). Similarly, higher yield strength for LB-PBF 17-4 PH SS fabricated with similar process parameters in this study has been reported as compared to that of the CM counterpart [6]. This is attributed to the finer microstructure produced as a result of the high cooling rate during the LB-PBF process. According to the Hall-Petch theory, strength will be increased as the grain size decreases [23]. In addition, the density of dislocations adjacent to the grain boundaries is higher in finer grain structures, which results in higher hardness value as compared to the coarse grain structures. It is well documented

that the hardness influences the wear resistance of conventional wrought materials, with a harder surface usually resulting in less wear [15]. Accordingly, the LB-PBF 17-4 PH SS with a slightly higher hardness value is likely to have less wear as compared to the CM specimens.

2.3.2 Wear properties

Figure 2.5 shows the measured wear rates for LB-PBF and CM 17-4 PH SS. The results of CM 17-4 PH SS specimens are consistent with those reported by Bressan et al. [15]. As seen, LB-PBF 17-4 PH SS possesses a lower wear rate as compared to CM 17-4 PH SS in dry condition regardless of the applied load. In other words, LB-PBF 17-4 PH SS is more wear resistant than the CM 17-4 PH SS in this condition. Under the lower applied load (i.e. 10N) in dry condition, the wear rates of LB-PBF and CM 17-4 PH SS are close, while the wear rate difference increases by increasing the load. It can be seen that by changing the wear condition from dry to lubricated, the wear rate decreases for both LB-PBF and CM 17-4 PH SS. However, in contrast to the dry condition, LB-PBF specimens have a higher wear rate than CM ones. Note the higher error for the 30 N dry cases, with the most severe wear. This high error is due to high experimental variation in the results and is very typical of dry severe wear. Rabinowicz [24] writes that “Wear is subjected to much statistical scatter and much experimental error.” The variation may be due to the formation of many wear particles in the contact.

In the dry condition, the wear mechanism will be more adhesive than when the contacts were lubricated. However, the addition of the lubricant drastically reduces the adhesion between the surfaces, and the dominant wear mechanisms changed to abrasion and surface fatigue. Surface fatigue may also occur in the dry cases, but in the adhesion it is severe, the material may be removed before it fatigues. A previous study showed lower fatigue resistance of LB-PBF 17-4 PH

SS fabricated with the same process parameters in this study as compared to the one of CM 17-4 PH SS [6]. This behavior may also result in higher wear in LB-PBF 17-4 PH SS than the CM ones due to surface fatigue. Higher wear rates for LB-PBF 17-4 PH SS as compared to the CM ones may also be related to its higher surface roughness. The average surface roughness of the LB-PBF specimens was measured to be 1.93 μm, while it was 0.88 μm for the CM ones. Although the roughness of the LB-PBF specimens is approximately double the roughness of the wrought specimens, it is not an order of magnitude difference. The authors theorize that the difference is due to the variations in the material structure. Consequently, the peaks of asperities are more likely to be in contact for the higher surface roughness condition (i.e. LB-PBF specimens) in the lubricated condition. This would result in higher local contact stresses, which causes surface fatigue and abrasion wear mechanism.

It is worth noting that surface roughness can also reduce adhesion in dry conditions. Therefore, the difference in roughness may also be the reason for variation in wear rate between the dry and lubricated conditions.

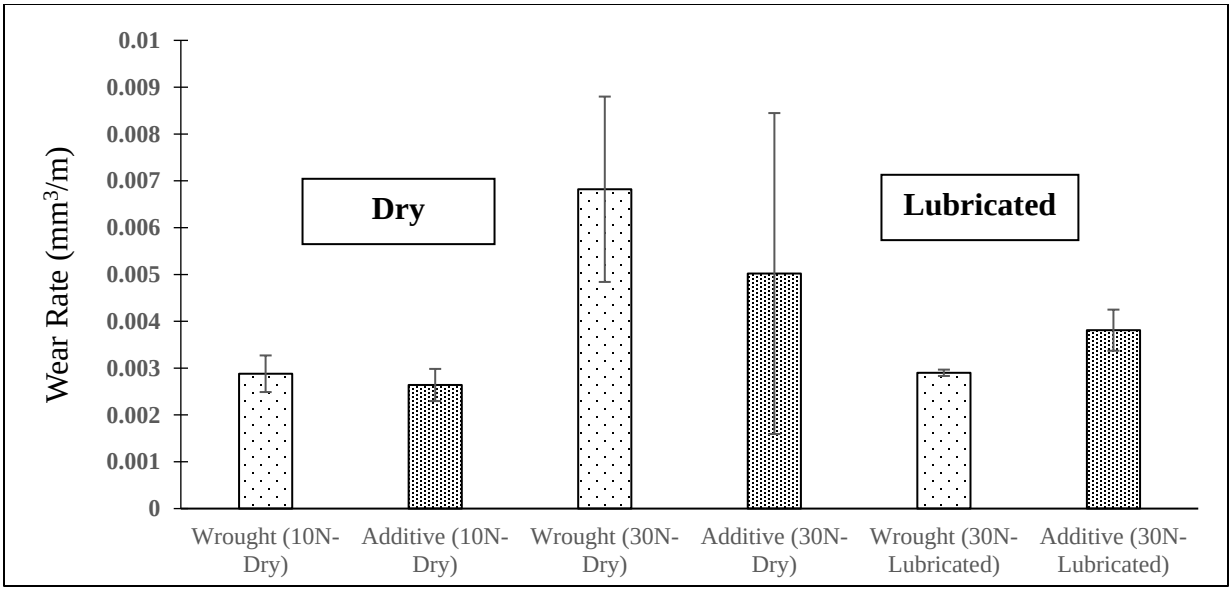

Figure 2.5: The wear rates of the 17-4 PH SS disks for wrought (CM) and additive (LB-PBF) specimens

2.3.3 Coefficient of friction (COF)

The coefficient of friction (COF) of each run is evaluated by averaging the friction of the ball on the disk tribometer test measured between 500-4000 s. This time window was used to reduce the effect of the run-in at the beginning of the test on the final test results. Figure shows the COF trend over time for each condition. Results of only one specimen from each condition (lubricated at 30N and dry at 10N or 30N) are shown for the LB-PBF and CM 17-4 PH SS in this figure. As seen, the COF is constant and smooth for both LB-PBF and CM 17-4 PH SS in the lubricated condition, which suggests a low wear regime. For the dry condition, however, the COF trends are very erratic, suggesting a severe wear regime. The initial increase in the coefficient of friction is due to the loading condition where the coefficient of friction increased from zero.

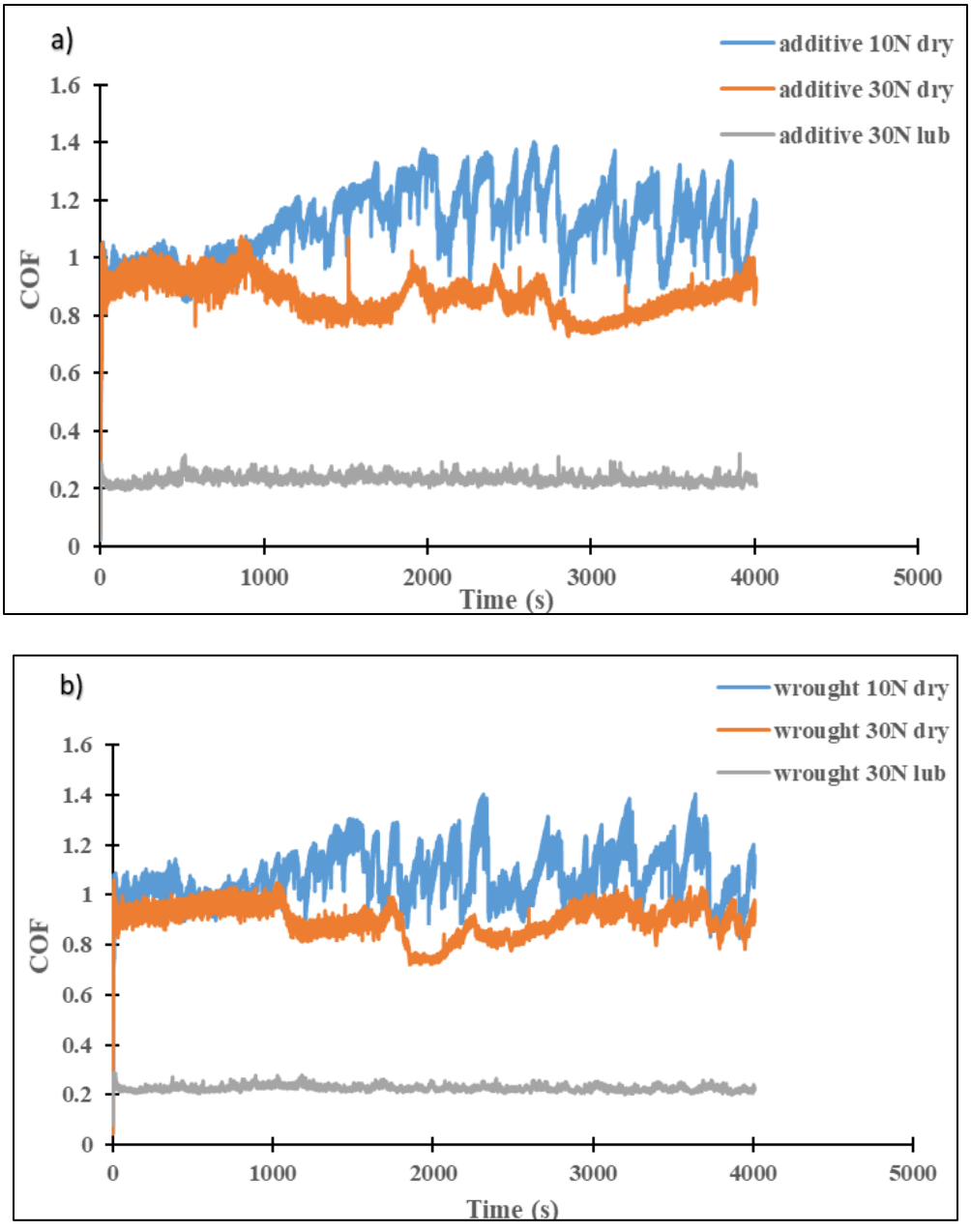

Figure 2.6. The COF trend over time measured for different load and surface conditions: (a) LB-PBF 17-4 PH SS, and (b) CM 17-4 PH SS

Figure 2.7 presents the COF results for the LB-PBF and CM 17-4 PH SS specimens, showing the mean COF values for LB-PBF and CM materials. An average steady state coefficient of friction (COF) was calculated for the additive and wrought specimens for each condition. Next,

the COF of the three specimens for each condition were averaged. There is a difference in the friction between each test condition, but not between the CM and LB-PBF samples. The dry COF at 30 N is less than the dry COF at 10 N, which agrees with several theories on adhesive friction [25-27].

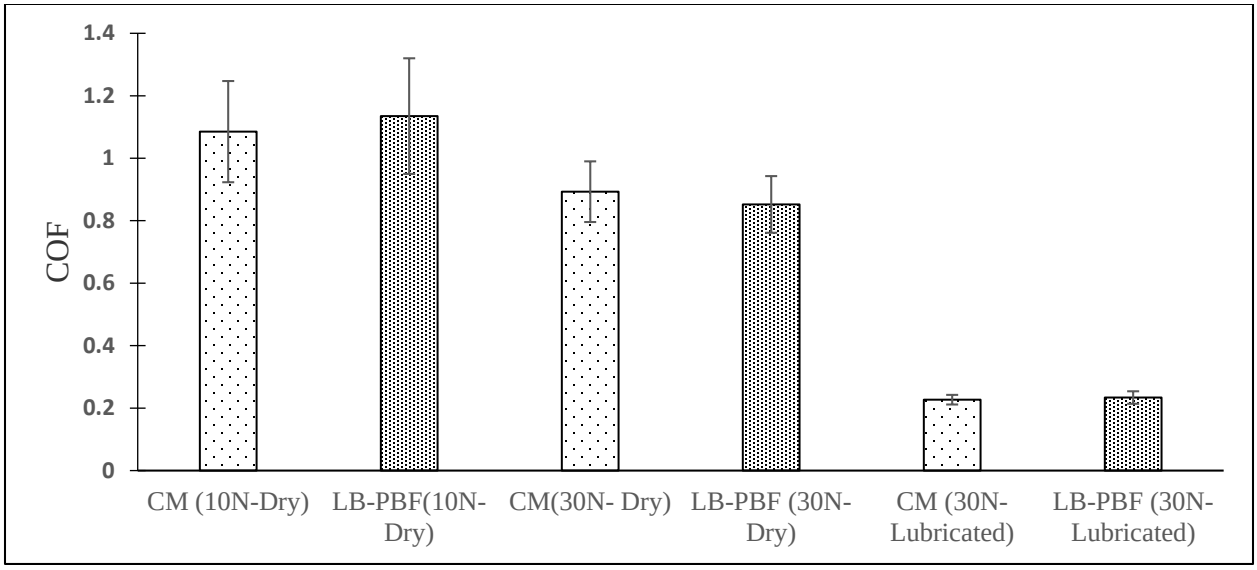

Figure 2.7. COF value for LB-PBF and CM 17-4 PH SS under various applied loads and friction conditions

2.3.4 Optical image of the surface

Optical images of the worn surfaces shown in Figure 2.8 help to indicate similarities and differences in the wear mechanisms of LB-PBF and CM 17-4 PH SS specimens during the ball on disk tests. Under 10 N applied load in dry condition, both LB-PBF and CM specimens have less worn surfaces (Figure 2.8 (a) and (d), respectively), than the situation under a 30 N applied load for both specimens (Figure 2.8 (b) and (e), respectively). The worn surfaces of the dry tests show signs of adhesion and scuffing (note places where surfaces appear to be smeared) regardless of the applied load. In lubricated conditions (Figure 2.8 (c) and (f)), the worn surfaces were much less

severe than the dry condition for both LB-PBF and CM specimens. The wear appears to be more dominated by abrasion, as indicated by the clear directional groove marks, but less smearing marks. These observations well correlated with the tribometer test data, where the COF values for lubricated tests were lower than those of dry conditions (see Figure 2.7). The overall review of these optical images indicates similar wear surfaces and mechanisms for the LB-PBF and CM specimens.

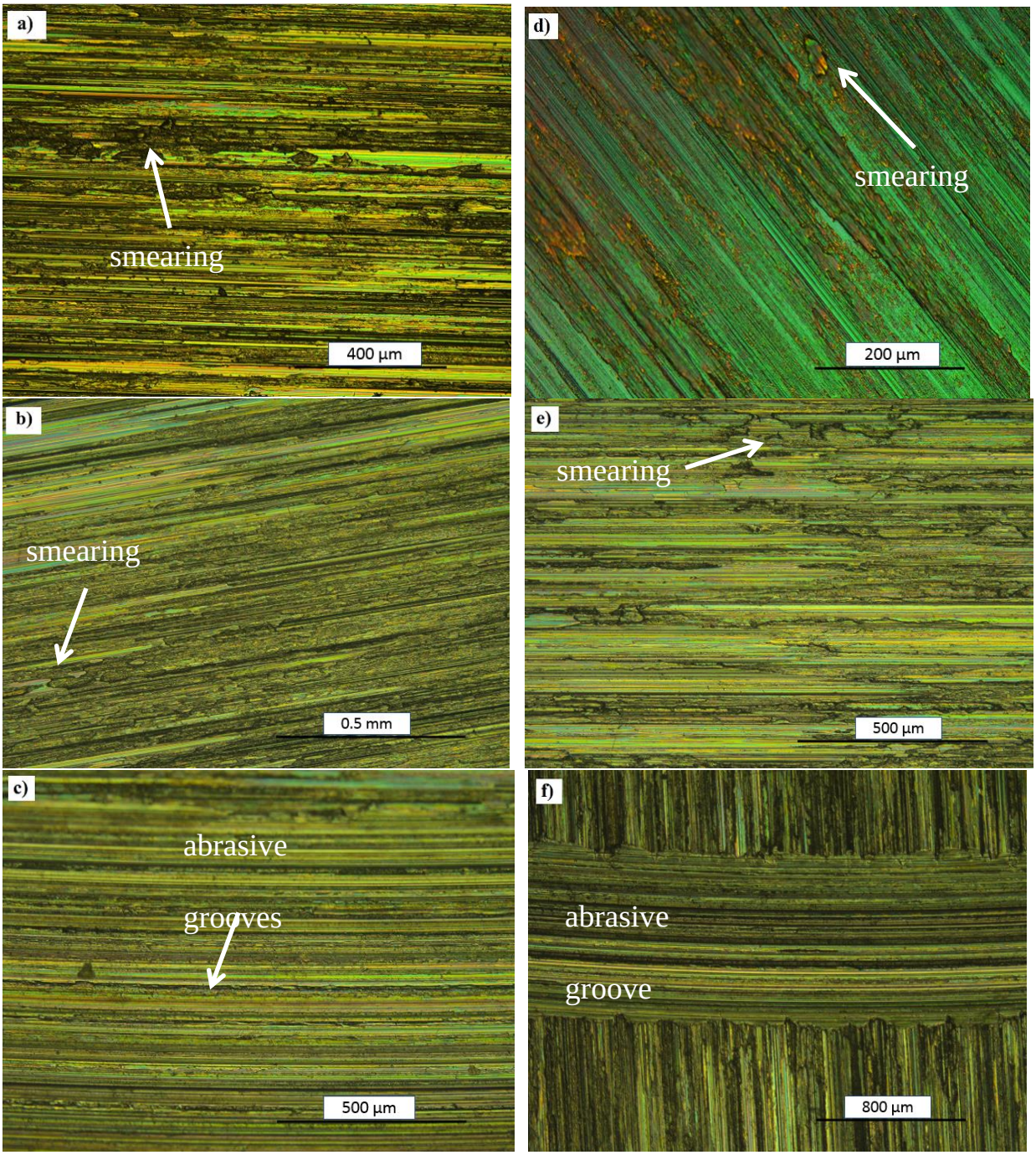

Figure 2.8. Optical images of worn surfaces of LB-PBF and CM 17-4 PH SS specimens in various conditions: (a) LB-PBF dry 10N, (b) LB-PBF dry 30N, (c) LB-PBF lubricated 30N, (d) CM dry 10N, (e) CM dry 30N, and (f) CM lubricated 30N.

2.3.5 Scanning Electron Microscope (SEM) Analysis

Figure 2.9 shows the SEM images of the worn surfaces of dry and lubricated conditions under 10 and 30 N applied loads for both LB-PBF and CM 17-4 PH SS specimens. The SEM images of the worn surfaces of the dry tests for both LB-PBF 17-4 PH SS (Figure 2.9 (a) and (b)) and CM ones (Figure 2.9 (d) and (e)) show clear indications of adhesive and scuffing wear, observed by the smearing patterns. Wear debris is clearly seen for the LB-PBF 17-4 PH SS 30 N dry load condition in Figure 2.9 (b). The adhered wear particles can be seen in the image of the LB-PBF 17-4 PH SS for 30 N dry condition specimen, which is an indicator of severe wear and also possible oxidation of this specimen. On the other hand, the CM specimen under the same condition (i.e. 30 N dry) has a relatively less erratically worn surface, as seen in Figure 2.9 (e). This could be related to the nature of the manufacturing process, where LB-PBF is a layer-wise process in contrast to casting as the conventional manufacturing method. There could be a weakness in the bond between these layers that allows for acceleration of the fatigue. As mentioned in recent research by Nezhadfar et al. [6], the fatigue properties of LB-PBF 17-4 PH SS are exacerbated by surface roughness and gas entrapped pores. Wear debris seen in the LB-PBF 17-4 PH SS specimen (Figure 9 (b)) may be due to the presence of such defects. The additional wear debris is also indicative of pitting and surface fatigue, and also oxidation. In terms of the lubricated condition, both LB-PBF and CM 17-4 PH SS specimens have relatively similar worn surfaces. The wear for the lubricated cases appears to show defined wear grooves, which are indicative of an abrasion-dominated wear regime.

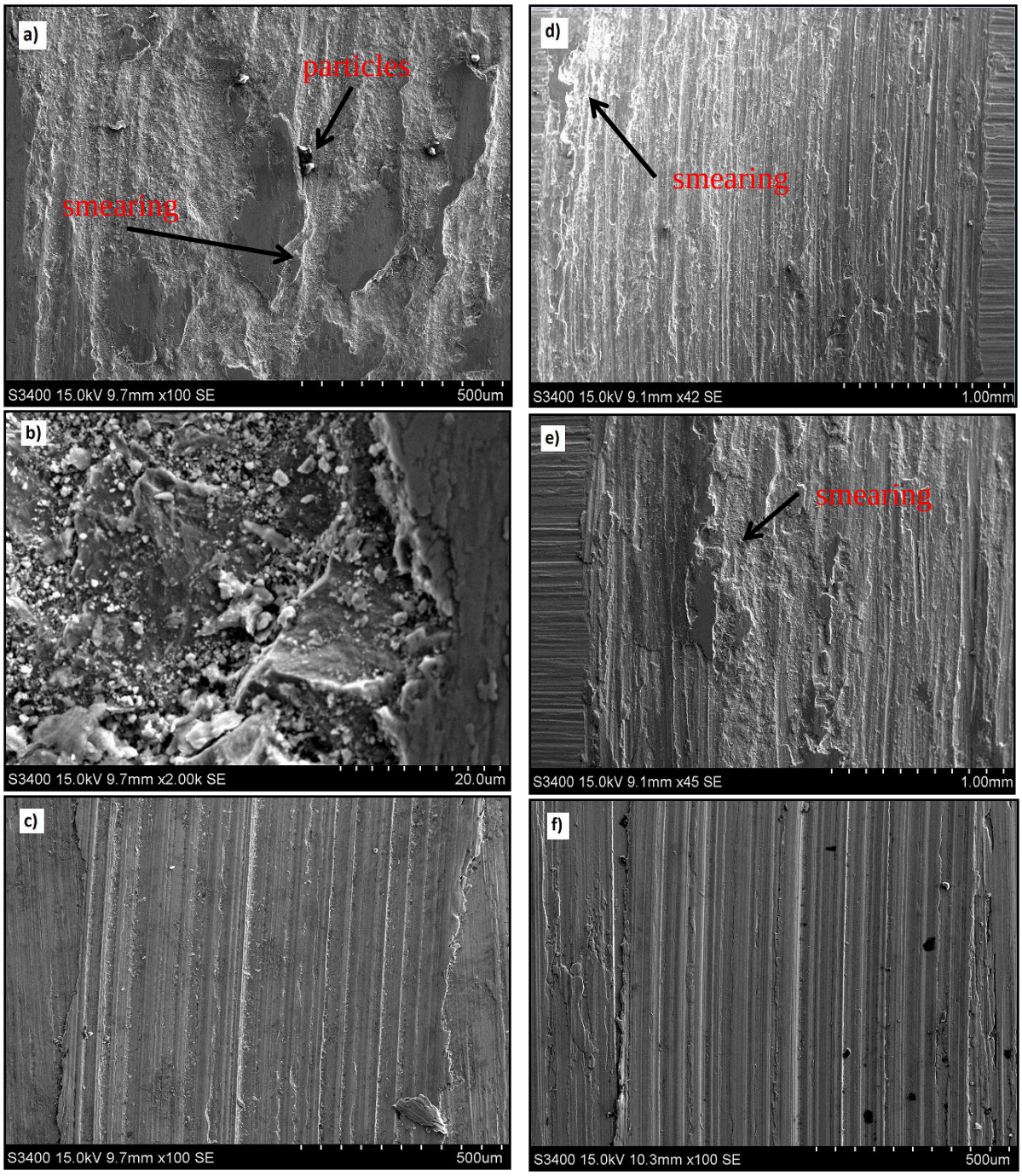

Figure 2.9. SEM images of worn surfaces of LB-PBF and CM 17-4 PH SS specimens in various conditions: (a) LB-PBF dry 10N, (b) LB-PBF dry 30N, (c) LB-PBF lubricated 30N, (d) CM dry 10N, (e) CM dry 30N, and (f) CM lubricated 30N

2.4 Conclusions

This study investigated the tribology behavior of additively manufactured 17-4 PH SS specimens via the LB-PBF process and compared it to that of wrought counterparts. The results obtained from a ball on the disk tribometer experiment were used to evaluate the friction and wear properties in dry and lubricated conditions under various applied loads. The following conclusions can be drawn based on the experimental results and observation:

1. LB-PBF 17-4 PH SS has a lower wear rate than the CM 17-4 PH SS in the dry condition regardless of the level of the load applied. This is probably due to the higher hardness of LB-PBF 17-4 PH SS as compared to the CM material, but could also be due to a difference in the roughness between the two samples.
2. LB-PBF 17-4 PH SS possesses a higher wear rate as compared to CM 17-4 PH SS in lubricated condition. This is attributed to the thinner lubricant film formed on the surface a result of higher surface roughness of LB-PBF specimens.
3. Although the wear mechanisms between LB-PBF and CM 17-4 PH SS appeared to be different, no statistical difference in their coefficient of friction (COF) was seen.
4. Adhesion was the dominant wear mechanism in dry condition, while abrasion and surface fatigue were the wear mechanisms for lubricated condition regardless of the manufacturing process (i.e. LB-PBF or CM).

Acknowledgements

The authors wish to acknowledge Auburn University mechanical engineering students E. Rhonemus, K. Bolton, S. Smith and Z. Tucker who initiated a tribological study of additive manufactured parts while participating in a class with C. Phillips under the guidance of R. Jackson. Additional acknowledgement goes to E. Rhonemus.

2.5 References

1. Ngo, T.D., et al., *Additive manufacturing (3D printing): A review of materials, methods, applications and challenges.* Composites Part B: Engineering, 2018. 143: p. 172-196.
2. Shrestha, R., et al., *An Investigation into Property-Performance Relationships for Laser Beam Powder Bed Fusion Additive Manufacturing.* Additive Manufacturing, 2019: p. 100807.
3. Yadollahi, A. and N. Shamsaei, *Additive manufacturing of fatigue resistant materials: Challenges and opportunities.* International Journal of Fatigue, 2017. 98: p. 14-31.
4. Shamsaei, N., et al., *An overview of Direct Laser Deposition for additive manufacturing; Part II: Mechanical behavior, process parameter optimization and control.* Additive Manufacturing, 2015. 8: p. 12-35.
5. Sames, W.J., et al., *The metallurgy and processing science of metal additive manufacturing.* International Materials Reviews, 2016. 61(5): p. 315-360.
6. Nezhadfar, P., et al., *Fatigue behavior of additively manufactured 17-4 PH stainless steel: Synergistic effects of surface roughness and heat treatment.* International Journal of Fatigue, 2019. 124: p. 188-204.
7. Shrestha, R., J. Simsiriwong, and N. Shamsaei, *Fatigue behavior of additive manufactured 316L stainless steel parts: Effects of layer orientation and surface roughness.* Additive Manufacturing, 2019. 28: p. 23-38.
8. Romano, S., et al., *Fatigue properties of AlSi10Mg obtained by additive manufacturing: Defect-based modelling and prediction of fatigue strength.* Engineering Fracture Mechanics, 2018. 187: p. 165-189.

9. Spierings, A.B., T.L. Starr, and K. Wegener, *Fatigue performance of additive manufactured metallic parts.* Rapid Prototyping Journal, 2013. 19(2): p. 88-94.

10. Nezhadfar, P., et al., *Fatigue crack growth behavior of additively manufactured 17-4 PH stainless steel: Effects of build orientation and microstructure.* International Journal of Fatigue, 2019. 123: p. 168-179.

11. Krauss, G. and G. Krauss, *Steels: heat treatment and processing principles*1989: ASM international Materials Park, OH.

12. Sterling, A.J., et al., *Fatigue behavior and failure mechanisms of direct laser deposited Ti–6Al–4V.* Materials Science and Engineering: A, 2016. 655: p. 100-112.

13. Pegues, J., et al., *Surface roughness effects on the fatigue strength of additively manufactured Ti-6Al-4V.* International Journal of Fatigue, 2018. 116: p. 543-552.

14. Bruce, R.W., *Handbook of lubrication and tribology, volume II: Theory and design*2012: CRC press.

15. Bressan, J., et al., *Influence of hardness on the wear resistance of 17-4 PH stainless steel evaluated by the pin-on-disc testing.* Journal of Materials Processing Technology, 2008. 205(1-3): p. 353-359.

16. Archard, J.F., *Contact and rubbing of flat surfaces.* J. Appl. Phys., 1953. 24: p. 981-988.

17. Mahesha, N.S., R. Hanumantharaya, and M.B. Davanageri, *Tribological Wear Behavior of AISI 630 (418 17-4 PH) Stainless Steel Hardened by Precipitation Hardening.* American Journal of Materials Science, 2016. 6(4A): p. 6-14.

18. Jin, J., W. Wang, and X. Chen, *Microstructure and Mechanical Properties of Ti+ N Ion Implanted Cronidur30 Steel.* Materials, 2019. 12(3): p. 427.

19. Leyland, A., et al., *Low temperature plasma diffusion treatment of stainless steels for improved wear resistance.* Surface and Coatings Technology, 1993. 62(1-3): p. 608-617.

20. Liu, R. and M. Yan, *Improvement of wear and corrosion resistances of 17-4PH stainless steel by plasma nitrocarburizing.* Materials & Design (1980-2015), 2010. 31(5): p. 2355-2359.

21. Li, G.-j., et al., *Microstructure and dry-sliding wear properties of DC plasma nitrided 17-4 PH stainless steel.* Nuclear Instruments and Methods in Physics Research Section B: Beam Interactions with Materials and Atoms, 2008. 266(9): p. 1964-1970.

22. Buciumeanu, M., et al., *Tribocorrosion behavior of additive manufactured Ti-6Al-4V biomedical alloy.* Tribology International, 2018. 119: p. 381-388.

23. Dieter, G.E. and D.J. Bacon, *Mechanical metallurgy*. Vol. 3. 1986: McGraw-hill New York.

24. Rabinowicz, E., *Friction and Wear of Materials*1995, New York: Wiley.

25. Li, L., I. Etsion, and F.E. Talke, *Contact Area and Static Friction of Rough Surfaces with High Plasticity Index.* Asme J. Tribol., 2010. 132(3): p. 031401-1-10.

26. Ghaednia, H., et al., *A review of elastic–plastic contact mechanics.* Applied Mechanics Reviews, 2017. 69(6): p. 060804.

27. Wang, X., Y. Xu, and R.L. Jackson, *Theoretical and Finite Element Analysis of Static Friction Between Multi-Scale Rough Surfaces.* Tribology Letters, 2018. 66(4): p. 146.

Chapter 3: An investigation of the friction an wear properties of high oleic vegetable-based and mineral oils

Abstract

This chapter discusses the investigation of the wear and chemical properties of several vegetable-based oils based on different oleic content and compares them to a standard mineral base oil and inherent chemistries. A ball-on-disk tribometer test was performed to analyze the tribological properties of the oil under 50 N of applied load and at varying speeds. The functional groups of oils were tested using Fourier Transform Infrared Spectroscopy (FTIR) and viscosity was determined using a rheometer. Bio-derived oils had a lower coefficient of friction (COF) than the standard mineral base oil at different speeds. The presence of oleic acid in the vegetable oils helped to reduce the friction between the surfaces as compared to that of the mineral base oil. The presence of oleic content played a vital role during the wear analysis where high oleic content oil had lower wear compared to other bio-based oils and the standard mineral base. Abrasion was observed to be the dominant wear mechanism from the optical profilometer that included grooves on all the surfaces of the disk samples. The results showed that high oleic content oil has good potential to be an alternative to the standard mineral base oil.

**This work has been published in International Journal of Agriculture, Environment and Bioresearch, Vol 6, Issue 6, Dec 2021, Page 1-20*

3.1 Introduction

The oil tanker "Prestige" sunk on September 13th, 2002, off the Galician coast which was one of the biggest spills in history and affecting several coastlines, ecological regions, aquatic species, and birds [1]. Mineral-based oils with additives/impurities are harmful to aquatic lives due to their toxic and non-biodegradable nature resulting in loss of several billions of dollars for cleanup purposes [2]. Similar incidents have resulted in huge public and governmental interests for alternatives to mineral-based oil.

Bio-based oil is the best substitute for conventional mineral-based oil. Some forms of bio-based oil are also regarded as green energy. The majority of the existing research is more focused on the development of bio-based fuels such as bio-diesel and blends of bio-oils that have a positive impact on the availability and environmental aspects [3][4]. Another major product of fossil-based oil is lubricants that prevent contact between asperities by forming a thin film or layer. Without adequate lubricants, the contact between two surfaces could lead to severe wear and eventually to catastrophic failure [5].

A lubricant acts as a protective layer for the longevity of the surfaces, transfers heat during operation, and reduces friction. A lubricant depends on the properties of the oil, and viscosity is a very important property that allows a bearing to operate in the hydrodynamic lubrication regime [6]. Viscosity is directly influenced by the intermolecular forces of the lubricant which at higher speed creates separation between surfaces and at low speed allows contact between surfaces. Therefore, lubricants are very important in everyday life and with an increase in environmental concern, research is conducted to use vegetable oils as base stocks for lubricants [7].

The boundary lubrication regime is a condition where there is solid contact between the surfaces and a formation of a low shear strength protective layer on the surface. In this condition,

the reduction of friction is limited as compared to that of hydrodynamic lubrication due to the formation of the boundary layers on the contact asperities [8]. The boundary lubrication film formation occurs due to two mechanisms: physisorption and chemisorption. In physisorption, active molecules align normally on the contacting surface to form a protective layer. In chemisorption, active chemical groups react with the surface to form a tribo-surface and produce a boundary layer [9].

Vegetable oils are getting more attention as base oils than conventional mineral oils because of their biodegradability and renewability aspects. The interest in the vegetable based oil is due to the comparable chemical and physical properties of synthetic esters and mineral base oils. Ting and Chen [10] studied the viscosity and working efficiency of soybean oil, epoxidized soybean oil (ESO), and hydrogenated soybean oil for use as base oils. The results showed that the epoxidized soybean oil had higher viscosity compared to original soybean oil whereas hydrogenated has a lower viscosity.

Castro et al. [11] studied the oxidation and wear properties of soybean oil, high-oleic soybean oil, and epoxidized soybean oil for base oil. Acceding to Castro et al. [11], high oleic soybean oil has good anti-wear properties due to lower polyunsaturated fatty acid content (~5%) as compared to soybean oil (~60%), forming a more stable polymeric film, whereas the presence of oxirane rings in ESO could reduce the binding properties resulting in more wear [11]. However, ESO showed a lower COF due to the formation of a tribochemical reaction on the surface as ESO could form polyester/polyether due to a tribopolymerization reaction.

Adhvaryu et al. [12] studied the tribological aspect of thermally and chemically modified soybean oils for environmentally friendly lubricants. The chemically modified soybean oil has greater wear protection than the thermally modified soybean oil, which was due to an increase in

the polar functionality group in the chemically modified soybean oil. Adding functionality groups helped for stronger adsorption potential on the metal surface with greater lateral interaction between ester chains.

Sharma et al. [13] explored the combination of antiwear and antioxidant additives to improve the oxidation behavior properties of soybean oil. The results showed that the combination of zinc dialkyldithiocarbamate antioxidant and antimony dithiocarbamates showed good results for improving both the antiwear and antioxidant properties of soybean oil. Lal and Carrick [14] conducted performance-based testing of mineral oil with high oleic vegetable oil for thermal and oxidative stability, viscosity, and low-temperature properties. High oleic vegetable oil had comparable properties to that of the mineral base with the addition of additives to improve the oxidative and thermal properties of vegetable oil, however, a wear analysis was not reported in the study.

Minami and Mistsume [15] studied the effect of phosphorous on the antiwear properties of vegetable oil and mineral base oil under boundary lubrication conditions. Additives were put into the mineral base oil, to improve the antiwear properties of vegetable oil, and wear reduction was dependent on the peroxide value of the base oil. The peroxide formation was mainly due to the autooxidation mechanism of the vegetable oil that was observed at room temperature.

Kraipat [16] studied the wear properties of different soybean oils using a four-ball wear tester and found that temperature, speed, and ZDDP additives have a significant effect on wear scar diameters. Wear scar diameter for epoxidized soybean oil and high oleic soybean oil was affected by the temperature, whereas for conventional soybean oil, the interaction between speed and additive played a significant role [16]. Adamczewska and Wilson [17] found less wear in a

pump test for a combination of vegetable oil and additives to that of mineral oils. This test was particularly focused on lubricants for farm tractors.

Clearly, some research has been conducted to study the friction and antiwear properties of vegetable-based oil as compared to the mineral base oil, but more is needed. High oleic content in oil has good friction and wear properties, however, a comparative study of vegetable-based oil with different oleic content without any inherent chemistries to that of mineral oil with inherent chemistries would help to provide vital information for further research on vegetable-based lubricants. This paper focuses on the comparative study of the vegetable-based oils (particularly high oleic content) and compares the friction and wear results with inherent chemistries on a mineral base. The chemical properties are analyzed to determine the functional groups and their effect on friction and wear properties. The results will help to determine the potential of vegetable-based oil lubricant as an alternative to conventional mineral-based oil.

Table 3.1: Oil sample and supplier name

Sample	**Trade Name**	**Composition**	**Supplier**
Oil A	Conventional Soybean oil	23% oleic acid	Zeeland Farm Services Inc. (Zeeland, MI)
Oil B	High Oleic Canola	80% oleic acid	DowDuPont (Wilmington, DE)
Oil C	Plenish	75% oleic acid	DowDuPont (Wilmington, DE)
Oil D	Vistive	70% oleic acid	Zeeland Farm Services Inc. (Zeeland, MI)
ISO 68	Paraflex HT	Base oil	Petro-Cananda Lubricants Inc. (Calgary, Canada)
Add	Additives	Mixture of chemicals	The Lubrizol Corporation (Wickliffe, OH)

3.2 Materials and Methods

3.2.1 Materials

Four bio-based oils with different compositions, a mineral base oil, and gear oil additives were obtained from various industries which can be found in Table 3.1. The disk samples were AISI 1018 steel with a surface roughness (R_a) of 0.5 micrometers and were machined to size. The resulting disks were 7 mm thick with a diameter of 69.9 mm as shown in Figure 1. A typical gear oil concentrate was used as an additive. Balls of 10mm high steel (Cr25) were used to conduct the ball on disk experiments with a Rockwell C hardness between 60 and 67. Dual laser infrared thermal temperature sensors were used to measure the temperature of the oil samples. A 120 V 600W lamp was used to supply heat which was controlled by a PCM solid state temperature controller via a thermocouple. Viscosity was determined using a rheometer for the temperature range of 25-100^{o}C using a sample size of 2ml. The functional groups of bio-oils were investigated using Fourier Transform Infrared (FTIR) spectroscopy. The samples were analyzed for 32 scans, between 4000 to 700 cm $^{-1}$ at a resolution of 4 cm $^{-1}$.

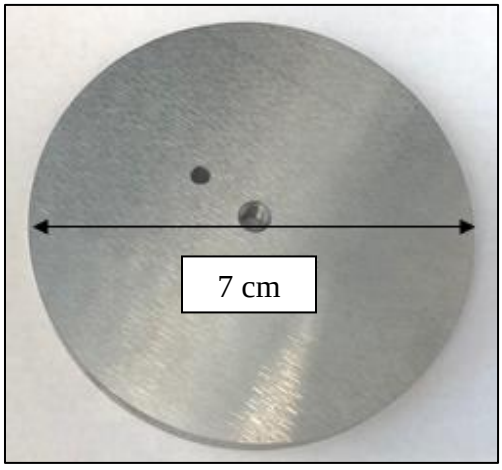

Figure 3.2: Picture of 1018 steel disk sample

3.2.2 Friction tests

A ball-on disk friction and wear test was performed using a tribometer. Approximately 17 ml of oil was poured on the holder to completely submerge the disk sample. The oil temperature was maintained at 90^{o}C using a heating lamp and a temperature controller with a thermocouple placed above the holder. The temperature was constantly being monitored using a dual laser infrared thermal temperature sensor and thermocouple. A load of 50N was applied to the ball against the disk at a radial distance of 16mm from the center. The total duration of the experiment was approximately 50 min which included applying the load, - at fourteen different speeds (0.0016, 0.00335, 0.0084, 0.0168, 0.0335, 0.084, 0.134, 0.167, 0.251, 0.335, 0.42, 0.502, 0.586, and 0.67) m/s and removing the load. Figure 2 is the schematic of the experiment and Figure 3 is a sample disk after the experiment with a Cr steel ball. The balls and disks were cleaned using a sequence of acetone and methanol before and after the experiment to avoid surface contaminants. Each condition was performed in triplicate in a random order to lower the possibility of bias due to unknown external influences. The data obtained from the test includes COF and velocity in a tabular format.

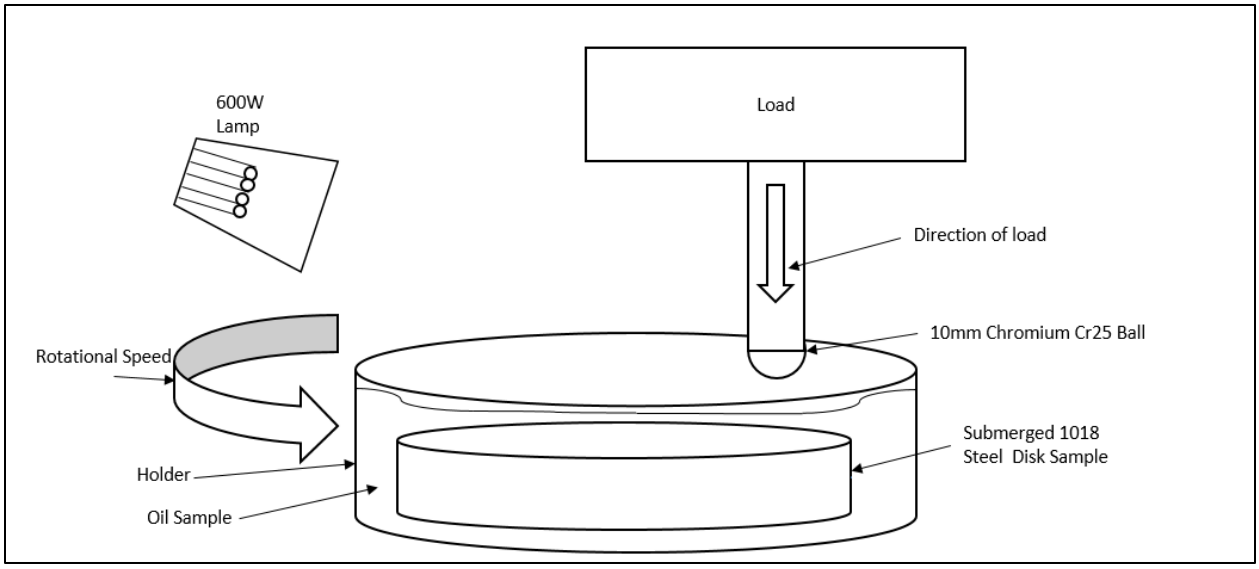

Figure 3.3: Schematic of a ball-on disk experiment

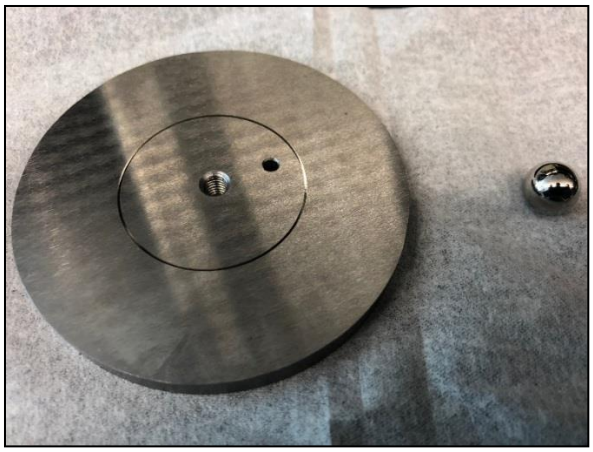

Figure 3.4: Sample disk and ball after test

3.2.3 Wear analysis methodology

Figure 3.5 represents the typical profile of the worn surface. A surface profilometer with a stylus of radius 12.5 µm, a force of 3 mg, was used to measure the profile of the worn surface. It was used to measure over a length of 8000 µm with a lateral resolution of 1.5 µm, and a vertical resolution of approximately 1 nm. The unworn portion of the profile was first extracted from the raw data to fit the linear line and was subsequently plotted on the worn surface to calculate the

wear groove cross-sectional area. Each specimen was scanned three times at different angles, all perpendicular to the groove, to check the variation in the results. The average wear cross-sectional area was calculated to evaluate the wear.

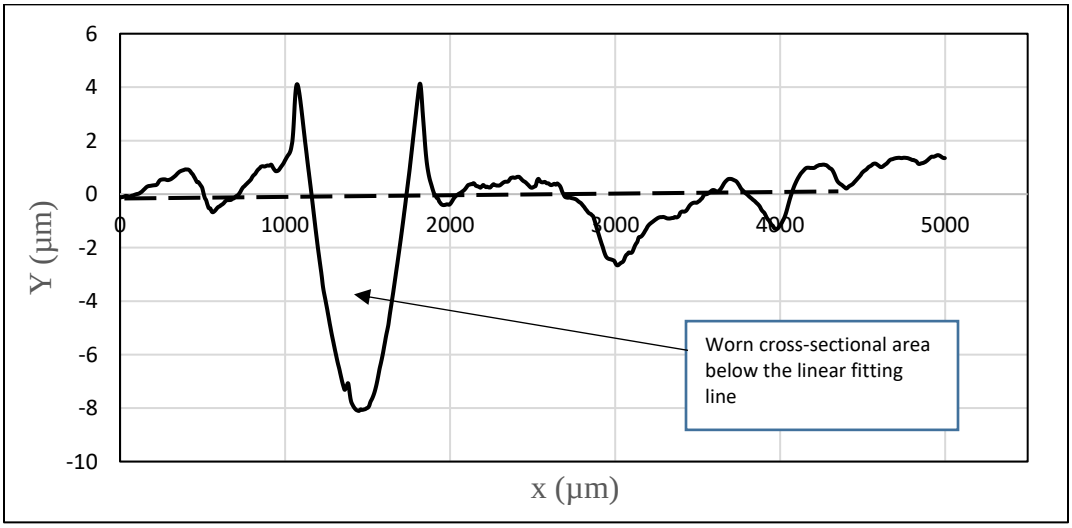

Figure 3.5: Typical profile of worn surface (Oil B – 50 N)

3.3 Results and Discussion

3.3.1 Effect of temperature on viscosity

Figure 3.5 shows the effect of temperature on viscosity from room temperature of 25^{o}C to 100^{o}C. ISO 68 has a high viscosity of around 0.16 Pa·s at room temperature but reduces to 0.036 Pa·s at 100^{o}C. Most of the trends show that the viscosity of oil reduces with an increase in temperature which is similar to results obtained by Fasina et al. [18]. However, there is an increase in viscosity of oil A as the temperature is increased from 90^{o}C to 100^{o}C which may be due to a polymerization reaction. Oil A had a higher polymerization rate due to lower oleic content as compared to Oil C and Oil D. Ting and Chen [10] had a similar result for conventional soybean oil, however, their graph was limited to 80^{o}C. With an increase in temperature, volatile components in the vegetable

oils also get vaporized which was observed in a study conducted by Castro et al. [11]. At a higher temperature of 175°C to 200°C higher molecular weight products were formed for conventional soybean oil which reduced the viscosity of the oil [11]. The volatile products (peroxides, alcohols, aldehydes, and other lower molecular weight compounds) formed during oxidation are vaporized due to a higher temperature and oxidation rate.

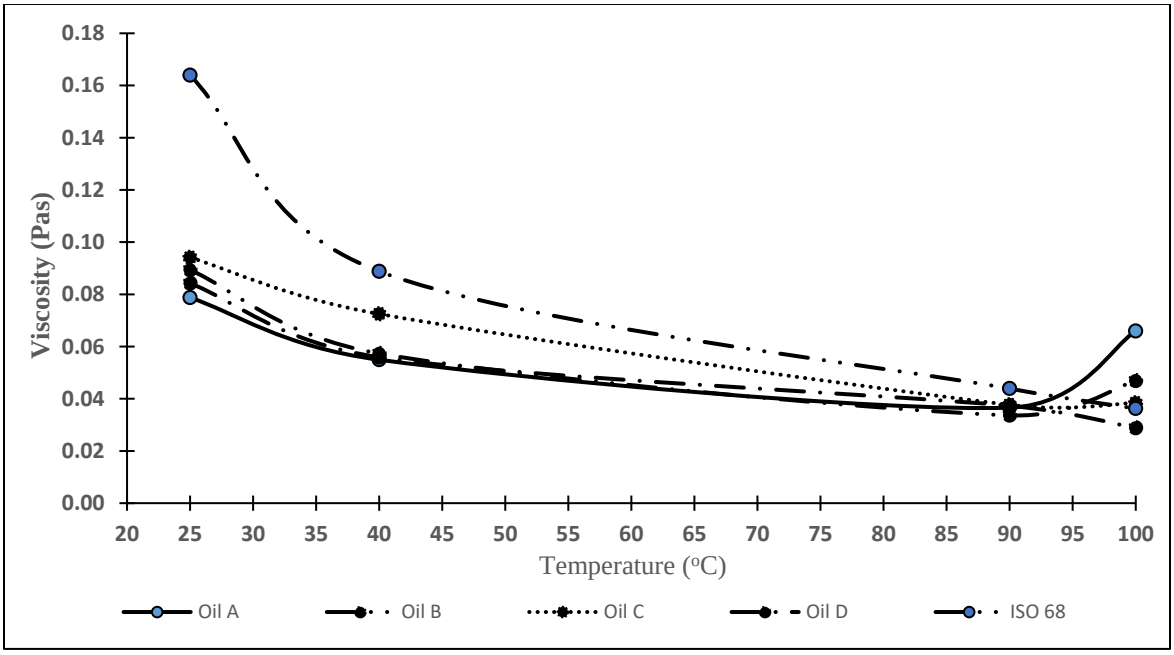

Figure 3.6: Measured viscosity as a function of temperature

3.3.2 Analysis of wear

Figure 3.6 shows the wear area analysis from the profilometer scans for all the experimental parameters after the conclusion of each test through all the speed ranges. At low speed, the metal surfaces are in contact resulting in higher wear. At a higher speed, a lubricating film is formed that could partially separate two surfaces. The fluid is pressurized at a higher speed to carry the applied load due to the elasto-hydrodynamic lift mechanism. However, according to established elasto-hydrodynamic models, the film is not theoretically enough to completely separate the surfaces (See

Appendix A). Due to this and wear occurring during all of the tests the investigators believe that the tested contact is always in the boundary lubrication regime, and dominated by solid contact. The effect of anti-wear additives is seen on ISO 68 base oil as the additives can form a coat of a protective layer on the metal surface by physisorption and adsorption mechanisms. The inclusion of additives at a higher percentage helps to reduce the wear that is observed in the boundary lubrication regime by creating a protective film between the surfaces. Wear rate is also influenced by the molecular structure of the oil that helps to determine either the physically or chemically adsorbed layers of the lubricants.

Polyunsaturated fatty acids (PUFA) are mostly found in vegetable oil and Oil A has a higher PUFA content (~60%) which is not ideal for lubrication [11]. The polyunsaturated fatty acids makes oil comparatively unstable due to oxidation agents (i.e low oxidative stability). Therefore the lower the PUFA, the better the oxidative stability of the vegetable oils. Oxidation degradation of the oils will reduce their lubricating properties. Fox et al. [19] also observed that the increase in the level of unsaturation in the fatty acid has a negative influence in the boundary lubrication regime. High oleic soybean oil has better wear properties due to a stable polymeric film and lower PUFA content (5%) compared to conventional soybean oil [11]. The wear result of Oil C was comparable to ISO 68 oil with a 0.25% conventional gear additive (add) concentration. Linoleic acid ($C_{18:2}$) which is the predominant n-6 polyunsaturated fatty acid (PUFA) is usually higher in Oil D and Oil B[20]. The reason for Oil D and Oil B to have higher wear could be because of higher concentration of PUFA [11][20]. Note that the recommended concentration of gear oil additive is 0.25-10% depending on the nature of the work such as for worm gears (3-10%) or spiral gears (1%)[21][22]. This demonstrates how the high oleic oils with low PUFA have better inherent

tribological properties than ISO 68 with some additives. This result suggests that high oleic bio-derived oils require less additives to reach the adequate performance achieved by mineral oils.

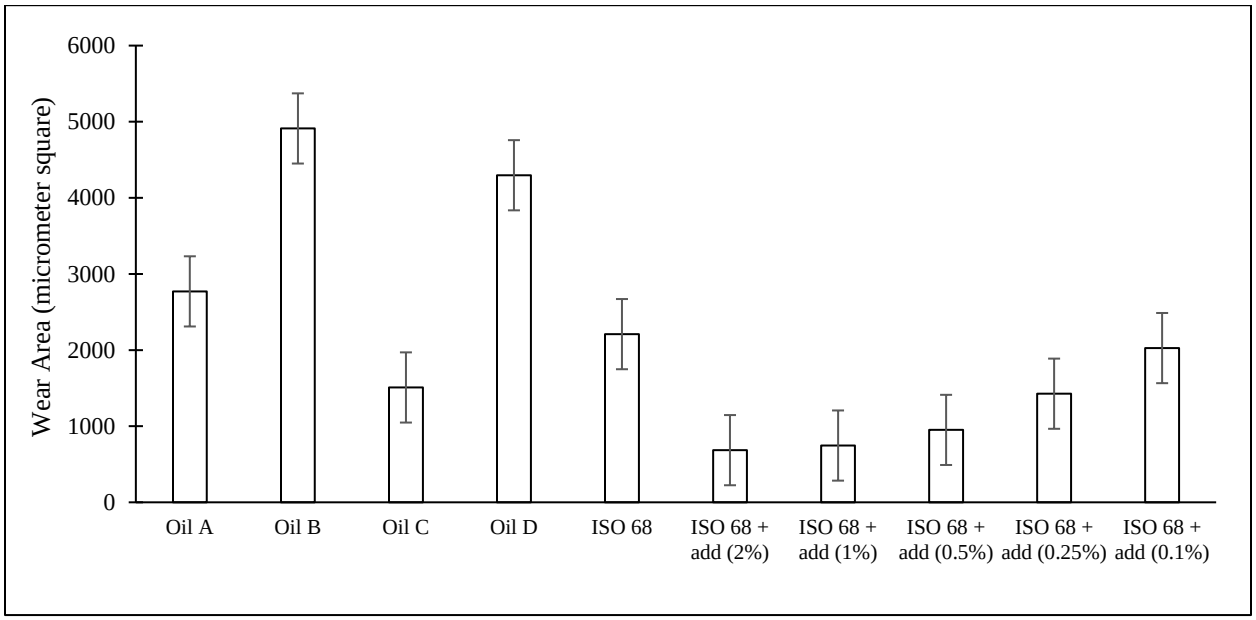

Figure 3.7: Wear area for all the experimental parameters

3.3.3 Functional groups of oil

The functional groups of the oil play a vital role in the friction and wear properties of the oil. Figure 3.7 (a) exhibits the Fourier-transform infrared spectroscopy (FTIR) of the oils without any additives. There are peaks across several wavenumber ranges 400-700 cm^{-1} as shown in Figure 3.7 (b), 1000-1700 cm^{-1} in Figure 3.7 (c), and 2800-3000 cm^{-1} in Figure 3.7 (d). Table 3.2 provides the functional group information based on wavenumber.

The region between 400-700 cm^{-1} is very hard to interpret which is referred as the fingerprint region since there are many peaks and it is exceptionally difficult to interpret. The region from 1000 cm^{-1} and above can be interpreted and provides vital information about the functional groups of the oil. In the case of ISO 68 base oil, there are peaks between 2912-2930 cm^{-1} of C-H stretching that represent a strong long-chain alkane group. There were peaks in this range

for each oil particularly between 2840-3000 cm^{-1} that represented the C-H bond stretching in each oil. The peaks observed between 2695-2800 cm^{-1} for Oil D and Oil C were C-H stretching that represented aldehydes.

The peaks between 1700-1720 cm^{-1} represented C=O stretching functional groups for acids and ketones. The C=O are saturated and thus stable that helps to form a film layer during boundary lubrication which was also observed by Castro et al.[11]. The peaks at 1425 and 1437 cm^{-1} represented the O-H stretching groups that were present in Oil B and Oil A. The peaks near 1717 cm^{-1} represented C=O stretching ketonic groups in both Oil B and Oil A that were observed by Adhvaryu et al. [2]. Oil C also included the presence of a sharp peak at 1447 cm^{-1} between 1457-1461 cm^{-1} represented CH_3 stretching, and medium peaks between 1462-1467 cm^{-1} represented C-H stretching.

Table 3.2: Wavenumber and functional groups

Wavenumber (cm^{-1})	**Functional Group**
400-700	Fingerprint Region
1425 and 1437	Hydroxyl
1457-1461	Alkyl group
1462-1467	C-H
1700-1720	Acids and Ketons
2695-2800	Aldehydes
2840-3000	C-H Bond
2912-2930	Long-Chain Alkane group

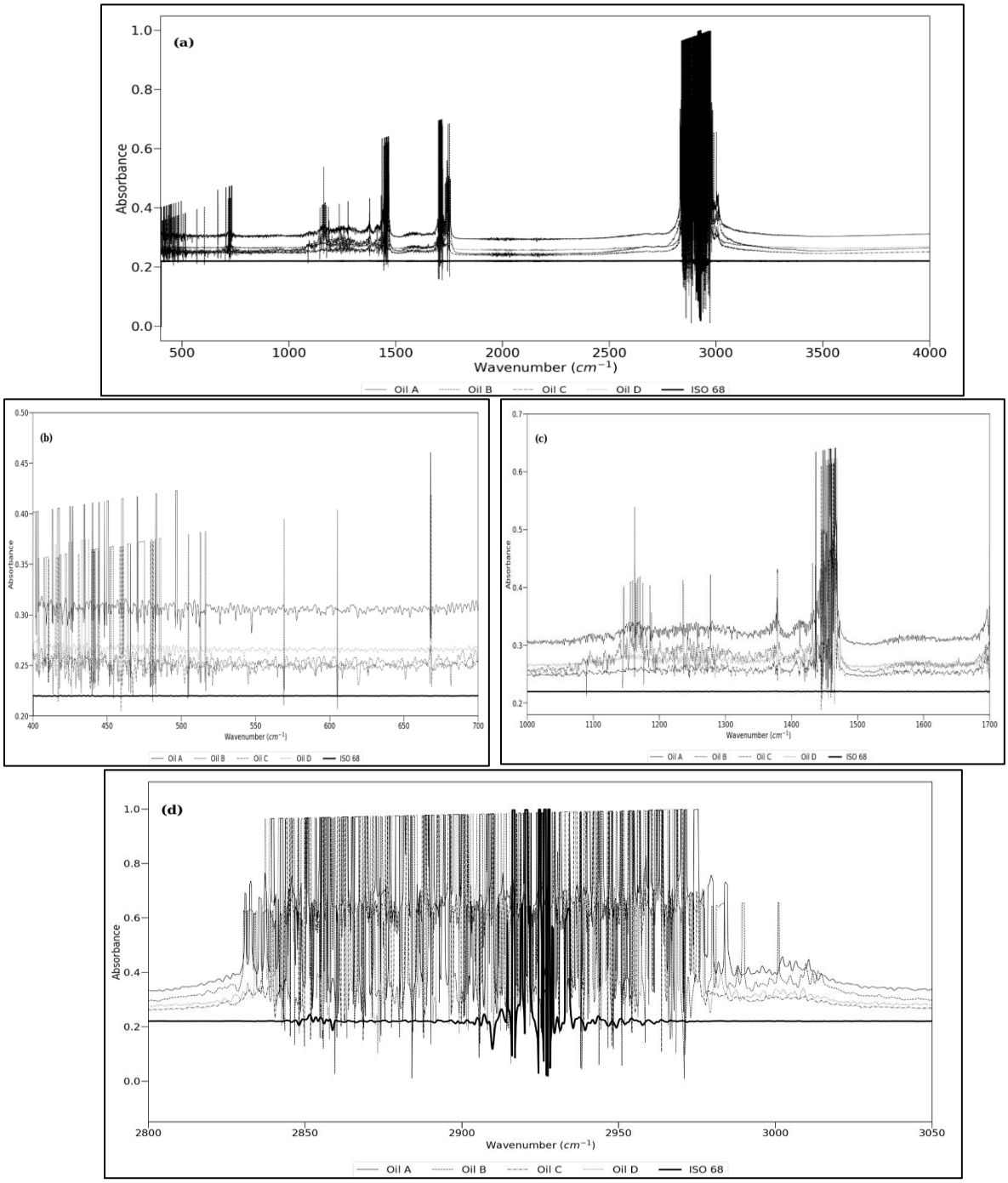

Figure 3.7: a) Overall view of FTI; b) FTIR for 400-700; c) FTIR analysis for wavelength between 1000-1700; and d) FTIR for wavelength between 2800 to 3500

3.3.4 Stribeck curve

The well-known Stribeck curve helps to describe the relationship between the COF, sliding speed, load, and viscosity in a lubricated contact [23]. The Hersey number is the dimensionless number obtained from the velocity (m/s) times the dynamic viscosity (Pa·s = N·s/m2), divided by the load per unit length of bearing (N/m) which is defined in Appendix A. As shown in Figure 3.8, the results plotted using the Stribeck curve show the transition of the COF from low to high speed. Plotting the results in this way helps to account for the differences in viscosity between the lubricants. The COF of Oils A, B, C, and D are lower than the ISO 68 at lower speed and continued in a similar pattern in the higher speed.

Elastohydrodynamic lubrication was used to calculate the minimum film thickness and λ (ratio between the film thickness and surface roughness) using a model by Chittenden et al. [24]. Details about calculation regarding λ is present in Appendix B. The λ for all the conditions were less than 0.1 that typically signifies boundary lubrication regime.

Vegetable oil contains polar functional groups (such as fatty acids) that are attracted to the metal surface and also due to reaction with the surface mainly by the presence of oxygen [25]. The effect of additives on ISO 68 could be seen in Fig. 8 at higher speeds. The COF of ISO 68 at high speed was 0.126, which was reduced with the inclusion of additives. Reyes and Neville [26] observed similar results when base oils were added with ZDDP, ZDDP plus the addition of Ca-sulphonate detergent, and MoDTP (Molybdenum Dithiophosphate). This reduction in COF indicates the effect of additives in the ISO 68. However, the additives never reduced the friction of the ISO 68 mineral oil to the friction range of the considered bio-oils, which suggests that they have inherently superior friction performance properties.

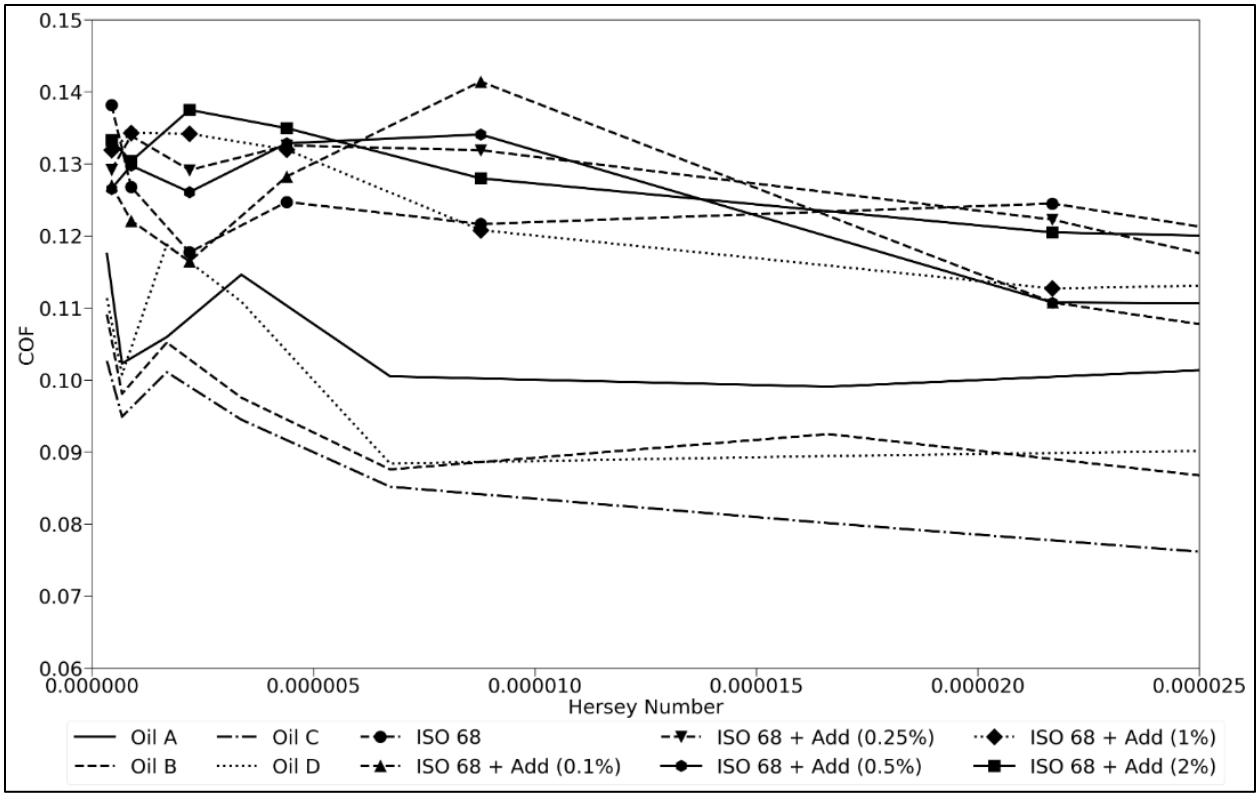

Figure 3.8: Stribeck Curve of the oil

3.3.5 Optical image of the surface

Optical images of the worn surfaces shown in Figure 3.9 help to diagnose the wear mechanism under different lubricating conditions during the ball on disk tests. The plowing line in Fig. 3.9 (a, b, c, and d) indicates the abrasive wear mechanism whereas the smearing surface indicates an adhesive wear mechanism. The dominant mechanism for wear in all the cases appears to be due to abrasive wear with some adhesion, that is similar for lubricated conditions as observed in a previous study [5]. The wear surface is mainly due to two-body abrasion where surface asperities are directly in contact with the boundary lubrication regime. The difference in hardness number between the ball and surface allowed the formation of abrasive grooves on the surface as observed in the images. The wear mechanism could have expanded from two-body to three-body abrasion

as the debris could have squeezed in between the ball and disk surface. The presence of smearing wear could be because of some adhesive wear still occurring. The volatile fraction of the Oil C and Oil D might have evaporated at around 90^{o}C, resulting in a decrease in the lubricant film thickness, causing the surfaces to come closer together. Castro et al. [11] observed a higher evaporation rate of high oleic soybean oil when the temperature was elevated due to the formation of volatile products that occurred via scission alpha to the hydroperoxide group. Film thickness is directly related to wear surface types which were also observed by Shahabuddin et al. [27]. Wear would have also been influenced by the protective tribo-films of fatty acids formed from the high oleic bio-oils. ISO 68 is more resistant to temperature so asperity contact causes the wear to mainly be by abrasion.

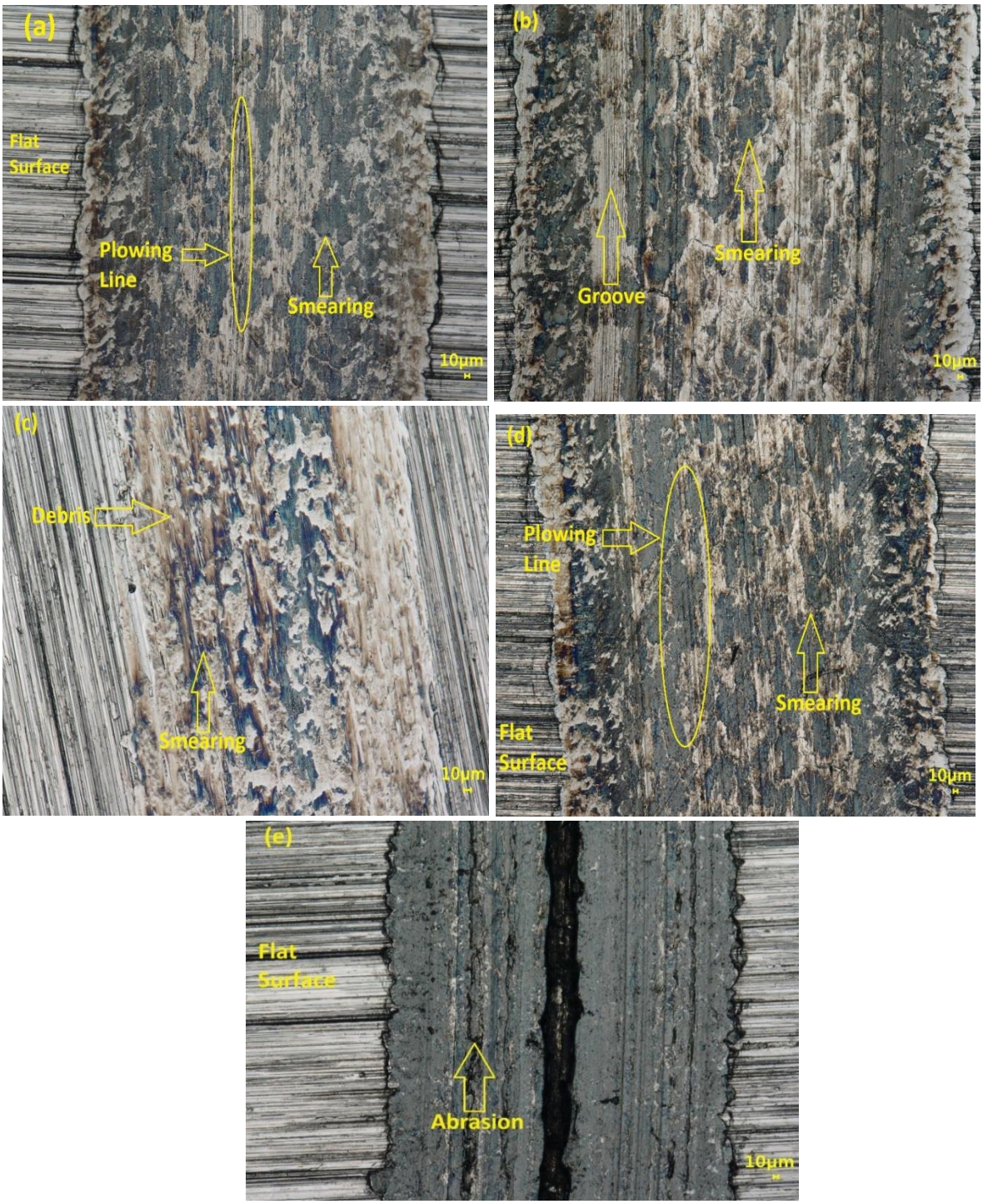

Figure 3.9: Surface profile from Optical Microscope: (a) Oil A, (b) Oil B, (c) Oil C, (d) Oil D, and (e) ISO 68

3.4 Conclusion

This study investigated the preliminary aspect of using vegetable oils without any additives as an alternative to the conventional mineral base oil with and without additives. The results obtained from the chemical and tribometer tests were used to evaluate the friction and wear properties of the oil. The following conclusions can be drawn based on the experimental results and observations:

1. The viscosity properties of the various bio-derived oils were comparable to the standard base oil at a temperature of around 90^{o}C. Oil A viscosity increased as the temperature at around 100^{o}C that could be the result of the deposition of the heavier molecular fraction of the oil. Oil C and Oil D had lower viscosity than mineral base even at 100^{o}C.
2. Oil C possesses lower wear than any other base oil as observed from the wear analysis. The Oil C wear area was comparable to mineral oil with 0.25% of additives that demonstrate the potential of the renewable source as a base lubricant that may not require as many additives as mineral oils.
3. Functional groups of the Oil B, C, and D mainly consisted of C=O stretching functional group from oleic acid content, which helped to attract with the metal surface to form a film layer during boundary lubrication.
4. All the considered bio-derived oils have a lower COF as compared to mineral oil at the boundary, mixed and hydrodynamic lubrication regimes. The presence of oxygenates in the vegetable oil reacts with the surface and improves the lubricity of the oil.
5. The abrasive wear mechanism was observed from the optical microscope images that also included the debris from the surface. The clear abrasive grooves could be seen on the

surface and Oil C had the lower wear volume, possibly due to the presence of higher oleic and lower PUFA content.

Acknowledgment

The author wishes to acknowledge Zeeland Farm Services, Inc, (Zeeland, MI), DowDuoPont (Wilmington, DE), The Lubrizol Corporation (Wickliffe, OH), and Petro-Canada Lubricants Inc. (Calgary, Canada) for their generous supply of the oils. The author would also like to thank United Soybean Board for funding this research. The author also wishes to acknowledge Dr. Rakish Shrestha, Dr. Swarna Saha, Dr. Rajdeep Shakya, and Sanjita Wasti for their help and guidance during the study.

3.5 References

[1] R. de la Huz, M. Lastra, J. Junoy, C. Castellanos, and J. M. Viéitez, "Biological impacts of oil pollution and cleaning in the intertidal zone of exposed sandy beaches: Preliminary study of the 'Prestige' oil spill," *Estuar. Coast. Shelf Sci.*, vol. 65, no. 1, pp. 19–29, 2005.

[2] A. Adhvaryu and S. Z. Erhan, "Epoxidized soybean oil as a potential source of high-temperature lubricants," *Ind. Crops Prod.*, vol. 15, no. 3, pp. 247–254, 2002.

[3] R. Shakya *et al.*, "Influence of biochemical composition during hydrothermal liquefaction of algae on product yields and fuel properties," *Bioresour. Technol.*, vol. 243, pp. 1112–1120, Nov. 2017.

[4] S. Thangalazhy-Gopakumar *et al.*, "Physiochemical properties of bio-oil produced at various temperatures from pine wood using an auger reactor," *Bioresour. Technol.*, vol. 101, no. 21, pp. 8389–8395, 2010.

[5] S. KC, P. D. Nezhadfar, C. Phillips, M. S. Kennedy, N. Shamsaei, and R. L. Jackson, "Tribological behavior of 17–4 PH stainless steel fabricated by traditional manufacturing and laser-based additive manufacturing methods," *Wear*, vol. 440–441, p. 203100, 2019.

[6] R. Jackson and J. Lei, "Hydrodynamically Lubricated and Grooved Biomimetic Self-Adapting Surfaces," *J. Funct. Biomater.*, vol. 5, no. 2, pp. 78–98, 2014.

[7] Y. Singh, A. Farooq, A. Raza, M. A. Mahmood, and S. Jain, "Sustainability of a non-edible vegetable oil based bio-lubricant for automotive applications: A review," *Process Saf. Environ. Prot.*, vol. 111, pp. 701–713, 2017.

[8] H. A. Spikes, "Boundary Lubrication and Boundary Films," in *Thin Films in Tribology*, vol. 25, D. Dowson, C. M. Taylor, T. H. C. Childs, M. Godet, and G. Dalmaz, Eds. Elsevier, 1993, pp. 331–346.

[9] H. Hirani, *Fundamentals of Engineering Tribology with Applications*. 2016.

[10] "Viscosity-and-working-efficiency-analysis-of-soybean-oil-based-bio-lubricants-_-Elsevier-Enhanced-Reader.pdf." .

[11] W. Castro, J. M. Perez, S. Z. Erhan, and F. Caputo, "A Study of the Oxidation and Wear Properties of Vegetable Oils : Soybean Oil Without Additives," no. 1, 2006.

[12] A. Adhvaryu, S. Z. Erhan, and J. M. Perez, "Tribological studies of thermally and chemically modified vegetable oils for use as environmentally friendly lubricants," *Wear*, vol. 257, no. 3–4, pp. 359–367, 2004.

[13] B. K. Sharma, J. M. Perez, and S. Z. Erhan, "Soybean oil-based lubricants: A search for synergistic antioxidants," *Energy and Fuels*, vol. 21, no. 4, pp. 2408–2414, 2007.

[14] K. Lal and V. Carrick, "Performance testing of lubricants based on high oleic vegetable oils," *J. Synth. Lubr.*, vol. 11, no. 3, pp. 189–206, 1994.

[15] I. Minami and S. Mitsumune, "Antiwear Properties of Phosphorous-Containing Compounds in Vegetable Oils," *Tribol. Lett.*, vol. 13, no. 2, pp. 95–101, 2002.

[16] K. Cheenkachorn, "A Study of Wear Properties of Different Soybean Oils," *Energy Procedia*, vol. 42, pp. 633–639, 2013.

[17] J. Z. Adamczewska and D. Wilson, "Development of ecologically responsive lubricants," *J. Synth. Lubr.*, vol. 14, no. 2, pp. 129–142, Jul. 1997.

[18] O. O. Fasina, H. Hallman, M. Craig-Schmidt, and C. Clements, "Predicting temperature-dependence viscosity of vegetable oils from fatty acid composition," *JAOCS, J. Am. Oil Chem. Soc.*, vol. 83, no. 10, pp. 899–903, 2006.

[19] N. J. Fox, B. Tyrer, and G. W. Stachowiak, "Boundary lubrication performance of free fatty acids in sunflower oil," *Tribol. Lett.*, vol. 16, no. 4, pp. 275–281, 2004.

[20] R. Seemamahannop, K. Bilyeu, Y. He, S. Kapila, V. Tumiatti, and M. Pompili, “Assessment of oxidative stability and physical properties of high oleic natural esters,” in *Proceedings - IEEE International Conference on Dielectric Liquids*, 2019.

[21] Anon, “Lubricant additives,” *Ind. Lubr. Tribol.*, 1973.

[22] Y. Su, L. Gong, and D. Chen, “An investigation on tribological properties and lubrication mechanism of graphite nanoparticles as vegetable based oil additive,” *J. Nanomater.*, 2015.

[23] P. L. Menezes, S. P. Ingole, M. Nosonovsky, S. V. Kailas, and M. R. Lovell, *Tribology for scientists and engineers: From basics to advanced concepts*, vol. 9781461419457. 2013.

[24] R. J. Chittenden, D. Dowson, J. F. Dunn, and C. M. Taylor, “Theoretical Analysis of the Isothermal Elastohydrodynamic Lubrication of Concentrated Contacts. I. Direction of Lubricant Entrainment Coincident with the Major Axis of the Hertzian Contact Ellipse.,” *Proc. R. Soc. London, Ser. A Math. Phys. Sci.*, vol. 397, no. 1813, 1985.

[25] J. C. J. Bart, E. Gucciardi, and S. Cavallaro, “2 - Principles of lubrication,” in *Woodhead Publishing Series in Energy*, J. C. J. Bart, E. Gucciardi, and S. B. T.-B. Cavallaro, Eds. Woodhead Publishing, 2013, pp. 10–23.

[26] M. Reyes and A. Neville, “The effect of anti-wear additives, detergents and friction modifiers in boundary lubrication of traditional Fe-base materials,” in *Tribology Series*, 2003.

[27] M. Shahabuddin, H. H. Masjuki, M. A. Kalam, M. M. K. Bhuiya, and H. Mehat, “Comparative tribological investigation of bio-lubricant formulated from a non-edible oil source (Jatropha oil),” *Ind. Crops Prod.*, vol. 47, pp. 323–330, 2013.

Chapter 4: Friction and wear properties of biomass-derived oils via thermochemical conversion processes

Abstract

Tribological properties of biomass-derived oils (bio-oils) were experimentally investigated, and the properties were compared with that of standard mineral oils used for lubrication purposes. Bio-oils were obtained from fast pyrolysis (using poultry and pine), gasification ("gasitar" using pine) and hydrothermal liquefaction processes (using *Scenedesmus* and *Nannocholoropsis*). The friction and wear tests were conducted using a ball on the disk tribometer test. The results showed that COF were around 0.02 for both gasitar and *Scenedesmus* bio-oil; whereas, catalytic and non-catalytic pyrolysis oils had around 0.1. The wear measurements showed that catalytic fast pyrolysis bio-oils had lower wear followed by non-catalytic bio-oil and "gasitar". *Nannocholoropsis* bio-oil had the highest amount of wear, and algal bio-oils showed higher wear compared to other oils. The bio-oil chemical analysis indicated that catalytic and non-catalytic fast pyrolysis bio-oil had higher oxygen content, while algal bio-oil had higher nitrogenates. Gasitar had higher hydrocarbon content with lower oxygen and nitrogenates making it a favorable lubricating oil.

**The work has been published in Biomass and Bioenergy, Volume 155, Dec 2021, 106269*

4.1 Introduction

According to the Energy Information Administration (EIA), the United States imported 41 thousand barrels of lubricants per day in 2017 [1], which depicts the size and importance of the lubrication industry. This trend is similar to the global lubrication market due to its widespread application in machinery such as weaving, drilling, milling, gears, and engines [2]. Lubricants are used to avoid direct contact to reduce friction and wear of sliding surfaces [3]. Commercial lubricants are formulated with a combination of mineral base oil (~75-80 wt.%) and additives. Up to 75-90 wt.% of most machinery lubricating oils are directly derived from petroleum refineries, mostly long-chain hydrocarbons (up to C_{50}), and the reserves are depleting rapidly [4]. Also, the continuous use of petroleum-based sources exacerbates environmental issues and climate change phenomena. Therefore, there is a shift towards alternative sources that is sustainable and still meet the need of the lubrication market. Research has been conducted to produce sustainable bio-based lubricants that could meet the requirements of existing industries [2], [4].

Bio-based lubricants are often produced from oil-seed crops such as soybean, canola, sunflower, and olive (referred to as first-generation biomass). Oils produced from first-generation biomass have been studied to replace petroleum-based mineral oil as they exhibit properties such as high viscosity index, low volatility and good lubricity [1], [2], [4]–[6]. However, these biomasses are primarily used as food and would create an ethical dilemma of food vs lubricants. Studies have been also focused on utilizing oils that were produced from non-food crops such as Jatropha. Sripada et al. (2013) carried out model compound studies on bio-lubricant production from methyl oleate and canola biodiesel by transesterification (at 80°-140°C) with trimethylolpropane (TMP), using sodium methoxide as the catalyst [7]. Kulkarni et al. [8] tried to take advantage of epoxidation (at 70°C) of double bonds under acidic conditions followed by acid-

catalyzed ring-opening with 2-ethylhexanol (at 120°C) to enhance the thermo-oxidative and cold-flow properties of mustard oil. Heikal et al. [9] utilized commercially available palm oil and Jatropha oil for the production of bio-lubricants, through two stages of transesterification. Shahabuddin et al. [10] , on the other hand, used Jatropha oil to compare the friction and wear properties. Their experiments included mixing bio-oil in different percentages (10-50%) with a mineral base lubricant and revealed that adding 10% bio-oil gave a better result. To date, all bio-lubricant studies that used oils (triglycerides) from both food and non-food oilseed crops were focused on either direct utilization of oils as lubricants or (trans)esterification of oils for lubricant production [4], [11]–[13].

Another sources that have been overlooked for the production of bio-lubricants are terrestrial and algal biomass. Bio-based oils produced from second and third-generation biomasses such as wood, eucalyptus, and algae can provide an alternative solution to the oils produced from first-generation oil seeds. There are several routes to convert these biomass sources to bio-oil, which could potentially be used as bio-lubricants. For example, Mahadevan et al.[14] used non-catalytic and catalytic fast pyrolysis to produce bio-oil from pine wood, while Shakya et al.[15] produced bio-oil from algae via hydrothermal liquefaction (HTL) process. Similarly, Nam et al. [16] utilized manure gasification and collected tar (referred as “gasitar”) as a bio-oil. Properties of these bio-oils depend not only on the source of biomass but also on the conversion processes. Shakya et al.[17] produced bio-oil via HTL from different species of algae such as *Nannochloropsis, Chlorella,* and *Pavlova*. The study found that the heating value, for example, of *Nannochloropsis* ranged between 35 and 37 MJ/kg. In another study, Pan et al. [18] found the heating value of bio-oil *Nannochloropsis* sp. via direct and catalytic pyrolysis was 24.4 and 32.2 MJ/kg, respectively. Although *Nannochloropsis* was used as a biomass in both processes, the variation in the heating

value was due to different conversion processes used. Bio-oils produced from HTL have different properties than the oils that were produced from pyrolysis. For example, the oil produced from HTL is highly viscous (40-67 cP) and also has lower oxygen content [17].

Most of the studies on pyrolysis and HTL have focused on biofuels production, and tar produced from gasification has been considered as waste and in fact, undesirable compounds since it causes problems in downstream processes. Nonetheless, only a handful of studies have looked into the tribological aspects of the bio-oils produced of lignocellulosic biomass as a stand-alone feedstock for the production of lubricants [19], [20]. Lu et al. [21] looked in the lubrication properties of diesel emulsified with fast pyrolysis bio-oil produced from rick husk at 10 wt%, 30 wt%, and 50 wt% along with different solid char. They observed that the bio-oil possessed better extreme-pressure, anti-wear and friction-reducing properties than commercial diesel oils. Oasmaa et al. [22] also tested bio-oil produced from fast pyrolysis with diesel using a four-ball wear test according to ASTM D2783. They observed that the wear was between 0.5 – 0.7 mm compared to 1.7mm for diesel fuel. Xu et al. [20] compared the tribological properties of bio-oil from pyrolysis, emulsified bio-oil, and diesel oil with the help of an engine cylinder piston ring tribotester and concluded that emulsified bio-oil performed better in terms of reducing wear. Varying load conditions (10-20 N) showed that the wear debris influences the wear rate by forming large clusters. In another study, Xu et al.[20] upgraded bio-oil (produced from microalgae-*Spirulina* sp.) using KF/Al $_2O_3$ and KF/HZSM-5 catalysts for studying friction and wear behaviors. The results showed that the KF/Al_2O_3 upgraded bio-oil showed better performance in terms of lubrication.

Previous studies have shown that bio-oils exhibited good lubricating properties. Table 4.1 presents the typical properties of bio-oil and different pathways. Standard minral base oil contains alkane group with long chains, unlike bio-oils which contains nitrogenates and oxygenates which

tends to increase the acidity and visocity. Bio-oil obtained from condensers have higher water content that results higher acidity and polymerizes with time. There are vaiations on how the bio-oil is obtained that results in variations in the tribological study. Most tribological research are focused on the bio-oil as biofuel and its tribological properties. However, a comparative study of bio-oils as lubricants produced from terrestrial and algal biomass for tribological properties is still lacking. Therefore, this paper focuses on the tribological properties of bio-oils as lubricants produced from pine and manure via fast pyrolysis, tar (referred to as "gasitar" throughout the manuscript) via gasification, and algae via HTL. Our goal is that this study will shed some light on what type of bio-oil has the potential to be used as a bio-lubricant.

Table 4.1: Comparison of typical properties of biomass and thermochemical pathways

Biomass	**Pathway**	**Viscosity (Pas)**	**HHV (MJ/kg)**	**Mositure Content (wt. %)**	**pH**	**C (wt. %)**	**H (wt. %)**	**N (wt. %)**	**O (wt. %)**	**Bio-oil derived**	**Ref**
Rice Husk	Pyrolysis	0.099	13.36	33.8	3.4	35.63	7	0	57.37	Condensers	[23]
Wheat Shell	Pyrolysis	-	6.02	84.4	6	69.9	9.7	11.5	8.8	Condensers	[24]
Poultry Fatty Wastes	Pyrolysis	4.630	40.33	0.7	2.9	63.25	11.26	1.03	23.64	Condensers	[25]
Swine Fatty Wastes	Pyrolysis	5.000	39.81	0.9	2.2	65.38	11.32	0.58	21.99	Condensers	[25]
Hardwood	Pyrolysis	0.012		31.8	2.4	55.5	6.7	0.1		Condensers	[26]
Bagasse	Pyrolysis	0.004	17.25	15	3.5	48.58	5.97	0.2	38.94	Condensers	[27]
Cotton Stalk	Pyrolysis	0.145		24.4	3.3	42.3	7.9	0.3	49.4	Condensers	[28]
Microalgae	Pyrolysis	0.100	29	-		61.52	8.5	9.79	20.19	Condensers	[29]
Spirulina	HTL	0.650	36.76	-		66.01	11.56	9.54	12.43	Reactor	[30]
Amphiroa fragilissima	HTL	0.002	23.25	-		66.2	4.2	0.7	28.6	Reactor	[31]
Amphiroa fragilissima	Pyrolysis	0.004	25.14	-		71.2	3.8	0.5	24.35	Condensers	[31]

Note: Viscosity (Absolute) was calculated by using density * kinematic viscosity for reported kinematic viscosity

4.2 Materials and Methods

4.2.1 Materials

Hybrid poplar biomass for non-catalytic and catalytic fast pyrolysis was obtained from Forest Concepts, LLC (Auburn, WA, USA). Poplar chips were processed through Crumble M24 rotary shear two times for uniform chip size. The samples were screened with a mesh pass 30+ (595 µm) and no pass mesh 60- (250 µm). Bio-oils produced from algae were from two different species, *Nannochloropsis* (obtained from Reed Mariculture Inc., CA, USA) and *Scenedesmus* (obtained from Arizona Center for Algae Technology and Innovation, Mesa, Arizona, USA). Poultry litter was collected from a local poultry farm (Auburn Alabama, USA). Pine residues (trees top) for a gasification process was obtained from a local forest at Auburn University (Auburn, AL, USA).

4.2.2 Pyrolysis and Gasification

Figure 4.1 presents a schematic of the fast pyrolysis and gasification process. The experimental setup consists of a hopper, a twin-screw auger, an injection screw, a fluidized bed reactor, a high-temperature filter (HTF), a pair of condensers, an electrostatic precipitator (ESP), and moisture absorbers. The fluidized bed reactor has a diameter of two inches (0.0508 m) and a freeboard diameter of 4 inches (0.1016 m). The overall height of the setup was 30 inches (0.762 m) with a freeboard of 6 inches (0.1524 m) high. Quartz sand (Macron, PA, USA) having a particle density of 2650 kg/m^3; bulk density of 1570 kg/m^3 and particle size of 150-300 µm, was used as the fluidizing bed material for fast pyrolysis and gasification experiments. For catalytic fast pyrolysis, marble small lump of calcium oxide (CaO) (Millipore, USA) was crushed and sieved to obtain particle sizes of 150-300 µm, similar to that of quartz sand. Around 300g of quartz sand (for gasification and non-catalytic fast pyrolysis) and the same amount of CaO (catalytic fast pyrolysis) were used for the experiments. For pyrolysis, the fluidized bed reactor was supplied with nitrogen

passing through multiple orifice distribution plates to purge out oxygen from the system at 15 l/min, which corresponds to a superficial velocity of 0.12 m/s and Reynold's number of 414 at NTP. For gasification, the air was passed through the orifice at 8-9 l/min. The temperature inside the reactor was maintained at 500^{o}C for pyrolysis and 850-900^{o}C for gasification by a set of electrical heaters. Char produced were collected from the bottom of the HTF, while its temperature was maintained at 350^{o}C by external heaters. Vapors and aerosols were passed through the pipe into the condenser train, which was maintained at 2^{o}C by circulating a water and ethylene glycol mixture using a chiller. The non-condensable gases then passed through an ESP with a 20 kV supply to the rod, where the oil phase is precipitated at the bottom of the ESP. Activated charcoal filters were used to absorb moisture from the gases, while a gas analyzer was used to track the composition of the gases. Bio-oils produced from catalytic and non-catalytic fast pyrolysis were collected from the bottom of the ESP for this study. Around 9 wt.% of bio-oil was obtained at the bottom of the ESP for fast pyrolysis process. Gasification was performed under constant operating conditions (~780^{o}C, equivalence ratio = ~ 0.32) with sand as bed materials. Gasitar samples were collected using acetone at the end of HTF during the gasification process. Acetone from the gasitar mixture was removed using an IKA rotary evaporator operated at 40^{o}C and 556 mbar of pressure. The amount of non-condensable gases produced were: H_2 (6.4 ± 0.19 Vol. %), CO (20.6 ± 1.07 Vol. %), CO_2 (14.8 ± 0.10 Vol. %), CH_4 (6.1 ± 0.18 Vol. %), C_2H_2 (0.054 ± 0.00 Vol. %), C_2H_4 (3.2 ± 0.015 Vol. %), and N_2 (48.9 Vol. %). The amount of gasitar produced was 10.1 g/kg dry biomass.

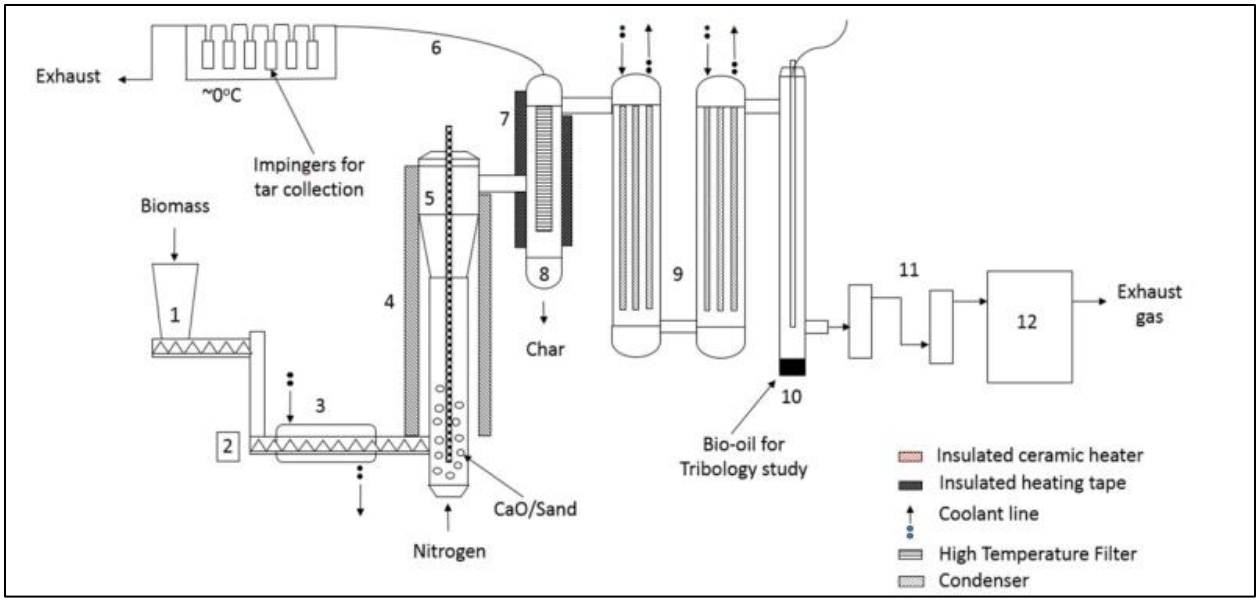

Figure 4.1: Schematic of bench-scale fluidized bed pyrolysis/gasification setup: 1, hopper; 2, injection screw; 3, heat exchanger; 4, pyrolysis/gasification heater; 5, reactor; 6, tar collector tube; 7, filter heater; 8, high temperature filter; 9, condensers; 10, electrostatic precipitator; 11, moisture absorbers; 12, gas analyzer for CO, CO_2, CH_4 and H_2

4.2.3 Hydrothermal liquefaction (HTL) of Algae

Hydrothermal liquefaction of algae was performed in a batch reactor of 1000 ml internal volume from Parr Instruments Inc (Moline, IL, USA). 15 wt.% dry algae and 85% of deionized water was mixed to make 100 g sample and added to the reactor. The reactor was purged with nitrogen gas (>99% purity, Airgas Inc., Charlotte, NC, USA) to create an inert atmosphere. The reactor was pressurized to 50 psi before heating to 320˚C for 30 min. After the experiment, the reactor was cooled, and the gases were discharged in the hood. Dichloromethane was used as the solvent for product separation and was removed at a later stage using a rotary evaporator at 60˚C and 720 mbar to obtain HTL bio-oil from algae.

4.2.4 Bio-oil Analysis

Bio-oils produced were analyzed for water content, total acid number (TAN), thermogravimetric analysis (TGA) and chemical composition. The functional groups of bio-oils were investigated using Fourier Transform Infrared (FTIR) spectroscopy. The samples were analyzed for 32 scans, between 4000 to 700 cm^{-1} at a resolution of 4 cm^{-1}, and the results obtained from FTIR were analyzed in Microsoft Excel. Water content analysis of the bio-oils was performed using a Karl Fischer titration method (Mettler Toledo V20). The titrant and solvent used for water content analysis were Combititrant 5 keto and Combisolvent keto (EMD Millipore), respectively. TGA was performed using PerkinElmer Pyris. Around 9.0 mg of sample was loaded in a 20 µl alumina crucible and heated from 25^{o}C to 600^{o}C, at a heating rate of 20^{o}C/min in the presence of nitrogen flowing at 20 mL/min. All experiments were performed in duplicates and statistical analysis of the data (ANOVA, Tukey's HSD) was performed to understand statistical difference of the obtained results. All the statistical analyses were performed at 95% confidence interval.

Chemical composition analysis of the bio-oils was performed using an Agilent 7890 GC/5975 MS equipped with a DB-1701 column (30 m × 0.25 mm, 25 µm). Each sample was made by diluting around 150 mg of bio-oils with 3 ml of methanol and 7 ml of dichloromethane. Ultrahigh-purity helium (99.999% Airgas Inc., Charlotte, NC, USA) was used as a carrier gas flowing at 1 ml/min. The initial temperature of the column was maintained at 50^{o}C for 2 min and the temperature was increased to 250^{o}C at a ramp rate of 3^{o}C/min. The chemical composition of the bio-oils was identified using the National Institute of Standards and Technology (NIST) mass spectral library. Total Acid Number (TAN) was measured using a Mettler Toledo T50 Titrator based on ASTM D664. The elemental analysis of the bio-oils was performed using a ‘Vario MICRO cube’ elemental analysis system (Elementar Americas Inc., New York, USA).

4.2.5 Tribological Tests

Bio-oils from pyrolysis and gasitar were first filtered through a 0.2 µm filter to remove char particles, while bio-oils from algae were already filtered before a rotary evaporation process to remove dichloromethane. The filtration system in this study was mainly focused to remove impurities on the product obtained from the thermo-chemical rather than purifying it into different composition levels. A ball on disk tribometer (Bruker/CETR UMT-3) test was employed to evaluate the tribological properties of the bio-oils. 1018 steel disks having a 2.75-inch diameter, 0.260-inch thickness with 0.5-micrometer average roughness were used for the test as shown in Figure 4.2. A 10 mm diameter 52100 high carbon chrome steel balls were used as a counterface. The disks were fixed in the holder and 2 ml of bio-oil was spread on the surface of the disk. A load of 50 N was applied for 30 min making a point contact while the disk was rotating at a speed of 63.7 rev/min. The COF data from the UMT-3 was directly obtained from the tribometer test in csv format.

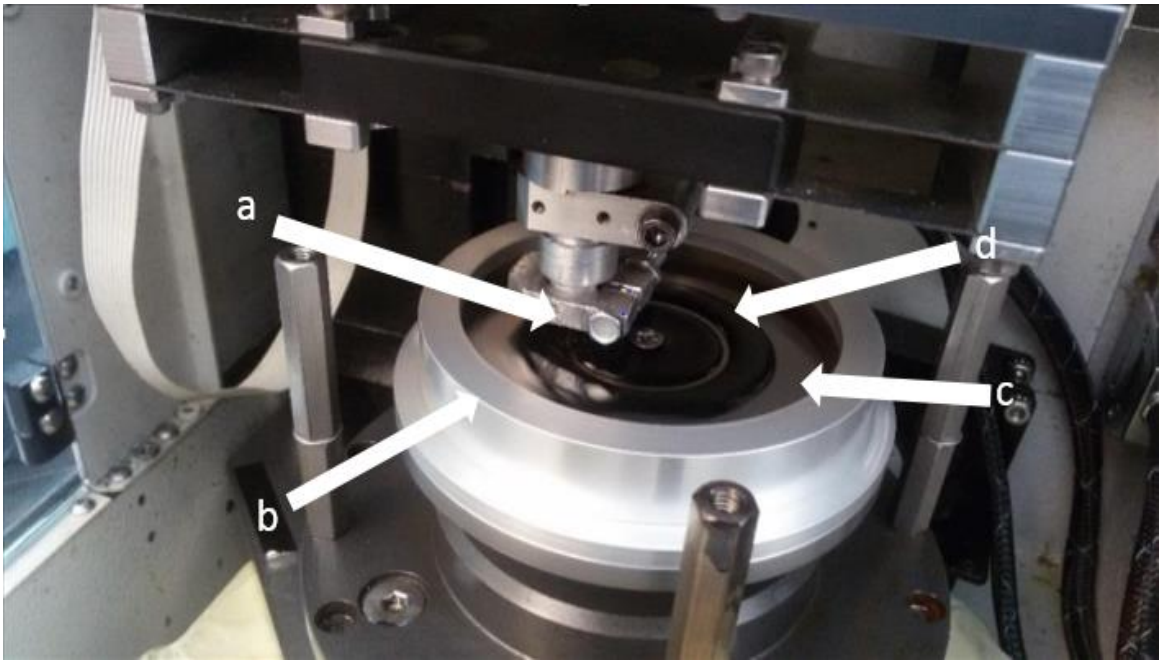

Figure 4.2: Ball on disk tribometer test (Bruker/CETR UMT-3): a) Ball holder, b) Disk holder, c) Sample disk, and d) Bio-oil sample (Catalytic pyrolysis bio-oil)

The wear grooves formed on the disk after the UMT tests were analyzed for the cross-sectional area by using a Veeco Dektak 150 stylus profilometer, shown in Figure 4.3. A stylus tip having a radius of 12.5 µm was passed perpendicularly across the wear groove with a force of 3.00 mg, where the length of the radial measurement was 4000.0 µm. The worn profiles were first removed and the remaining data were fitted with a line to characterize the height of the original surface. The linear line equation and wear groove data were plotted in MATLAB to calculate the cross-sectional area of the removed material.

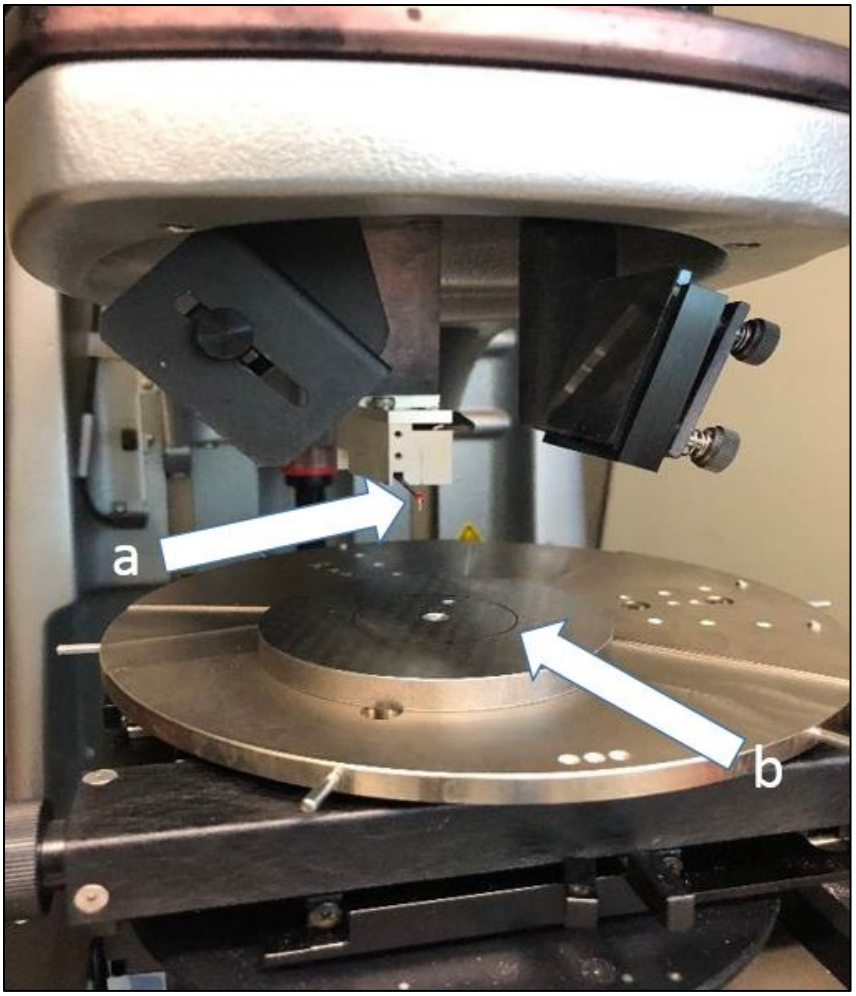

Figure 4.3: Vecco Dektak 150 for profilometer test: a) Stylus, and b) Sample disk (Non-catalytic)

4.3 Results and Discussion

Bio-oils are composed of many complex chemical compounds and functional groups which require additional processes to separate major composition. The scope of this research is to obtain bio-oils after the thermo-chemcial process and study its lubrication properties since these bio-oils were produced from many different processes and raw materials.

4.3.1 Bio-oil Characterization

All the bio-oils were analyzed in terms of elemental composition, moisture content, TAN and dynamic viscosity. Table 4.2 summarizes the properties of bio-oils used in the study. Gasitar had the lowest moisture content, while it was highest for poultry litter derived bio-oil. Further, gasitar had the lowest TAN and elemental analysis showed a higher percentage of carbon and hydrogen, while non-catalytic fast pyrolysis bio-oils were more acidic. TAN of non-catalytic and catalytic bio-oils are higher due to the presence of polymeric chains of cellulose, hemicellulose and lignin of poplar. These chains results in the production of bio-oil having higher oxygen content during pyrolysis process which is observed in Table 4.2. The presence of oxygen in bio-oil is highly associated with the acidity of bio-oil. Catalytic fast pyrolysis bio-oil and gasitar were less viscous compared to algal bio-oils (*Scendesmus* and *Nannochloropsis*), poultry and non-catalytic fast pyrolysis bio-oils. The bio-oils produced from the same process parameters and method for *Scenendesmus* and *Nannochloropsis* vary in dynamic viscosity. This could be due to variation in the composition of algae species in terms of proteins, carbohydrates, and lipids. The standard mineral base oils had the dynamic viscosity of 0.16 ± 0.03 and 0.25 ± 0.03 (Pa.s at 25^{o}C) for standard 68 and standard 100 respectively. Non-catalytic, catalytic bio-oil and gasitar had a lower percentage of nitrogen and sulfur content with higher carbon and hydrogen content. Nitrogenates were higher for algal and poultry litter bio-oils.

Table 4.2: Selected bio-oil properties

Properties	Bio-oils					
	Non-catalytic	Catalytic	Gasitar	Nannochloropsis	Poultry	Scenedesmus
C (wt. %)	65.5 ± 0.1 ^{c}	66.7 ± 0.1 ^{c}	88.5 ± 0.2 ^{a}	71.2 ± 0.3 ^{b}	60.8 ± 0.8 ^{d}	66.3 ± 0.8 ^{c}
H (wt. %)	7.3 ± 0.04 ^{c}	7.5 ± 0.04 ^{c}	6.5 ± 0.01 ^{c}	11.4 ± 0.6 ^{a}	9.6 ± 0.03 ^{b}	10.0 ± 0.11 ^{a,b}
N (wt. %)	0.2 ± 0.04 ^{c}	0.2 ± 0.03 ^{c}	0.6 ± 0.08 ^{c}	5.5± 0.2 ^{b}	8.1 ± 0.05 ^{a}	5.9 ± 0.03 ^{b}
S (wt. %)	0.09 ± 0.05 ^{b}	0.07 ± 0.05 ^{b}	0.07 ± 0.07 ^{b}	0.45 ± 0.04 ^{a}	0.36 ± 0.02 ^{a}	0.5 ± 0.01 ^{a}
O* (wt. %)	26.95 ± 0.14 ^{a}	25.50 ± 0.15 ^{a}	4.29 ± 0.19 ^{e}	11.45 ± 1.06 ^{d}	21.06 ± 0.84 ^{b}	17.23 ± 0.75 ^{c}
Moisture (wt. %)	5.9 ± 0.2 ^{c}	4.0 ± 0.02 ^{c}	0.7 ± 0.14 ^{d}	1.3 ± 0.04 ^{d}	7.1 ± 0.2 ^{a}	3.5 ± 0.3 ^{b}
TAN	130.0 ± 6.6 ^{a}	106.9 ± 1.4 ^{b}	5.0 ± 0.14 ^{e}	30.3 ± 0.9 ^{d}	42.3 ± 0.5 ^{c}	24.9 ± 0.1 ^{d}
HHV (MJ/kg)	27.0 ± 0.01 ^{a}	33.4 ± 0.02 ^{f}	38.3 ± 0.15 ^{d}	35.9 ± 0.2 ^{b}	31.5 ± 0.1 ^{e}	32.3 ± 0.1 ^{c}
Dynamic Viscosity (Pa.s)	2.5 ± 0.1 ^{a,b}	0.8 ± 0.04 ^{b}	0.05 ± 0.01 ^{b}	3.9 ± 1.2 ^{a}	2.3 ± 0.05 ^{a,b}	1.2 ± 0.06 ^{b}

Different letters in the superscript of each group (row) denote the values are statistically different at properties level.
*By difference for oxygen = 100% – (C% + H% + N% + S%)

GC/MS analysis of the bio-oils detected more than 100 compounds based on the NIST library of mass spectra. The compounds were selected for GC/MS peaks having an area percentage exceeding 0.1% of total ion chromatogram. The compounds were mainly categorized into six major groups: acids, phenols, hydrocarbons, oxygenates, nitrogenates, and others (compounds not considered by the major groups). Figure 4.4 represents the peak area percentage of the major groups for bio-oils produced from different biomass. It can be seen that there is higher oxygenates in the pyrolysis bio-oil especially non-catalytic and catalytic bio-oils followed by poultry derived bio-oils. This increase is due to higher aromatic hydroxyl groups particularly phenolic compounds. These are mainly formed from thermal decomposition of lignin during the pyrolysis process. These includes carboxylic acids from the decomposition of biomass that helps to form a lubrication film during boundary lubrication. These fatty acids tends to be affected by load, temperature and speed that results in breaking of the film layer [32][33]. Poultry bio-oil had slightly higher nitrogenates and N-O compounds than non-catalytic and catalytic bio-oil. Oxygenates in these bio-oils consist of acids, ketones, aldehydes, furans, hydroxyl and ether compounds which belong to the carbonyl

groups. Research has shown that these polar groups help to create a monolayer film that is effective at reducing friction and wear [34]. Gasitar had higher hydrocarbons compared to all the other bio-oils, which consisted of aromatics. Hydrocarbons play an important role to form an adsorption oil film on surfaces to avoid direct metal contact. This is one of the desired properties of lubricants, and the hydrocarbon content of the bio-oils help to form a thin layer between contact metal surfaces [35]. Nitrogenates and N-O compounds were prevalent in the case of algal bio-oil which were mostly associated with the heavier aromatic hydrocarbon groups. Nitrogen is the second highest element present in the algal oil which tends to be associated with carbon mainly due to respiration of fixed CO_2. This causes the algal oil to be highly viscous and offers resistance to fluidity of bio-oil [36][37]. The replenish action was not observed during the tribometer test which could have been the reason due to the heavier and viscous fraction of the algal oils. Details about the chemical compounds for GCMS can be found in Appendix C.

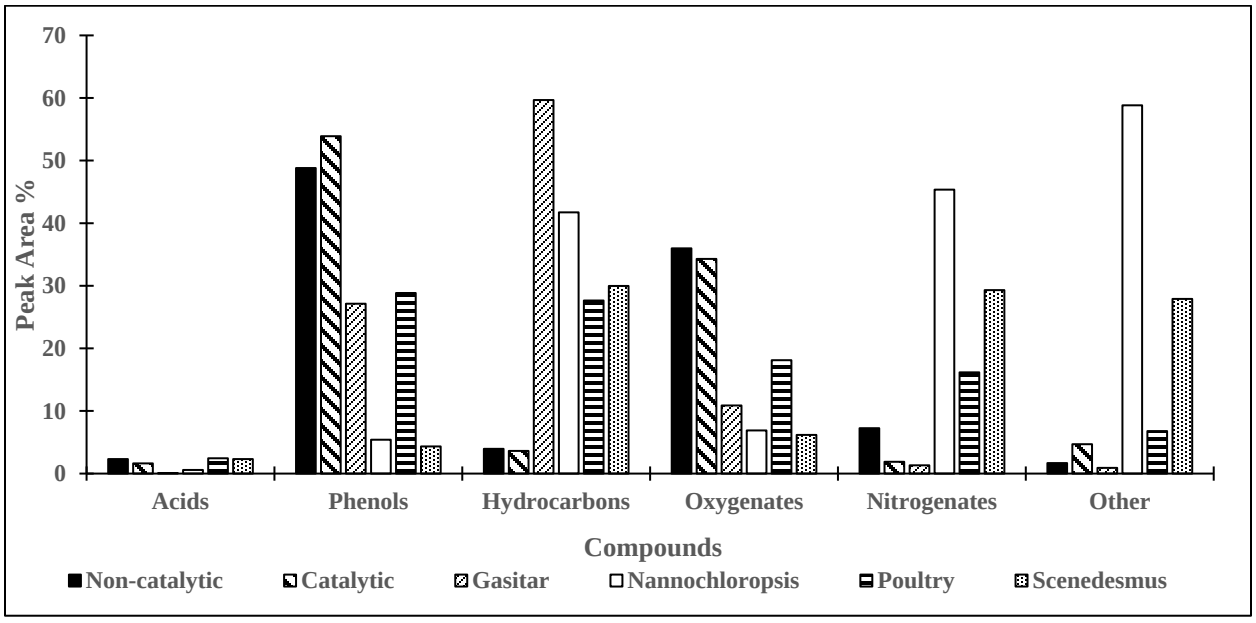

Figure 4.4: GCMS analysis of bio-oil

Figure 4.5 shows FTIR spectroscopy data of the bio-oils. The data show functional groups associated with the bio-oils. There was significant stretching at 3100-3500 cm $^{-1}$ which confirms the O-H functional group for non-catalytic, catalytic, poultry and gasitar and corroborated which with the result from GC/MS. The band at 3400 cm^{-1} is related to hydroxyl and amino groups that is consistent with previous studies [38].The peaks between 3000-3100 cm^{-1} in gasitar represented the aromatic carbons. The aromatics helps to improve the efficiency for competitive adsorption between polar compounds in terms of lubrication [39]. The band peak between 2800-3000 cm $^{-1}$ represents alkanes hydrocarbon stretch region which is very high for standard base oils. The stretching was relatively higher for poultry and *Nanochloropsis*. Alkanes helps to provide rigitdity to the film and is a contributing factor for reducing COF [40]. The peaks presented in between 1600-1750cm^{-1} represent ketonic, and esters groups presents non-catalytic, catalytic, and poultry bio-oil. This stretching was also observed in the ester groups of Yufu et al. [41]. The esterified algal bio-oil showed superios lubrication properties that required further procession of the bio-oil. The C-C functional vibration stretching is relatively higher for poultry bio-oil. The sharp peak at around 1454 cm^{-1} represents alkane groups present in poultry bio-oil, while the vibration at 1200 cm^{-1} represents higher oxygenates present in bio-oil particularly C-O compounds. Those compounds were mainly present in non-catalytic and catalytic bio-oil. The stretching between 650-800 cm^{-1} represents alkanes and alkenes groups.

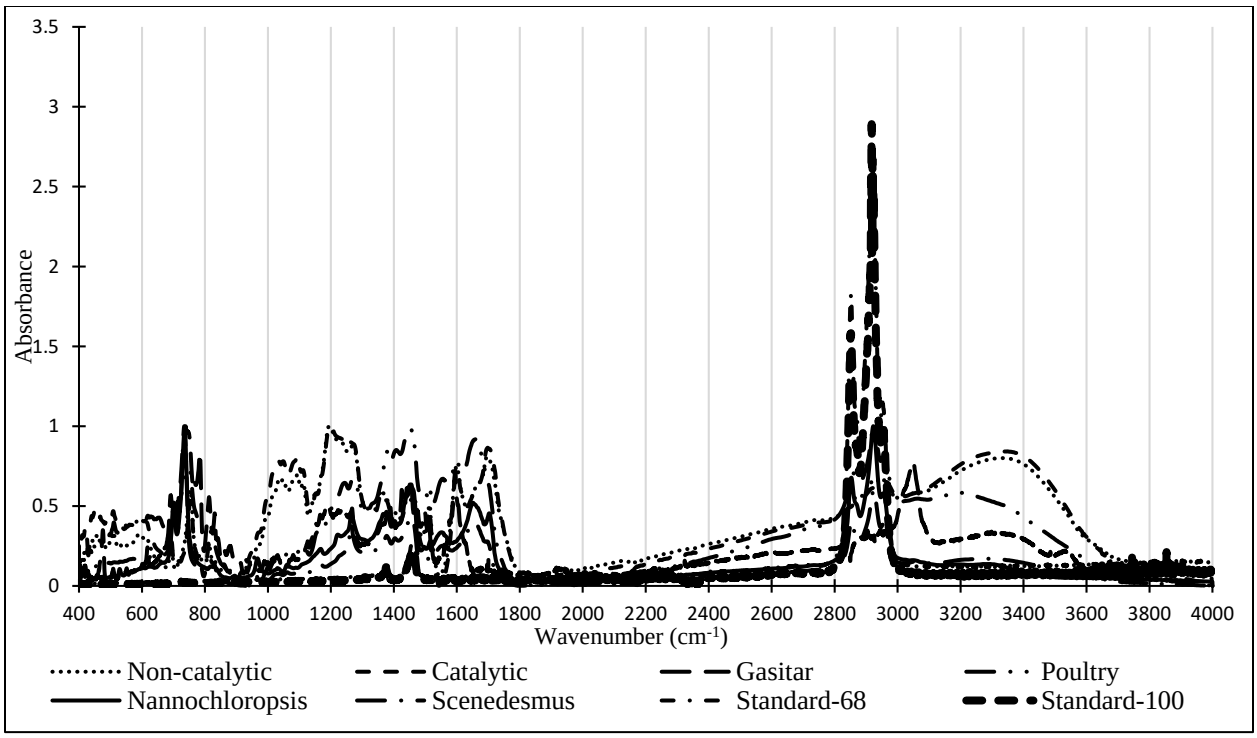

Figure 4.5. FTIR data of bio-oil

Thermogravimetric analysis (TGA) indicates the volatility of bio-oils with an increase in temperature. The TGA analysis was performed on bio-oils samples to determine the mass-loss rate for different bio-oil starting from 25^{o}C to 600^{o}C at a heating rate of 10^{o}C/min. A majority of the mass loss occurred below 400^{o}C, however, it took around 530^{o}C for algal (*Scenedesmus* and *Nannochloropsis*) bio-oils (Figure 4.6). Most of the bio-oils started losing their mass from the temperature as low as 100^{o}C (some of the losses could be due to moisture present in bio-oils) so it is important to increase the stability of bio-oils before using them as lubricants. Most gear lubricants operate between 90^{o}C and 120^{o}C, so bio-oils could be applicable for gear lubrication [42]. Most of the mass loss occurred between 25^{o}C – 500^{o}C and the remained mass for all the bio-oils samples was below 2 mg at 600^{o}C. The TGA test on standard base oil showed that the majority of mass loss occurred at around 450^{o}C. Mass loss started around 325^{o}C, which is approximately

200ºC higher than the bio-oils. The carboxylic acids present in the bio-oil are adsorbed on the metal surface thus forming monolayer film of hydrocarbon end of fatty acids oriented away from metal surface. This layer is affected by load, temperature, speed, viscosity and composition [43]. The carboxylic acids and other lower molecular compounds such as ketones and aldehydes are reactive, volatile and with the temperature rise these could affect the reduce frictional properties of bio-oil [44].

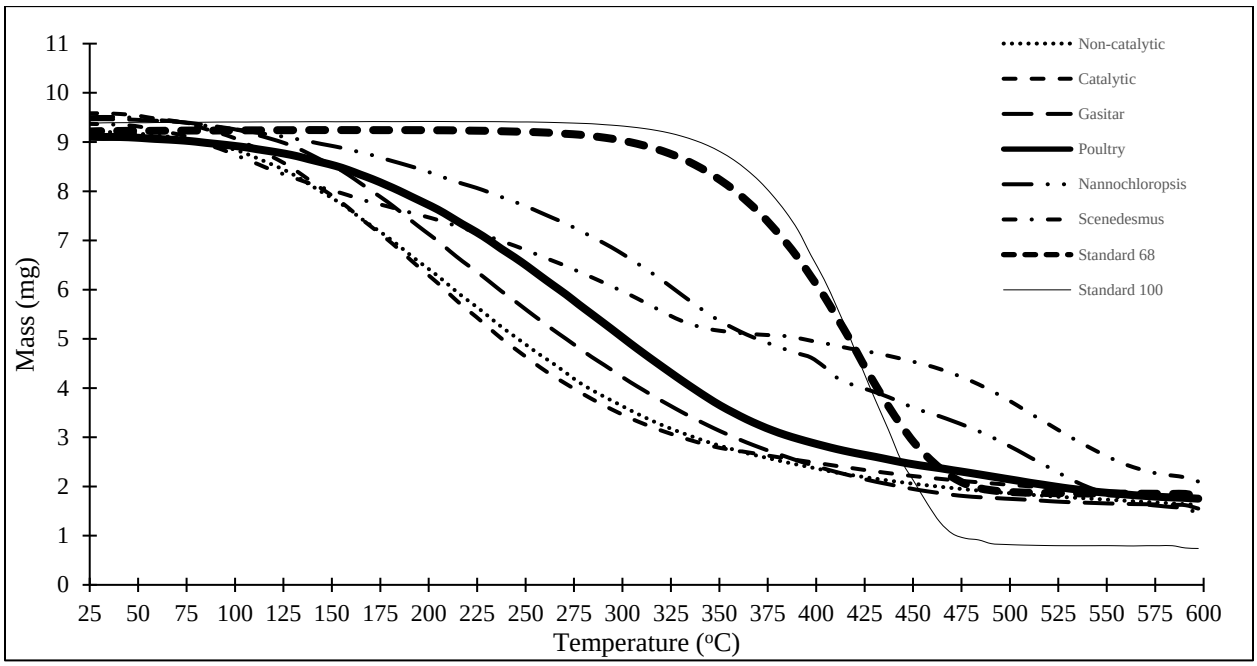

Figure 4.6: Thermogravimetric analysis of bio-oil

4.3.2 Tribological Properties of Bio-oils

4.3.2.1 Coefficient of Friction (COF)

COF is defined as a ratio between friction force and normal force.The COF obtained from the tribometer test is shown in Figure 4.7. The tests were designed to be well into the boundary lubrication regime resulting in solid asperities contact dominated. The bio-oil sample attached

itself with the contacting surface to create a film layer however with 50N load and 63.7 rev/s the film layer gets rubbed off and solid surfaces come into contact. The COF was lower for gasitar and *scenedesmus* as compared to other bio-oils and standard base oils. The bio-oils obtained from pyrolysis have higher oxygenates, particularly polar organic compounds, which contribute to form a film layer on the metal surfaces. Gasitar having a comparatively good mixture of aromatic hydrocarbons along with hydroxyl groups could be the reason for the lower COF. It also had a lower dynamic viscosity, which could have played an important role and allowed the oil to replenish the wear groove surface. Also, algae bio-oils have a lower COF which could be due to the combination of alkanes and alkene-based hydrocarbons and that could have helped to form a film layer via adsorption on the metal surface. However, algal bio-oils were more viscous than any other of the bio-oils, which caused flow-ability problems during the experimental runs. Catalytic, non-catalytic, gasitar, and poultry litter bio-oils had a mixture of hydrocarbons and oxygenates, which could be the reason for a lower COF than the standard base oils. Based on the average COF, gasitar exhibited good lubrication. The COF result was better than the standard base oils with all of the bio-oils tested.

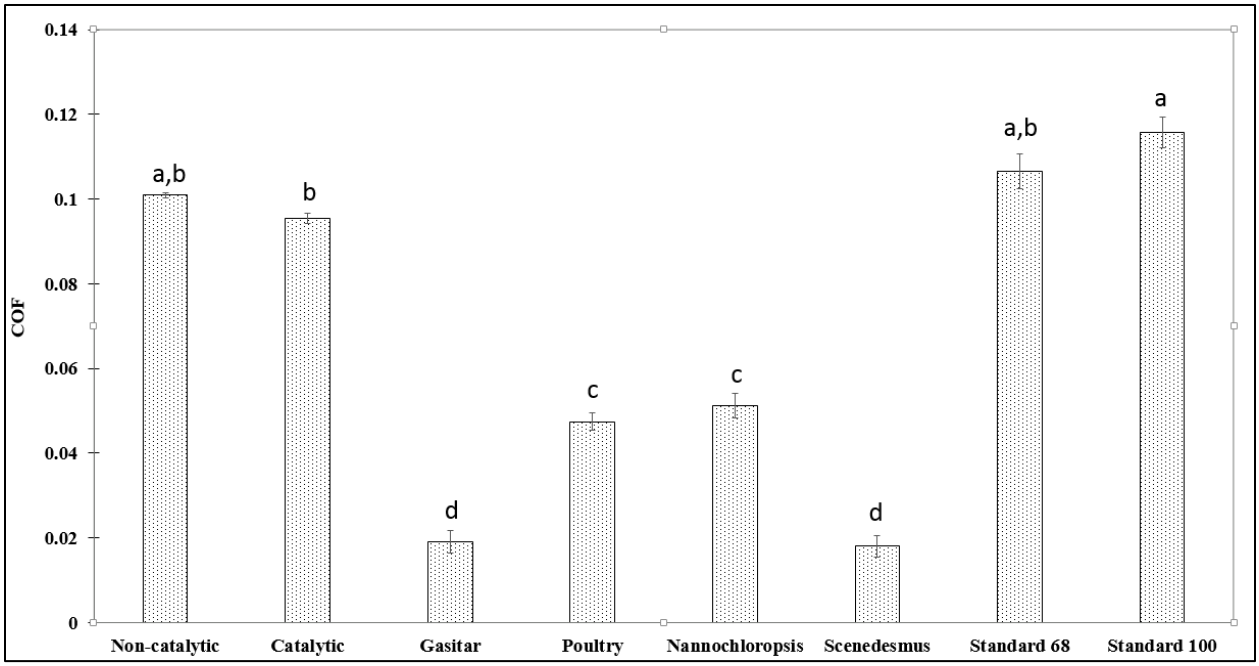

Different letters above the bar denote that the values are statistically different for different bio-oils

Figure 4.7: COF of bio-oil along with standard base oils

4.3.2.2 Wear

Wear areas of the samples were obtained from the profilometer test. The data obtained from the profilometer were analyzed in Excel and MATLAB to obtain the worn cross-sectional area of the grooves which is represented in Figure 4.8 (a). The wear area was quite high for disk samples tested with *Nannochloropsis* and *Scenedesmus* bio-oils compared to all the other tests as shown in Figure 4.8 (b). Fig ure 4.8 (c) represents the wear area data without algal oil samples. The data indicate clearly that algal bio-oil produced a higher wear cross-section area compared to all other tests. The reason could be due to the higher viscosity of algal bio-oil which could have hampered the replenishment mechanism of the lubricant. During the tribometer test, the oil film thickness helps to avoid contact between the metal surfaces formed, algal bio-oils having higher viscosities were readily displaced by the ball. The higher viscosity caused flow-ability issues which hampered the replenishment action and could have led to the direct contact between asperities, causing higher

wear. The pyrolysis oil has a comparatively lower viscosity and also contains polar organic compounds. The polar organic compounds such as ketones and aldehydes could have formed a thin layer to avoid direct metal contact. The catalytic bio-oil had comparatively lower wear cross-sectional area than any other oils, which could due to lower polar group and the replenishing action might have been boosted due to lower viscosity. Gasitar had a lower oxygen content and higher aromatic hydrocarbon content, which could have provided a good resistance to wear. Further, it also had lower viscosity compared to all other bio-oils and might have effectively improved the replenishment action and form a thin layer to avoid direct contact. These bio-oils have comparatively better performance than standard mineral base oils with the viscosity of 68 and 100 cSt. With the inclusion of additives, that would be used in fatty formulated industrial lubricants these bio-oils have a good prospect to be used as a lubricant.

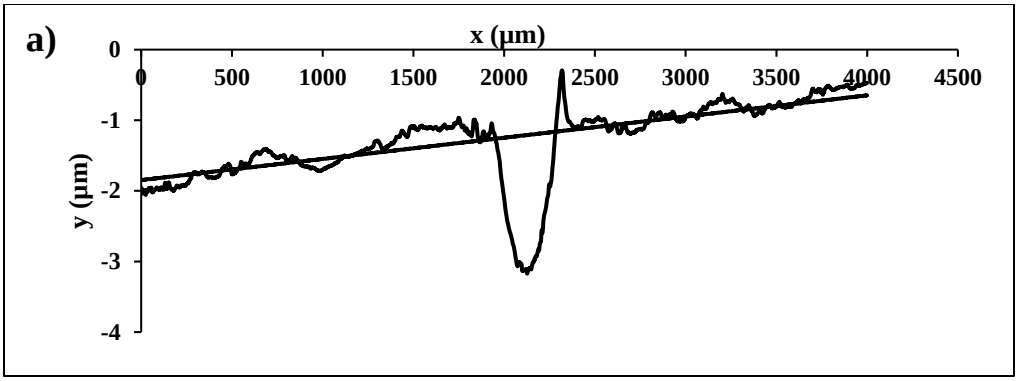

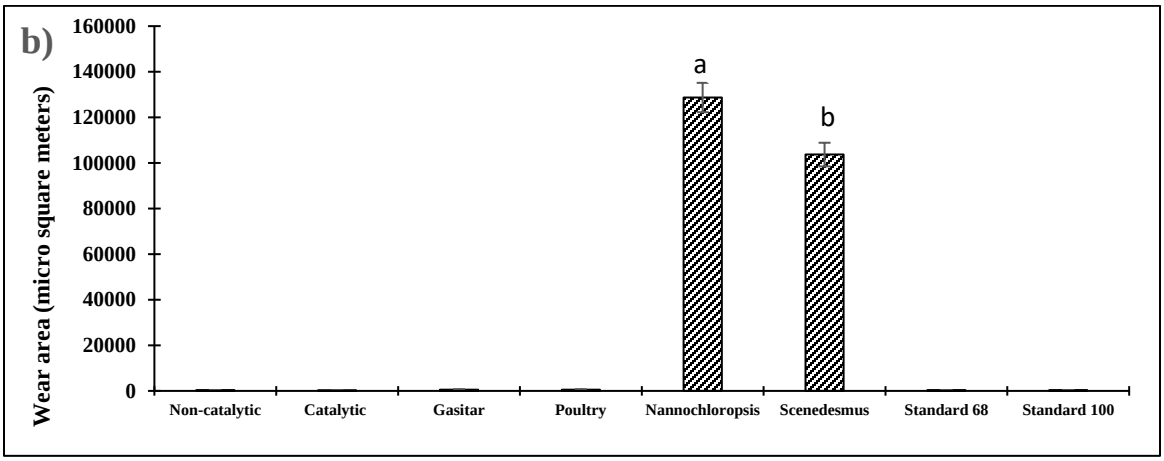

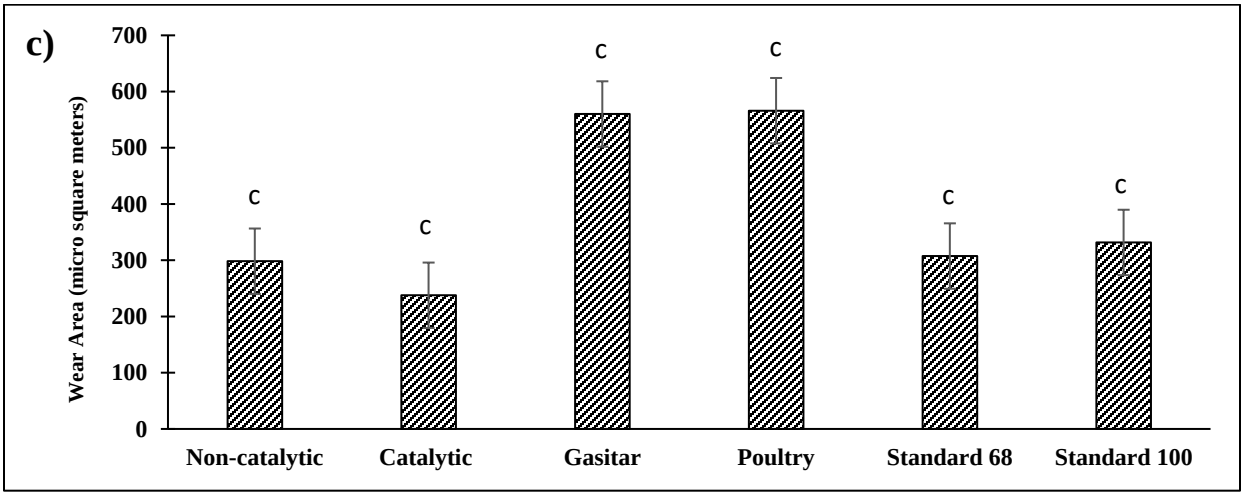

Different letters above the bar denote that the values are statistically different for different oils

Figure 4.8: a) Wear profile with a mean line to evaluate the wear area of test specimen (catalytic bio-oil test run); b) wear area of the bio-oil and standards oils; and c) wear area without algal bio-oil

4.3.2.3 Digital Images of Wear Surface

Digital images presented in Figure 4.9 were obtained from the digital microscope. These images helped to better visualize and evaluate the wear grooves. The wear groove of each sample disk tested with algal bio-oils had higher wear width as well as higher depth. Those groove dimensions were comparatively less for all other cases as discussed in the wear section. The shallow grooves observed on algal disk samples could be due to scuffing. The algal bio-oil might not have been sufficient enough to avoid contact between surfaces. The images observed for poultry-based oil also indicated that the wear was due to scuffing. The images observed in all other sample disks indicate that wear mechanisms were slightly different from that of algal bio-oil. The wear images for standard mineral base oils (both 68 & 100) could be due to abrasion. The wear images of gasitar, catalytic and non-catalytic oils tested disks could be due to micro plowing of the surfaces since wear groove from microscope images were very small.

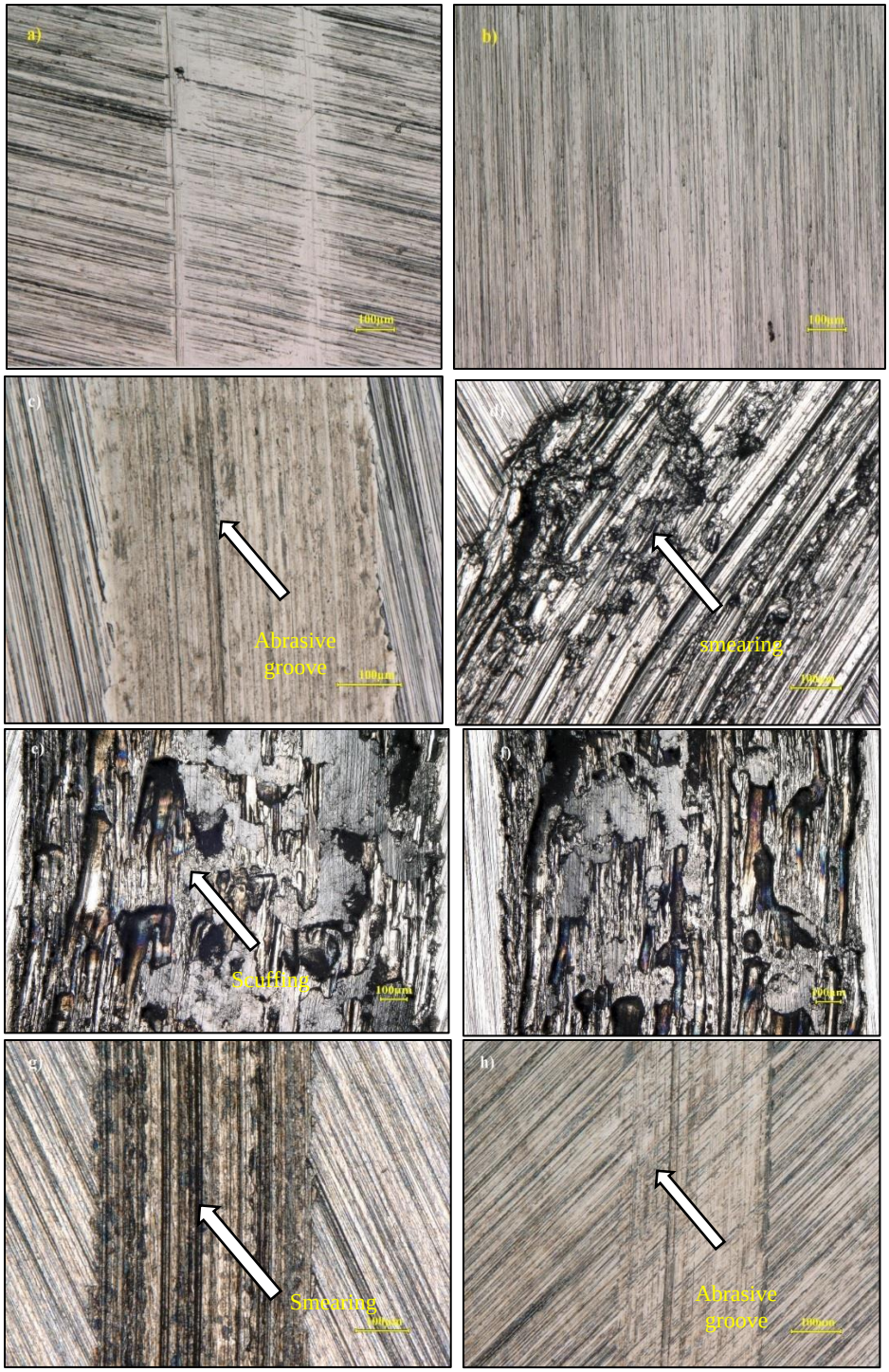

Figure 4.9: Wear surfaces of disk samples: (a) Non-catalytic, (b) Catalytic, (c) Gasitar, (d) Poultry, (e) Nannochloropsis, (f) Scenedesmus (g) Standard 68, and (h) Standard 100

4.4 Conclusions

The tribological tests revealed that gasitar had a low COF (0.02), however, wear results indicated that catalytic pyrolysis bio-oil had a lower wear cross-sectional area compared to all other tests. The algal bio-oil tested sample disk had grooved surfaces as observed from digital microscope images, which could be due to scuffing wear mechanism. The images of disk samples tested with pyrolysis and gasitar exhibited wear grooves indicating micro plowing wear mechanism. The chemical analysis of bio-oil samples indicated that gasitar had a lower oxygen and higher hydrocarbon composition, pyrolysis bio-oil had higher oxygenates, and algal bio-oils had a higher nitrogenates composition. The study shows that catalytic pyrolysis bio-oil and gasitar have good prospects to be used as lubricants, however catalytic pyrolysis bio-oil chemical analysis still indicates the presence of oxygenating groups which could have a cascading effect at an elevated temperature. Gasitar contains hydrocarbons and some oxygenates, and with the addition of additives, it could be an alternative to current fossil-based lubricants.

Acknowledgements

The author (S.K.C.) would like to acknowledge Dr. Hyungseok Nam for providing tar (“gasitar”) samples from gasification, and Dr. Rajdeep Shakya for helping with GC/MS analysis. This work was supported by the Alabama Agricultural Experiment Station and the Hatch Program of the National Institute of Food and Agriculture, U.S. Department of Agriculture.

4.5 References

[1] U. S. E. Information, "U.S. Imports of Lubricants," *Energy Information Administration*, 2018. [Online]. Available: https://www.eia.gov/dnav/pet/hist/LeafHandler.ashx?n=PET&s=MLUIMUS2&f=A. [Accessed: 01-Feb-2019].

[2] W. Dresel and M. Theo, *Lubricants and lubrication*. Wiley, Weinheim, 2006.

[3] S. KC, P. D. Nezhadfar, C. Phillips, M. S. Kennedy, N. Shamsaei, and R. L. Jackson, "Tribological behavior of 17–4 PH stainless steel fabricated by traditional manufacturing and laser-based additive manufacturing methods," *Wear*, vol. 440–441, p. 203100, 2019.

[4] T. M. Panchal, A. Patel, D. D. Chauhan, M. Thomas, and J. V. Patel, "A methodological review on bio-lubricants from vegetable oil based resources," *Renew. Sustain. Energy Rev.*, vol. 70, pp. 65–70, Apr. 2017.

[5] S. Z. Erhan and S. Asadauskas, "Lubricant basestocks from vegetable oils," *Ind. Crops Prod.*, vol. 11, no. 2–3, pp. 277–282, Mar. 2000.

[6] H. S. Abdalla and S. Patel, "The performance and oxidation stability of sustainable metalworking fluid derived from vegetable extracts," *Proc. Inst. Mech. Eng. Part B J. Eng. Manuf.*, vol. 220, no. 12, pp. 2027–2040, 2006.

[7] P. K. Sripada, R. V Sharma, and A. K. Dalai, "Comparative study of tribological properties of trimethylolpropane-based biolubricants derived from methyl oleate and canola biodiesel," *Ind. Crops Prod.*, vol. 50, pp. 95–103, 2013.

[8] R. D. Kulkarni, P. S. Deshpande, S. U. Mahajan, and P. P. Mahulikar, "Epoxidation of mustard oil and ring opening with 2-ethylhexanol for biolubricants with enhanced thermo-oxidative and cold flow characteristics," *Ind. Crops Prod.*, vol. 49, pp. 586–592, 2013.

[9] E. K. Heikal, M. S. Elmelawy, S. A. Khalil, and N. M. Elbasuny, “Manufacturing of environment friendly biolubricants from vegetable oils,” *Egypt. J. Pet.*, vol. 26, no. 1, pp. 53–59, 2017.

[10] M. Shahabuddin, H. H. Masjuki, and M. A. Kalam, “Experimental investigation into tribological characteristics of biolubricant formulated from Jatropha oil,” *Procedia Eng.*, vol. 56, pp. 597–606, 2013.

[11] N. A. Zainal, N. W. M. Zulkifli, M. Gulzar, and H. H. Masjuki, “A review on the chemistry, production, and technological potential of bio-based lubricants,” *Renew. Sustain. Energy Rev.*, vol. 82, pp. 80–102, 2018.

[12] S. Ray, P. V. C. Rao, and N. V Choudary, “Poly-α-olefin-based synthetic lubricants: a short review on various synthetic routes,” *Lubr. Sci.*, vol. 24, no. 1, pp. 23–44, Jan. 2012.

[13] *A Comprehensive Review of Lubricant Chemistry, Technology, Selection, and Design*. 2009.

[14] R. Mahadevan, R. Shakya, S. Neupane, and S. Adhikari, “Physical and chemical properties and accelerated aging test of bio-oil produced from in situ catalytic pyrolysis in a bench-scale fluidized-bed reactor,” *Energy and Fuels*, vol. 29, no. 2, pp. 841–848, 2015.

[15] R. Shakya, S. Adhikari, R. Mahadevan, E. B. Hassan, and T. A. Dempster, “Catalytic upgrading of bio-oil produced from hydrothermal liquefaction of Nannochloropsis sp.,” *Bioresour. Technol.*, vol. 252, pp. 28–36, Mar. 2018.

[16] H. Nam, A. L. Maglinao, S. C. Capareda, and D. A. Rodriguez-Alejandro, “Enriched-air fluidized bed gasification using bench and pilot scale reactors of dairy manure with sand bedding based on response surface methods,” *Energy*, vol. 95, pp. 187–199, Jan. 2016.

[17] R. Shakya, J. Whelen, S. Adhikari, R. Mahadevan, and S. Neupane, “Effect of

temperature and Na2CO3 catalyst on hydrothermal liquefaction of algae," *Algal Res.*, vol. 12, pp. 80–90, 2015.

[18] Y. F. Pan Pan 1, Changwei Hu, Wenyan Yang, Yuesong Li, Linlin Dong, Liangfang Zhu, Dongmei Tong, Renwei Qing, "The direct pyrolysis and catalytic pyrolysis of Nannochloropsis sp. residue for renewable bio-oils," *Bioresour. Technol.*, vol. 101, no. 12, pp. 4593–4599, Jun. 2010.

[19] T. X. &Dan Y. Z. Hui Qiang Yu, Xiao Yang Wei, Zheng Cui, Xian Guo Hu, "Friction and wear behaviors of a cylinder liner–piston ring with emulsified bio-oil as fuel," *Tribol. Trans.*, vol. 56, no. 3, pp. 359–365, 2013.

[20] Y. Xu, X. Zheng, X. Hu, K. D. Dearn, and H. Xu, "Effect of catalytic esterification on the friction and wear performance of bio-oil," *Wear*, vol. 311, no. 1–2, pp. 93–100, 2014.

[21] Q. Lu, Z. B. Zhang, H. T. Liao, X. C. Yang, and C. Q. Dong, "Lubrication properties of bio-oil and its emulsions with diesel oil," *Energies*, vol. 5, no. 3, pp. 741–751, 2012.

[22] A. Oasmaa, E. Leppämäki, P. Koponen, J. Levander, and E. Tapola, "Physical characterization of biomass-based pyrolysis liquids. Application of standard fuel oil analyses Oasmaa, A. et al. VTT Publ., 1997, 306, 1–86," *Fuel Energy Abstr.*, vol. 39, no. 2, p. 97, 1998.

[23] X. Guo, S. Wang, Q. Wang, Z. Guo, and Z. Luo, "Properties of Bio-oil from Fast Pyrolysis of Rice Husk," *Chinese J. Chem. Eng.*, vol. 19, no. 1, pp. 116–121, Feb. 2011.

[24] M. Bertero, G. De La Puente, and U. Sedran, "Fuels from bio-oils: Bio-oil production from different residual sources, characterization and thermal conditioning," *Fuel*, vol. 95, pp. 263–271, May 2012.

[25] A. Ben Hassen-Trabelsi, T. Kraiem, S. Naoui, and H. Belayouni, "Pyrolysis of waste

animal fats in a fixed-bed reactor: Production and characterization of bio-oil and bio-char," *Waste Manag.*, vol. 34, no. 1, pp. 210–218, Jan. 2014.

[26] M. Ikura, M. Stanciulescu, and E. Hogan, "Emulsification of pyrolysis derived bio-oil in diesel fuel," *Biomass and Bioenergy*, vol. 24, no. 3, pp. 221–232, 2003.

[27] M. R. Asadullah, M., Rahman, M. A., Ali, M. M., Rahman, M. S., Motin, M. A., Sultan, M. B., Alam, "Production of bio-oil from fixed bed pyrolysis of bagasse," *Fuel*, vol. 86, no. 16, pp. 2514–2520, Nov. 2007.

[28] J. lu Zheng, W. ming Yi, and N. na Wang, "Bio-oil production from cotton stalk," *Energy Convers. Manag.*, vol. 49, no. 6, pp. 1724–1730, Jun. 2008.

[29] X. Miao, Q. Wu, and C. Yang, "Fast pyrolysis of microalgae to produce renewable fuels," *J. Anal. Appl. Pyrolysis*, vol. 71, no. 2, pp. 855–863, Jun. 2004.

[30] M. Saber, B. Nakhshiniev, and K. Yoshikawa, "A review of production and upgrading of algal bio-oil," *Renew. Sustain. Energy Rev.*, vol. 58, pp. 918–930, May 2016.

[31] J. Arun, K. P. Gopinath, P. S. SundarRajan, R. Malolan, and P. AjaySrinivaasan, "Hydrothermal liquefaction and pyrolysis of Amphiroa fragilissima biomass: Comparative study on oxygen content and storage stability parameters of bio-oil," *Bioresour. Technol. Reports*, vol. 11, p. 100465, Sep. 2020.

[32] N. W. M. Zulkifli, M. A. Kalam, H. H. Masjuki, K. A. H. Al Mahmud, and R. Yunus, "The Effect of Temperature on Tribological Properties of Chemically Modified Bio-Based Lubricant," *Tribol. Trans.*, vol. 57, no. 3, pp. 408–415, May 2014.

[33] M. A. Maleque, H. H. Masjuki, and A. S. M. A. Haseeb, "Effect of mechanical factors on tribological properties of palm oil methyl ester blended lubricant," *Wear*, vol. 239, no. 1, pp. 117–125, Apr. 2000.

[34] M. R. Reeves, Carlton J. Menezes, Pradeep L. Jen, Tien Chien Lovell, “The influence of fatty acids on tribological and thermal properties of natural oils as sustainable biolubricants,” *Tribol. Int.*, vol. 90, pp. 123–134, Oct. 2015.

[35] S. Dutta, C. Hartkopf-Fröder, K. Witte, R. Brocke, and U. Mann, “Molecular characterization of fossil palynomorphs by transmission micro-FTIR spectroscopy: Implications for hydrocarbon source evaluation,” *Int. J. Coal Geol.*, vol. 115, pp. 13–23, Aug. 2013.

[36] A. Demirbaş, “Production of Biodiesel from Algae Oils,” *Energy Sources, Part A Recover. Util. Environ. Eff.*, vol. 31, no. 2, pp. 163–168, Dec. 2008.

[37] A. Kumar and S. Bera, “Revisiting nitrogen utilization in algae: A review on the process of regulation and assimilation,” *Bioresour. Technol. Reports*, vol. 12, p. 100584, 2020.

[38] S. Xiu, A. Shahbazi, V. Shirley, and D. Cheng, “Hydrothermal pyrolysis of swine manure to bio-oil: Effects of operating parameters on products yield and characterization of bio-oil,” *J. Anal. Appl. Pyrolysis*, vol. 88, no. 1, pp. 73–79, 2010.

[39] R. F. Tsinghua and Y. Qiu, “The effect of aromatic hydrocarbons in lubricant base oils on the efficiency of adsorptive additives,” *Lubr. Sci.*, vol. 14, no. 2, pp. 195–210, Feb. 2002.

[40] A. Jabbarzadeh, “Friction anisotropy in confined alkanes: Linear and branched molecules,” *Tribol. Int.*, vol. 97, pp. 108–115, 2016.

[41] Y. Xu, X. Hu, K. Yuan, G. Zhu, and W. Wang, “Friction and wear behaviors of catalytic methylesterified bio-oil,” *Tribol. Int.*, vol. 71, pp. 168–174, 2014.

[42] B. R. Höhn and K. Michaelis, “Influence of oil temperature on gear failures,” *Tribol. Int.*, vol. 37, no. 2, pp. 103–109, Feb. 2004.

[43] A. H. M. Maleque, H. Masjuki, “Effect of mechanical factors on tribological properties of

palm oil methyl ester blended lubricant," *Wear*, vol. 239, no. 1, pp. 117–125, 2000.

[44] B. M. Negahdar, Leila, Gonzalez-Quiroga, Arturo, Otyuskaya, Daria, Toraman, Hilal E., Liu, Li, Jastrzebski, Johann T.B.H. Van Geem, Kevin M., Marin, Guy B., Thybaut, Joris W., Weckhuysen, "Characterization and Comparison of Fast Pyrolysis Bio-oils from Pinewood, Rapeseed Cake, and Wheat Straw Using 13C NMR and Comprehensive GC × GC," *ACS Sustain. Chem. Eng.*, vol. 4, no. 9, 2016.

Chapter 5: Conclusion and future recommendation

5.1 Conclusion

A tribological study of different materials and lubricants has been performed. Firstly, additively manufactured parts were produced using laser beam powder bed fusion (LB-PBF). Friction and wear properties were compared with conventional wrought samples under dry and lubricated conditions. Secondly, with the intent to look out for alternatives to conventional fossil-based lubricant, high oleic vegetable-based oils were studied from a tribological standpoint. Lastly, second and third-generation biomasses were utilized to produce bio-oils. The lubrication properties of the bio-oils were compared with conventional base oil. Each of the objectives was fulfilled, and the findings, analysis, and conclusions are summarized below:

Objective I: Disk samples were made using LB-PBF technology and conventional wrought samples were tested under a load of 10N and 30N under dry and lubricated conditions. LB-PBF 17-4 PH SS has a lower wear rate than conventional 17-4 PH SS for dry condition, which could be due to the higher hardness of AM and also due to differences in the roughness between two samples. The AM samples had slightly higher hardness (417 ± 21 HV) than the CM samples (392 ± 24 HV) and the roughness of LB-PBF was 1.93 µm while it was 0.88 µm for CM. The higher roughness of AM led to the formation of effectively thinner lubricant film formation as compared to the CM specimens. The results showed a lower friction and wear regime for both AM and CM in the lubricated condition, while the COFs were erratic and wear was severe for dry conditions. Optical images of the worn surfaces indicated that 10N applied load in the dry condition had lower worn surfaces than a 30N applied load in the dry condition for both CM and AM samples. The images showed signs of adhesion and scuffing regardless of the loads under dry conditions. The

directional grooves on the surfaces indicated an abrasive wear mechanism for lubricated conditions. The observation was concurrent with the lower COF results for lubricated conditions. Wear debris were observed in SEM images for dry conditions indicating operation in a severe wear regime. Overall, AM parts showed comparable tribological properties as compared to CM, however results did suggest surface fatigue could negatively effect AM part wear.

Objective II: Vegetable-based oils with different oleic content were tested for tribological properties under 50N of applied load at varying speeds and compared with a standard mineral base oil with additives. Viscosity plays a vital role and the rheometer test indicated that the vegetable-based oil viscosity decreases with an increase in temperature. The effect of PUFA was found in different vegetable-based oils as higher PUFA makes oil unstable due to oxidation. Oils having lower PUFA showed good wear-resistant properties as compared with higher PUFA containing vegetable oils. The FTIR test showed that the presence of strong C=O bonds and could have helped to form a film layer during boundary lubrication. Varying speeds were applied during the tribometer test and the minimum film thickness was evaluated using elastohydro dynamic lubrication (EHL) equations which indicated the boundary lubrication regime for the test. A Stribeck curve showed lower COF values for vegetable-based oil as compared to the standard mineral base. The presence of polar functional groups such as fatty acids which are attracted to the metal surface could be the reason for lower COF at lower speeds. Optical images showed that the dominant wear mechanism for all the cases was abrasive wear along with some adhesion. The wear mechanism could have expanded from two body to three-body due to debris being trapped in between the ball and disk surface. With the test temperature being at approximately 90^{o}C, the volatile fraction could have evaporated, reducing the lubricant film thickness for vegetable-based

oils. Overall, the vegetable-based oil showed better tribological properties compared to the conventional mineral oil.

Objective III: Bio-oils were obtained from fast pyrolysis (using poultry and pine), gasification ("gasitar" using pine), and hydrothermal liquefaction processes (using Scenedesmus and Nannocholoropsis). A ball on disk tribometer test was conducted for thermochemically produced bio-oils under a load of 50 N at a rotating speed of 63.7 rev/min for 30 minutes. Bio-oil analysis showed catalytic and gasitar oils had a lower viscosity as compared to other bio-oils. The variation could be due to different thermochemical processes and different compositions of the biomass. GCMS analysis showed the presence of ketones, aldehydes, and furans belonging to the carbonyl group that helped to form a film layer on the metal surface. Gasitar had a higher hydrocarbon content compared to other bio-oils which is favorable for lubrication purposes. The aromatics present in the bio-oils helped to improve the efficiency for competitive adsorption between polar compounds in terms of lubrication. TGA analysis showed that most of the bio-oils mass loss occurred at around 400^{o}C starting from as low as 100^{o}C, making it favorable for typical lubrication applications. Tribometer results showed that gasitar and scenedesmus had lower COF values as compared to other bio-oils and the mineral base oil. Algal oils had higher wear as compared to any of the other oils. This could be due to the presence of a heavier fraction of oils particularly due to nitrogenates and high viscosity. Optical images of the wear surfaces showed directionally smeared which may be due to scuffing. Algal and poultry oils had severe wear due to the presence of nitrogenates reducing the replenishing action of the bio-oil.

5.2 Future Recommendation

Tribology is a very important branch of science and needs continuous research along with the evolving technology. Additive manufacturing is emerging as a new technology in the manufacturing world and more research is required in terms of surface roughness, lubrication, and wear properties. Sustainable bio-based products are required to replace conventional lubricants to reduce fossil-based products. Vegetable-based oils show promising results as compared to conventional base oils. Second and third-generation biomass as raw material would make a higher impact on the lubrication industry since they are sustainable and generally carbon neutral source. Bio-lubricant from bio-wastes could help to make a sustainable future from lubrication perspective. With the knowledge gained from this study, the research on bio-based oils can be further expanded.

Additive manufacturing has different methods and process conditions to produce parts, one of which is the LB-PBF process. Other process materials other than 17-4 PH SS should also be tested for the tribological study. The surface roughness of AM parts were relatively higher than the conventional, so more surface refinement and improvement methods should be investigated. Tribometer tests under different speeds, load, and at an elevated temperature conditions should give future information about the potential use of AM parts on a commercial scale. Some research has been conducted in terms of modeling fatigue behavior and surface roughness, however experimental results will help to give a better picture.

Vegetable-based bio-oils showed better tribological properties than conventional base oil under similar conditions. The presence of PUFA greatly varies the performance of vegetable-based oils. Fatty acids helps to improve the friction and wear properties, especially for higher oleic content oils. However, a comparative study of vegetable-based oil with commercial additives

would help to provide results than can be compared with conventional base oils on the market. This result will help to understand the influence of additives to improve the oxidative stability of the vegetable-based oils.

Second and third-generation bio-oils have shown good potential and could be a sustainable alternative to conventional base oils. Gasitar and catalytic pyrolysis produced oils have shown comparable properties to conventional oils. Further research is required to understand the tribological properties of these particular bio-oils. A tribometer test with disk samples completely submerged, different loading conditions, elevated temperature, and varying speed would help to provide a better picture of these oils. Another avenue for future research would be to upgrade the bio-oils using hydrotreatment and compare the tribological properties with that of the conventional base oils. Additionally, additives could be used to optimize the bio-oils and the results could be compared for tribological properties.

Appendix A

$$Hersey\ Number = \frac{Dynamic\ viscosity\ x\ Speed\ x\ Radius}{Load}$$

Appendix B

Input parameters:

Radius of ball = 5mm

Elastic modulus of ball = 210 GPa

Poisson ratio of ball = 0.29

Elastic Modulus of sample = 205 GPa

Poission ration of sample = 0.3

Pressure viscosity coefficient (1/GPa) = 0.1

Mini speed (m/s) = 0.0016

Max speed (m/s) = 0.67

Load (N) = 50

Elastohydrodynamic lubrication was used to calculate the minimum film thickness and lambda ratio. Minimum film thickness is the minimum separation two surfaces to avoid direct contact. Chittenden et al. [24] studied the minimum film thickness and central film thickness with major axis of the Herztian contact ellipse which was used to compute the minimum film thickness.

The minimum film thickness is calculated as:

$$Hmin = 3.64\,.G^{0.49}.U^{0.68}.W^{-0.073}\left(1 - e^{-0.67\left(\frac{Ry}{Rx}\right)^{\frac{2}{3}}}\right) \ldots.(a)$$

G, U, and W are dimensional less parameters and are calculated as:

$G = \propto_p E^{|}$…..(b)

$U = \frac{\eta u}{E^{|} R_x}$…....(c)

$W = \frac{F}{E^{|} R_x^2}$…...(d)

where

α_p = Pressure viscosity coefficient

$E^{`}$ = Equivalence modulus of elasticity

η = viscosity

u = entering velocity of the fluid

F = load

R = radius of the contacting surfaces

For varying dynamic viscosity minimum film thickness was evaluated as shown in table C1

Table B.1: Minimum film thickness of each oil

Sliding Speed	**Oil A**	**Oil B**	**Oil C**	**Oil D**	**ISO 68**
m/s	**h_{min} (nm)**	**h_{min} (nm)**	**h_{min} (nm)**	**h_{min} (nm)**	**h_{min} (nm)**
0.0016	0.09	0.08	0.09	0.09	0.1
0.00335	0.95	0.89	0.96	0.96	1.07
0.0084	1.5	1.41	1.53	1.53	1.69
0.0168	1.97	1.86	2.01	2.01	2.22
0.0335	2.39	2.25	2.43	2.43	2.7
0.084	2.78	2.62	2.83	2.83	3.13
0.134	3.14	2.96	3.2	3.2	3.56
0.167	3.49	3.29	3.55	3.55	3.94
0.251	3.82	3.6	3.89	3.89	4.31
0.335	4.14	3.9	4.21	4.21	4.67
0.42	4.44	4.19	4.52	4.52	5.01
0.502	4.74	4.47	4.83	4.83	5.35
0.586	5.03	4.74	5.12	5.12	5.67
0.67	5.31	5	5.41	5.41	5.99

The lambda ratio is the minimum film thickness (h_{min}) in relation to the RMS roughness of the contacting surface.

$$\lambda = \frac{\text{hmin}}{\sqrt{R_{q1}^2 + R_{q2}^2}} \quad \text{.....(b)}$$

where, h_{min} = minimum film thickness

R_q = RMS roughness of two contacting surfaces

From minimum film thickness, lambda ratio was evaluated by dividing by the average sample roughness as shown in table C2

Table B.2: Lambda ratio of each oil

Sliding Speed (m/s)	Oil A	Oil B	Oil C	Oil D	ISO 68
0.0016	0.000622	0.000553	0.000622	0.000622	0.000691
0.00335	0.006565	0.00615	0.006634	0.006634	0.007394
0.0084	0.010365	0.009743	0.010573	0.010573	0.011678
0.0168	0.013613	0.012853	0.013889	0.013889	0.015341
0.0335	0.016515	0.015548	0.016792	0.016792	0.018657
0.084	0.01921	0.018105	0.019556	0.019556	0.021629
0.134	0.021698	0.020454	0.022112	0.022112	0.0246
0.167	0.024116	0.022734	0.024531	0.024531	0.027226
0.251	0.026397	0.024876	0.02688	0.02688	0.029783
0.335	0.028608	0.02695	0.029092	0.029092	0.03227
0.42	0.030681	0.028953	0.031234	0.031234	0.03462
0.502	0.032754	0.030888	0.033376	0.033376	0.036969
0.586	0.034758	0.032754	0.03538	0.03538	0.03918
0.67	0.036693	0.034551	0.037384	0.037384	0.041392

Appendix C: Supplementary Information

List of compounds in each group

Oxygenates	Acid	Phenols	Hydrocarbons	Nitrogenates	Others
Phenol, 3-ethyl-	Acetic acid	Phenol	Benzene, 1-methyl-4-(phenylmethyl)-	2-Amino-3-hydroxypyridine	Ethylene glycol diglycidyl ether
	Benzoic acid, 4-hydroxy-3-methoxy	Phenol, 3-methoxy-	(1-Methylbuta-1,3-dienyl)benzene	1H-Benzimidazole, 2-ethyl-	(5-Bromopyridin-2-yl)carbamic acid, methyl ester
Phenol	Propanoic acid	Benzene, ethoxy-	.alpha.-Methylstyrene	1H-Isoindole-1,3(2H)-dione, 2-(9-azabicyclo[6.1.0]non-4-en-9-yl)-, (1.alpha.,4Z,8.alpha.)-	1,4-Bis(trimethylsilyl)-1,3-butadiyne
Naphtho[2,1-b]furan, 1,2-dimethyl-		Phenol, 2-methyl-	[14]Annulene, 1,6:8,13-bis(methano)-, syn	1-Isobutyl-6,7-dimethoxy-3,4-dihydro-isoquinoline	1-Isobutyl-6,7-dimethoxy-3,4-dihydro-isoquinoline
Furfural		Phenol, 4-methyl-	1,1'-Biphenyl, 3-methyl-	1-Naphthalenecarbonitrile	2-Amino-3-hydroxypyridine
Furan, 2-ethyl-		Phenol, 3-methyl-		2-Butenamide, 3-methyl-N-1H-purin-6-yl-	3,5-Cyclohexadiene-1,2-dione, 3,4,5,6-tetrachloro-

Ethylene glycol diglycidyl ether		Phenol, 2,4-dimethyl-	11H-Benzo[b]fluorene	4(1H)-Pteridinone, 5,6,7,8-tetrahydro-6-methyl-	4(1H)-Pteridinone, 5,6,7,8-tetrahydro-6-methyl-
Ethanone, 1-(4-hydroxy-3,5-dimethoxyphenyl)-		Phenol, 3-ethyl-	1H-Indene, 2-phenyl-	4-Fluoro-2,6-dimethoxypyrimidine	6-Chloro-3-(2-chloroethyl)-1,2-dihydro-2-oxoquinoline
Ethanone, 1-(2-furanyl)-		Phenol, 4-ethyl-2-methoxy-	1H-Phenalene	6-Chloro-3-(2-chloroethyl)-1,2-dihydro-2-oxoquinoline	9,10-Bis(bromomethyl)anthracene
Ethanol, 2-[4-(1,1-dimethylpropyl)phenoxy]-		Phenol, 2-ethyl-5-methyl-	1-Isopropenylnaphthalene	6-Chrysenol	Cyclopenta[c]thiapyran
Durohydroquinone		Phenol, 3-methyl-6-propyl-	2,4-Dimethylstyrene	Benzo[c]cinnoline, 4,7-dimethyl-	N-(4-Methoxyphenyl)-2-hydroxyimino-acetamide
Dibenzofuran		Phenol, 2-ethyl-4,5-dimethyl-	2-Phenylnaphthalene	Benzonitrile	
Cyclopentanone		Phenol, 2,6-dimethoxy-	3,3'-Dimethylbiphenyl	Benzonitrile, 2-methyl-	
Benzofuran, 2,3-dihydro-		Phenol, 2-methoxy-4-(1-propenyl)-, (E)-	3H-Benz[e]indene, 2-methyl-	N-(4-Methoxyphenyl)-2-hydroxyimino-acetamide	
Benzo[b]naphtho[1,2-d]furan		Phenol, 3-methoxy-2,4,6-trimethyl-	4H-Cyclopenta[def]phenanthrene	Isoquinoline	
Benzaldehyde, 6-hydroxy-4-methoxy-2,3-dimethyl-		Phenol, 2-methoxy-4-(1-propenyl)-	9,10-Dimethylanthracene		
Acetophenone			9H-Fluorene, 9-methyl-		
Acetic acid, phenyl ester			Acephenanthrylene, 4,5-dihydro-		
9H-Fluoren-9-ol			Anthracene, 1-methyl-		
4-tert-Butoxystyrene			Anthracene, 2-ethyl-		
3-Phenanthrol			Benz[a]azulene		
2-Cyclopenten-1-one, 3-methyl-			Benzanthrene		

2-Propanone, 1-hydroxy-			Benzene, 2-butenyl-		
2-Furanmethanol			Biphenyl		
1H-Indenol			Indane		
1-Butanone, 1-(2,4,6-trihydroxy-3-methylphenyl)-			Naphthalene		
[1,1'-Biphenyl]-4-carboxaldehyde			Phenanthrene		
			Pyrene		
			Pyrene, 1-methyl-		